Robustness of mission plans for unmanned aircraft

by

Moritz Niendorf

A dissertation submitted in partial fulfillment
of the requirements for the degree of
Doctor of Philosophy
(Aerospace Engineering)
in the University of Michigan
2016

Doctoral Committee:

Associate Professor Anouck Renee Girard, Chair
Associate Professor Ryan M. Eustice
Professor Daniel J. Inman
Professor Pierre Tshimanga Kabamba (Deceased)
Professor Ilya Vladimir Kolmanovsky

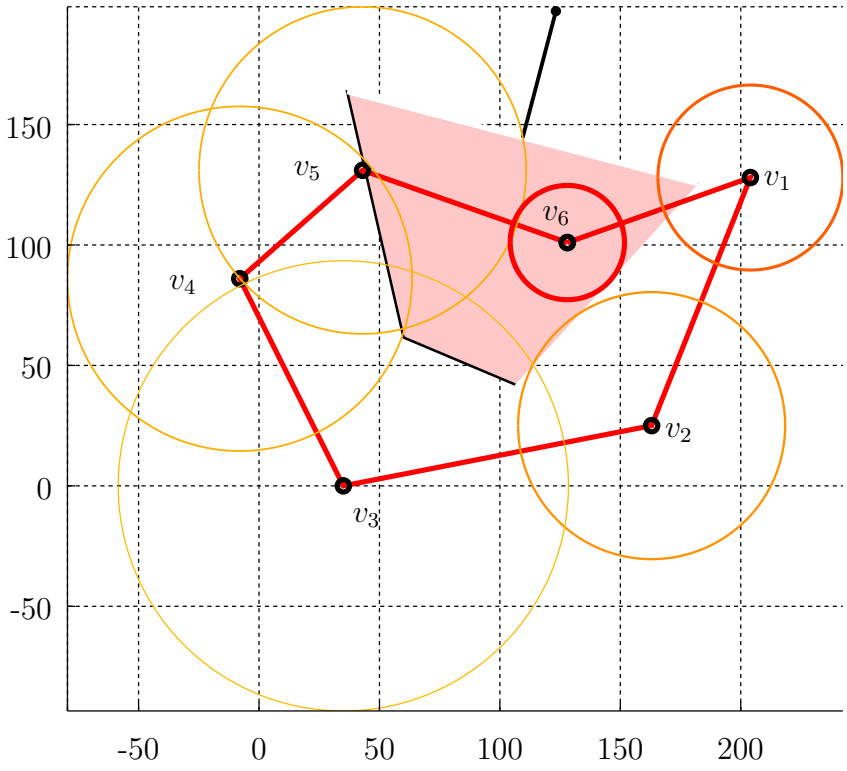
150
100
50
0
-50
-50
0
50
100
150
200
v_1
v_2
v_3
v_4
v_5
v_6

2016

To my family, friends, and mentors.

ACKNOWLEDGEMENTS

I first and foremost would like to thank my advisors, Professors Anouck Girard and Pierre Kabamba. Thank you for all the support you have given me over the course of my graduate career. Your guidance was instrumental to the success of this work and your mentoring was invaluable to my personal and professional growth.

I am very grateful to Professors Ryan Eustice, Daniel Inman, and Ilya Kolmanovsky for joining my committee and offering very useful feedback about my research.

I am very appreciative of the help I have received over the years from my lab mates, especially Ricardo Bencatel, Jonathan Las-Fargeas, Dave Oyler, Johnhenri Richardson, and Jinwoo Seok, as well as of the help I received from Shasha Magpantay and Christopher Petersen. I would like to thank Florian Adolf of the German Aerospace Center (DLR e.V.) for his valuable advice regarding mission planning for unmanned aircraft.

I would like to acknowledge the United States Air Force for funding my research. I would also like to thank the Air Force Research Laboratory, the University of Michigan Department of Aerospace Engineering, and the Rackham Graduate School for their support. Furthermore, I would like to thank the staff in the Department of Aerospace Engineering and the Rackham Graduate School for facilitating my studies.

Thank you to all the friends I made during my time in Ann Arbor. You have supported me, entertained me, and taught me quite a bit on top of what I learned in school. Completing this research would not have been possible without the enjoyable life you created for me outside of my studies.

Lastly and mostly, thank you to my family for all your support over the duration of my graduate studies.

TABLE OF CONTENTS

LIST OF FIGURES

LIST OF TABLES

LIST OF ABBREVIATIONS

LP Linear programming

ILP Integer linear programming

UAV Unmanned aerial vehicle

TSP Traveling salesman problem

eTSP Euclidean TSP

snTSP Symmetric non sequence-dependent TSP

anTSP Asymmetric non sequence-dependent TSP

ssTSP Symmetric sequence-dependent TSP

asTSP Asymmetric sequence-dependent TSP

wsmoTSP Weighted-sum multi-objective TSP

MST Minimum spanning tree

eMST Euclidean minimum spanning tree

M1T Minimum 1-tree

ABSTRACT

Robustness of mission plans for unmanned aircraft

by

Moritz Niendorf

Chair: Anouck Renee Girard

This thesis studies the robustness of optimal mission plans for unmanned aircraft. Mission planning typically involves tactical planning and path planning. Tactical planning refers to task scheduling and in multi aircraft scenarios also includes establishing a communication topology. Path planning refers to computing a feasible and collision-free trajectory.

For a prototypical mission planning problem, the traveling salesman problem on a weighted graph, the robustness of an optimal tour is analyzed with respect to changes to the edge costs. Specifically, the stability region of an optimal tour is obtained, i.e., the set of all edge cost perturbations for which that tour is optimal.

The exact stability region of solutions to variants of the traveling salesman problems is obtained from a linear programming relaxation of an auxiliary problem. Edge cost tolerances and edge criticalities are derived from the stability region. For Euclidean traveling salesman problems, robustness with respect to perturbations to vertex locations is considered and safe radii and vertex criticalities are introduced. For weighted-sum multi-objective problems, stability regions with respect to changes in the objectives, weights, and simultaneous changes are given. Most critical weight perturbations are derived.

Computing exact stability regions is intractable for large instances. Therefore, tractable approximations are desirable. The stability region of solutions to relaxations of the traveling salesman problem give under approximations and sets of tours give over approximations. The application of these results to the two-neighborhood and the minimum 1-tree relaxation are discussed. Bounds on edge cost tolerances and approximate criticalities are obtainable likewise.

A minimum spanning tree is an optimal communication topology for minimizing the cumulative transmission power in multi aircraft missions. The stability region of a minimum spanning tree is given and tolerances, stability balls, and criticalities are derived. This analysis is extended to Euclidean minimum spanning trees.

This thesis aims at enabling increased mission performance by providing means of assessing the robustness and optimality of a mission and methods for identifying critical elements. Examples of the application to mission planning in contested environments, cargo aircraft mission planning, multi-objective mission planning, and planning optimal communication topologies for teams of unmanned aircraft are given.

CHAPTER 1

Introduction

1.1 Motivation

The use of unmanned aerial vehicles (UAVs) has grown steadily in recent years. With the increase in their use and the advances in technology, these aircraft are tasked with increasingly large and complex missions. Such missions include but are not limited to surveillance of multiple points of interest over extended periods of time, search and rescue applications, pipeline inspections, mapping, communication relaying, crop dusting, and delivery tasks.

These missions are typically designed such that given the circumstances of the mission, e.g., the tasks to be completed, vehicle specifications, and a model of the environment, a flight path and sequence of actions to be performed by the aircraft are selected such that they optimize a mission objective. If multiple vehicles are used to jointly perform a mission, some communication between the UAVs to coordinate the mission execution is typically required. The goal of this research is to enable increased UAV mission performance by providing means to assess the robustness of a given mission plan, by providing methods to detect suboptimality in mission plans due to changes in the circumstances of the mission, and by identifying critical elements of a mission.

Mission planning for UAVs is an inherently complex problem due to the high

dimensionality of the solution space. The addition of time-varying mission specifications such as a priori unknown changes in the environment or the flight performance of the aircraft further increases the complexity of the problem.

Planning efficient missions for unmanned aircraft typically involves two steps:

1. Tactical planning refers to scheduling the order in which locations are visited and the determination of a communication topology in multi-UAV missions;

2. Path planning is concerned with the computation of a feasible and collision-free trajectory.

Figure 1.1 depicts one of many possible realizations of such a planning approach. This specific approach is discussed in detail in Ref. [1]. An unmanned aircraft is located at a and operates in a dense urban environment. Multiple waypoints ($b - f$) indicated by the circled arrows are placed by the operator. A path planning algorithm computes shortest paths between each waypoint pair. This step corresponds to solving the path planning problem. The waypoints are then ordered such that the total distance traveled is minimized. This step corresponds to solving the tactical planning problem. The yellow flight path is collision-free, feasible for a simplified dynamics model of the aircraft, and visits the waypoints in an optimal sequence. In a post-processing step, this path is further optimized, which leads to the final flight path shown in blue.

During mission execution the unmanned aircraft might encounter points where the overall mission performance would benefit from modifying the original mission plan. In these cases, the integration of tactical planning and path planning using feedback between both of these layers may lead to faster, more efficient, and more reliable mission completion even under changing conditions. Fig. 1.2 depicts the interaction between tactical planning and path planning.

Consider the scenario in Fig. 1.3 that illustrates one example of the interaction of

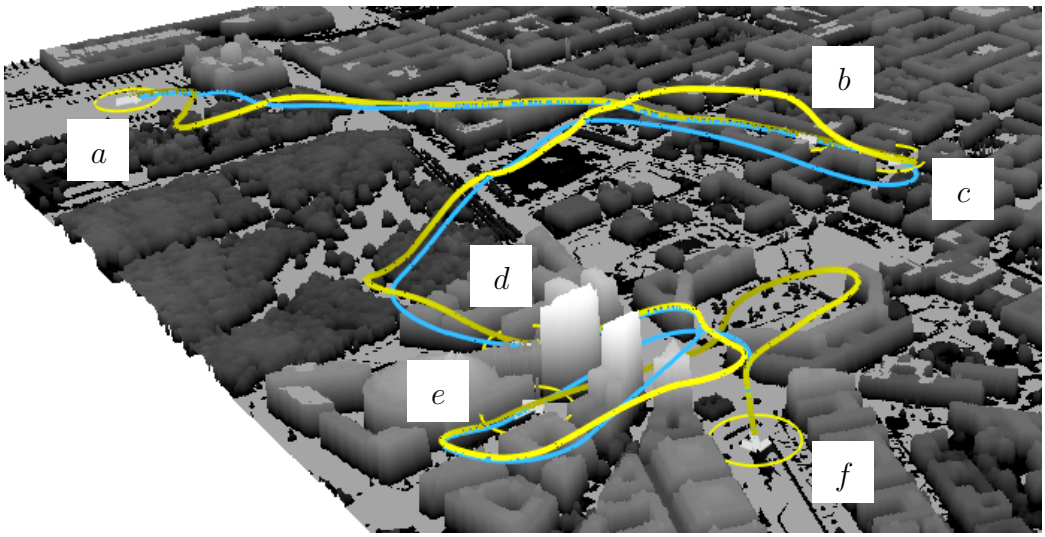

Figure 1.1: **UAV mission planning example:** An unmanned aircraft is located at a and operates in a dense urban environment. Multiple waypoints ($b - f$) indicated by the circled arrows are placed by the operator. A path planning algorithm computes shortest paths between each waypoint pair. The waypoints are then ordered such that the total distance traveled is minimized. The yellow flight path is collision-free, feasible for a simplified dynamics model of the aircraft, and visits the waypoints in an optimal sequence. In a post-processing step, this path is further optimized, which leads to the final flight path (blue) [1].

tactical planning and path planning for unmanned aircraft in the presence of obstacles. An unmanned aircraft is located at location c. It is tasked to take off, visit multiple locations of interest indicated by the green dots, and return to the airfield. Obstacles are indicated by the polygons. Depending on the mission, these obstacles could be storm cells in a large scale scenario, buildings in an urban scenario, or for example areas in which manned aircraft operate that need to be avoided. First, the shortest path between each location pair is computed. This corresponds to the path planning in Fig. 1.2. Then, a tactical planning problem is solved using the previously computed path cost information to obtain the optimal tactical plan, i.e., the order in which to visit the locations. This corresponds to tactical planning in Fig. 1.2. If the obstacles are moved, the shortest path between each location pair is recomputed and the tactical planning problem is resolved. Given the obstacle locations in Fig. 1.3b, the nominal

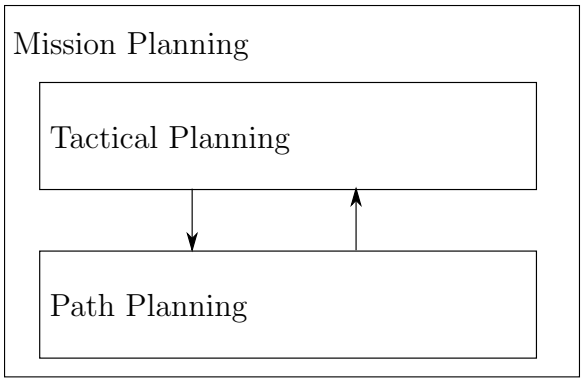

Figure 1.2: **UAV mission planning schematic:** A tactical planning layer computes a sequence of tactical goals and determines a communication topology based on the initial locations of the aircraft in multi-UAV scenarios. The path planning layer computes a flight path that satisfies the tactical goals. If changes occur at the tactical layer, they are propagated to the path planning layer and a new flight path is computed. If changes at the path planning layer occur, such as replanning the flight path between two tactical goals because of an unforeseen obstacle, this information is provided to the tactical planning layer that adapts the tactical plan if beneficial. Finally, in multi-UAV scenarios, the optimality of the communication topology is assessed during mission execution and adapted to the current situation.

tactical plan remains optimal. This nominal plan contains the subsequence (a, b, c). For the case depicted in Fig. 1.3c, the obstacle locations are altered again. In this case, a different tactical plan containing the subsequence (a, c, b) is optimal.

Considering the scenario laid out in Fig. 1.3 raises the following two questions:

1. How robust is an optimal tactical plan with respect to changes in the environment?

2. Are tactical plans more susceptible to changes in the costs of certain paths than to changes to the costs of other paths?

In multi-UAV scenarios, where tactical planning involves determining a communication topology, even just following the planned flight paths might lead to situations where the initial communication topology becomes suboptimal.

Obtaining methods to assess the robustness of a mission plan has multiple potential benefits: First, by comparing robustness margins for individual elements of the

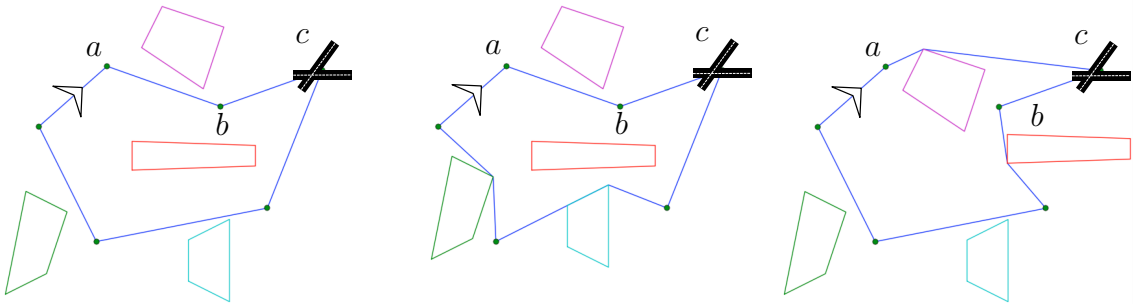

(a) Nominal (b) Path changed (c) Tactical plan changed

Figure 1.3: **Tactical planning and path planning interaction:** Consider the nominal scenario in Fig. 1.3a. An aircraft is located at an airfield c. It is tasked to take off, visit multiple locations of interest indicated by the green dots, and return to the airfield. Obstacles are indicated by the polygons. First, the shortest path between each location pair is computed. Then, a tactical planning problem is solved using the path cost information to obtain the optimal tactical plan, i.e., the order in which to visit the locations. If the obstacles are moved, the shortest path between each location pair is recomputed and the tactical planning problem is resolved. Given the obstacle locations in Fig. 1.3b, the nominal tactical plan remains optimal. This nominal plan contains the subsequence (a, b, c). For the case depicted in Fig. 1.3c, the obstacle locations are altered again. In this case a different tactical plan containing the subsequence (a, c, b) is optimal.

problem data, the notion of criticality of an element of the problem data, which is a dimensionless parameter, can be defined. Using criticality analysis, efforts in the acquisition of problem data can be focused on the most critical elements. Second, robustness analysis provides information about how robust the optimal solution is with respect to modeling errors but also to changing conditions. Finally, by analyzing the robustness of a given mission plan, expressions can be determined that allow to ascertain the optimality of a mission plan without resolving the planning problem. Therefore, this work aims at enabling adaptive and efficient mission planning for unmanned aircraft in time-varying environments by addressing the problem stated in the following section.

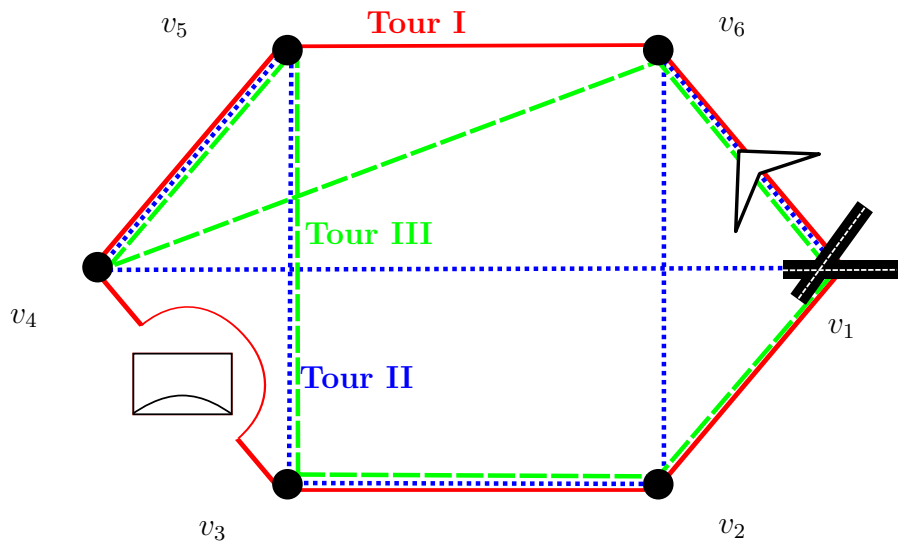

Figure 1.4: **Mission planning in contested environments:** The air defense unit between task locations v_3 and v_4 increases the path cost. This raises the question of how robust tour I (red - solid line) is with respect to such changes.

1.2 Problem Statement

The central problem addressed in this thesis can be stated as follows: Given the circumstances of the mission (e.g., the tasks to be completed, vehicle specifications and a model of the environment), and a performance metric, find methods to assess the robustness and the optimality of a given mission plan such that the optimality of a plan under changing conditions can be ascertained and critical elements of the mission can be identified.

1.3 Motivating examples

The following four examples illustrate the type of mission planning problems and scenarios considered in this work.

1.3.1 UAV mission planning in contested environments

Consider the prototypical mission planning scenario in Fig. 1.4. An unmanned aircraft starting from an airfield v_1 is tasked to visit locations v_2 - v_6 and return to the airfield. It is assumed that a path planning algorithm computes flight paths between location pairs. The path length is assigned as edge weight to the edge connecting that location pair in a representation of the problem as a weighted graph. Then, tactical planning corresponds to solving a classical instance of the symmetric traveling salesman problem (TSP) on the weighted graph.

Assume that the UAV operator provides and approves three alternative schedules in the form of tours, where tour I $(v_1, v_6, v_5, v_4, v_3, v_2, v_1)$ is cost optimal and tours II $(v_1, v_6, v_2, v_3, v_5, v_4, v_1)$ and III $(v_1, v_6, v_4, v_5, v_3, v_2, v_1)$ are backups. Shortly before take-off, new intelligence suggests the presence of anti-aircraft units that must be avoided between locations v_3 and v_4. The path planning algorithm computes a new flight path between this location pair and updates the edge weight. This raises the question of how robust the optimal schedule is with respect to changes in the problem data.

1.3.2 Cargo aircraft mission planning

Consider the prototypical mission planning scenario in Fig. 1.5. A cargo aircraft starting at location v_1 visits three locations and delivers one distinct piece of cargo at each location. The goal is to find a minimum time route. The travel time is proportional to the distance traveled. The best tour is (v_1, v_2, v_3, v_4, v_1) as indicated in the figure. Furthermore, the cargo is stacked according to this itinerary in the cargo aircraft to minimize time when unloading. Optimizing the load in a cargo aircraft based on the anticipated itinerary is a common practice [2]. In this example, the cargo for location v_4 is at the bottom of the stack and the load for location v_2 at the top. If the aircraft deviates from the originally optimal tour, any cargo on top of the

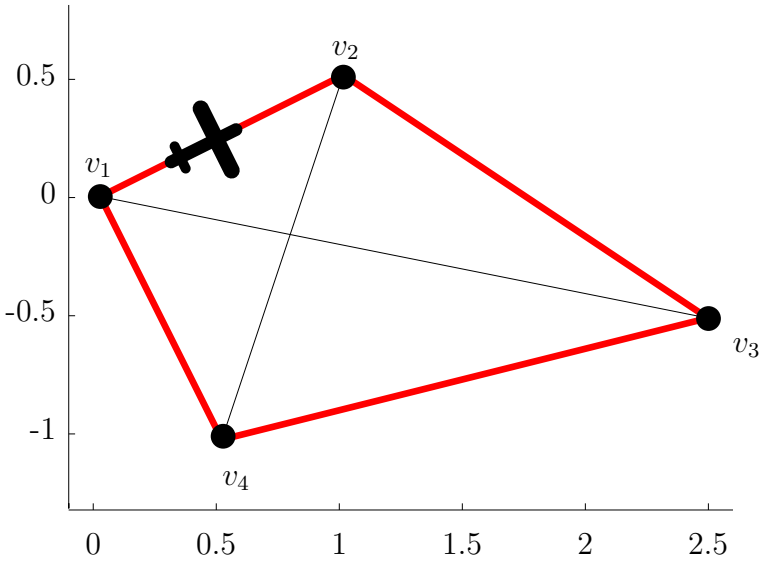

Figure 1.5: **Mission planning for cargo aircraft:** The load inside a delivery aircraft following a time optimal tour v_1, v_2, v_3, v_4, v_1 is stacked according to the travel itinerary. If the aircraft deviates from the planned tour, for example to avoid unfavorable weather, additional time is needed to unload the cargo. This raises the question under which conditions might such a deviation still result in a faster tour completion than the original tour.

cargo for that location must be unloaded and reloaded back into the aircraft. The unloading and loading operation is assumed to consume one time unit, where solely unloading the cargo on top of the stack is assumed to not add additional time. Hence, if the aircraft follows the original route, the time to complete the route is only the travel time. If the aircraft, however, deviates from the original tour and first visits location v_4, an additional cost for unloading and reloading the freight for locations v_2 and v_3 of two time units is added. Hence, the cost of traveling from one location to another does not only depend on the location pair but also on the sequence of locations visited a priori. This property makes this problem a sequence-dependent problem. If the travel times between destinations are time-varying for example due to weather conditions, the question arises under which conditions deviating from the original route results in a faster tour completion than following the original tour in spite of the time penalty due to unloading and reloading cargo.

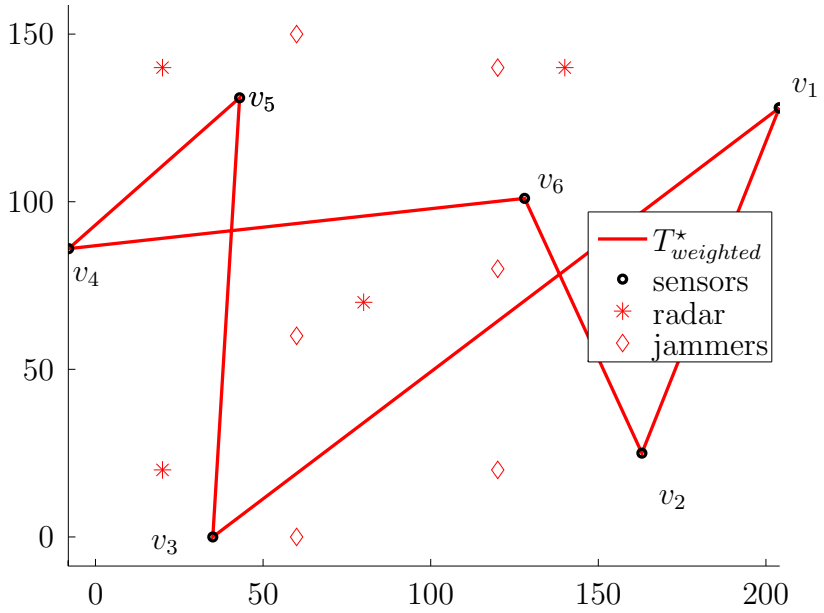

Figure 1.6: **Multi-objective mission planning:** An unmanned aircraft is used to query multiple unattended ground sensors at multiple locations repeatedly. The locations of the unattended ground sensor are enumerated v_1 through v_6. Hostile radar sites as well as hostile communication jamming devices need to be avoided while minimizing the distance traveled. The figure depicts the optimal tour to this problem formulated as a wsmoTSP with respect to a certain choice of weights that trade off the objectives.

1.3.3 Multi-objective UAV mission planning

Consider the prototypical mission planning scenario in Fig. 1.6 that is based upon scenarios in Ref. [3] and Ref. [4]. An unmanned aircraft is used to query multiple unattended ground sensors at multiple locations repeatedly. A traditional approach to obtain optimized flight patterns in this case is to pose this problem as a symmetric TSP, in which the unmanned aircraft is required to visit each unattended ground sensors once, starting from any sensor and returning to the original place of departure resulting in a tour. The locations of the unattended ground sensor are enumerated v_1 through v_6. Hostile radar sites and hostile communication jamming devices are present within the area of operation and need to be avoided while keeping the mission time short and the flown path fuel efficient. This problem can be formulated as an instance of a multi-objective TSP. Multi-objective optimization problems are

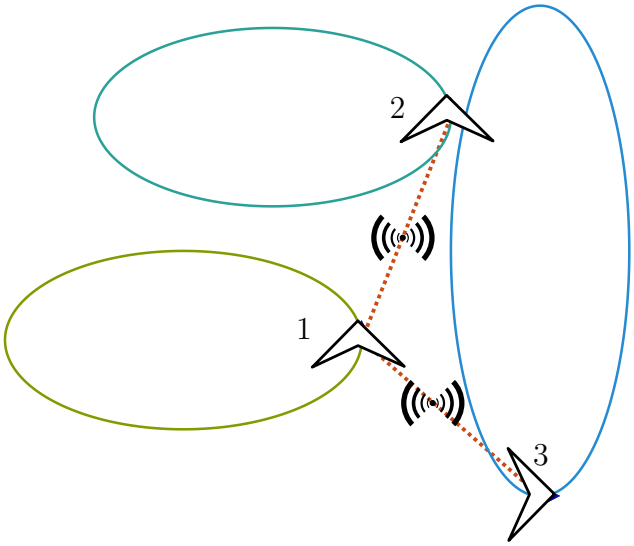

Figure 1.7: **Communication topology planning:** Three UAVs follow elliptical flight paths at a velocity that results in the same period for each trajectory. The location of each aircraft along its trajectory at time t_0 and the optimal choice of communication links (dotted lines) at that time are shown.

often solved using a weighted-sum approach [5]. Fig. 1.6 depicts the optimal solution with respect to a certain choice of weights that trade-off the different objectives and are determined by a human operator. However, the operator faces the difficulty of choosing and tuning these weighting parameters. It is therefore interesting to characterize the robustness of an optimal tour with respect to the weights, because in discrete optimization problems small changes in the problem data may lead to significant changes in the solution [6].

1.3.4 Communication topologies in multi-UAV missions

Consider the prototypical mission planning scenario depicted in Fig. 1.7: Three UAVs survey an area of interest by following elliptical flight paths at a velocity that results in the same period for each trajectory. The location of each aircraft along its trajectory at time t_0 is shown in the figure.

While performing this mission all aircraft must maintain communication links

between each other such that each aircraft can receive data from any other aircraft by means of single or multi hop communication while minimizing the transmission power to reduce energy expenditure and electromagnetic signature. The transmission power to establish a connection between any pair of aircraft is inversely proportional to a power of the Euclidean distance between these aircraft. An optimal communication topology in this case with respect to cumulative transmission power is a minimum spanning tree (MST) on the communication graph, where the UAVs correspond to the vertices of that graph and the weight of an edge of that graph is the distance between the two vertices covered by that edge. Specifically, this MST is an Euclidean minimum spanning tree (eMST), where the edge weight is the Euclidean distance between the vertices that are covered by that edge. The initial optimal communication topology is depicted by the dotted lines in the figure.

As the aircraft move during the mission their relative positions with respect to each other change. This results in changing weights of the edges of the communication graph over time. Thus, the following questions are raised: How robust is the optimal set of communication links and can the criticality of each individual communication link be assessed.

1.4 Technical Approach

The three single vehicle scenarios outlined above can be modeled as variants of the traveling salesman problem. This formulation allows for the analysis of mission planning comprised of tactical planning and path planning in the following manner:

- Given a set of locations of interest, feasible flight paths and their associated cost are computed for every location pair accounting for mission circumstances such as the capabilities of the aircraft and the environment.

- Given the cost of traveling between each location pair, a traveling salesman

problem is formulated and solved on an auxiliary weighted graph, where the vertices correspond to the locations of interest and the cost of an edge connecting two vertices is the cost of the flight path between the two corresponding locations of interest.

The results presented in this thesis are applicable to a wide variety of mission planning scenarios, path planning methods, and performance metrics that can be expressed as outlined above. This integrated approach to mission planning has for example been studied to minimize distance traveled in an obstacle rich environment using accurate path costs between pairs of locations for unmanned rotorcraft and unmanned fixed-wing aircraft [1, 7].

The problem stated in Section 1.2 can be specialized to this case of integrated path planning and tactical planning as follows:

Problem formulation 1.4.1 (Robustness of task schedules)**.** *Given the solution to an instance of a variant of the traveling salesman problem, find methods to assess the robustness and the optimality of the best tour such that the optimality of that tour can be ascertained with respect to changes in the problem data and the criticality of elements of the problem data can be computed.*

This thesis presents the exact and approximate analysis of stability regions and tolerances for an optimal solution to variants of the traveling salesman problem on a weighted graph. The edge cost tolerance is the supremum of cost increases of an edge (resp. infimum of cost decreases) under which the tour remains optimal, provided the other edge costs in the graph are unchanged. The stability region corresponding to a given tour is defined as the set of all edge cost perturbations for which that tour is optimal. It can therefore be understood as a robustness margin of an optimal solution. Additional stability information such as tolerances can be derived from the stability region. Criticality measures for elements of the problem data which are

dimensionless parameters are introduced. The higher the criticality of an element, the more susceptible the optimal tour to changes in that element. Exact stability regions can be obtained through application of sensitivity analysis to the relaxation of an integer linear programming (ILP) formulation of the TSP.

However, methods to obtain exact stability regions typically scale poorly with the size of the instance, as even checking whether an optimal TSP tour remains optimal after the cost of a single edge has been changed cannot be achieved in polynomial time unless $P = NP$ [8]. Hence, this thesis develops a general method to obtain over and under approximations of the stability region of an optimal solution to an instance of the TSP based on neighborhoods and relaxations. Using these results, specific methods based on the two neighborhood of an optimal tour and the minimum 1-tree (M1T) relaxation are shown. Approximate tolerances and criticalities can be computed from the approximate stability regions. Furthermore, stability regions for Euclidean traveling salesman problems (eTSP) with respect to perturbations to the vertex locations are derived. Finally, this thesis introduces the notion of safe radii for vertices.

The problem of choosing an optimal communication topology for a UAV mission can be modeled as a variant of the minimum spanning tree problem as follows, where tactical planning in this case corresponds to the choice of a communication topology:

- Given a set of aircraft and a region of interest, feasible flight paths are computed for each aircraft.

- Given the flight path for each vehicle, a minimum spanning tree problem is formulated on an auxiliary weighted graph, where the vertices correspond to the aircraft and the cost of an edge connecting two vertices at each instant in time quantifies the cost of communication between the two corresponding aircraft at that instant in time.

This problem can be understood as an instance of a minimum spanning tree problem on a weighted graph with potentially time-varying edge costs. Even in the initial computation phase it is therefore relevant to assess whether the initial communication topology is optimal for the entirety of the mission or if due to the time-varying costs of communication other topologies are better during the mission. The problem stated in Section 1.2 can be specialized for this case of integrated path planning and tactical planning:

Problem formulation 1.4.2 (Robustness of communication topologies)**.** *Given the solution to an instance of the minimum spanning tree problem, find methods to assess the robustness and the optimality of a minimum spanning tree such that the optimality of that tree can be ascertained with respect to changes in the problem data and the criticality of elements of the problem data can be computed.*

With regard to this problem, this thesis presents the analysis of stability regions for minimum spanning trees on a weighted graph and their application to communication networks for teams of UAVs. A polyhedral description of the stability region and derived stability metrics such as edge weight tolerances and stability balls are given. Finally, a small perturbation analysis yields an approximate stability region in the space of vertex location changes for eMSTs.

Analyzing the robustness of a given solution with respect to changing parameters can be done by exhaustively sampling the space of input parameters. However, solving the underlying optimization problem might be computationally expensive and the quality of the analysis depends on the chosen sampling density. This thesis presents multiple approaches to perform robustness analysis by obtaining the exact or approximate stability regions of an optimal solution. The stability region associated with an optimal solution is the set of all perturbations to the input parameters for which that solution remains optimal. This methodology differs from an alternative way to address uncertain data, where the uncertainty is modeled and stochastic optimiza-

tion techniques are used to find a solution that minimizes the expected value of the objective function. Stability analysis as presented in this thesis does not require any a priori knowledge of the nature of the uncertainty. Additional insight, such as criticality of elements of the input data as well as the smallest perturbation that causes a solution to become suboptimal can be derived.

1.5 Contributions

The contributions of this thesis are:

- The analysis of the stability region of solutions to classes of the TSP with respect to perturbations in the edge costs through a linear programming relaxation of an auxiliary problem is shown. A description and representation of the stability regions in half space representation are given. The problem of obtaining exact stability regions is shown to be intractable. The derivation of edge cost tolerances from the stability regions is demonstrated and edge criticalities are defined. Finally, for the special case of Euclidean TSPs, the derivation of approximate stability regions with respect to perturbations to vertex locations, safe radii, and vertex criticalities are given.

- Stability regions for optimal solutions to weighted-sum multi-objective TSPs in the space of weight changes with respect to a given set of tours are given. From the stability region, most critical weight perturbations are derived. Furthermore, stability regions for optimal solutions to wsmoTSPs in the space of edge cost changes with respect to each cost function are presented. Finally, linearized stability regions for optimal solutions to wsmoTSPs for simultaneous perturbations in the individual cost functions and weights are derived.

- Over and under approximations of the stability region of optimal solutions to symmetric non sequence-dependent TSP are given. Upper and lower bounds

on edge cost tolerances, approximate edge criticalities, approximate stability regions with respect to perturbations in vertex locations, safe radii and vertex criticalities are shown to be obtainable.

- An approach to sensitivity analysis of optimal communication topologies for teams of UAVs through the analysis of stability regions of minimum spanning trees and derived robustness measures.

Obtaining the stability region of an optimal solution has multiple benefits:

The stability region provides robustness margins with respect to simultaneous increases and decreases in any arbitrary set of edges. Analyzing the stability region of an optimal solution allows for evaluation of how robust a solution is to modeling errors and changing problem data. Modeling and data acquisition efforts should be directed towards elements of the problem data that have a small robustness margin.

Stability analysis can be used to determine whether a previously computed solution remains optimal among a set of feasible solutions after cost changes occur to an arbitrary number of edges by testing whether a perturbation is contained within the stability region of that solution.

Exploiting the notion of criticality of an element of the problem data, which is a dimensionless parameter, further insight can be gained. The higher the criticality of an edge, the more susceptible the optimal solution is to changes in the cost of that edge. It can therefore be used to identify most vulnerable edges in a problem instance.

Regarding the traveling salesman problem, the suggested computation methods are polynomial in time in the cardinality of the set of tours considered. Hence, obtaining exact stability information for large instances is intractable as it requires the enumeration of all possible tours. However, assuming expert knowledge, the set of tours could be designed and approved by an operator or for example obtained through the use of the k-opt heuristic.

By analyzing the stability region of an optimal solution to a wsmoTSP, the need for fine-tuning weights can be alleviated by ascertaining the range of weights for which that solution is optimal. Modeling and data acquisition efforts should be directed towards objective functions whose associated weights or cost vectors have a small robustness margin.

The benefit of developing tractable methods to obtain over and under approximations of the stability region is twofold. First, as obtaining exact stability regions is intractable for larger instances, the proposed methods allow for the approximate assessment of robustness margins of tours. Second, the approximate stability regions could for example be exploited when designing a supervisory control system for an agent that is executing a TSP tour or in the design of adaptive algorithms that re-optimize solutions after perturbations to the problem data occur.

In the development of under approximations of stability regions of traveling salesman tours, stability regions for minimum spanning trees and minimum 1-trees in half space representation are derived and characterized. These results are leveraged for the sensitivity analysis of solutions to the MST problem and its application to optimal communication topologies for teams of UAVs.

1.6 Organization

The remainder of this thesis is organized as follows. A literature survey relevant to mission planning problems for unmanned aircraft, stability analysis for combinatorial optimization problems, exact and approximate stability analysis of solutions to traveling salesman problems, and stability analysis for minimum spanning trees is provided in Chapter 2.

Chapter 3 formulates several relevant variants of the traveling salesman problem, minimum spanning tree problems, and gives definitions of the concepts used for

stability analysis throughout this thesis.

Methods to compute stability regions for the best tour in a set of tours for the symmetric TSP and the extension of these results to the asymmetric problem as well as their sequence-dependent counterparts are studied in Chapter 4. Additionally, results for the Euclidean TSP (eTSP) and wsmoTSP are derived and criticality measures for edges and vertices presented. The content of Chapter 4 is based on material presented in Refs. [9–13].

Chapter 5 derives a polyhedral description of stability regions of MSTs based on results in the literature. It follows the ideas outlined in the previous chapter in deriving stability measures from the stability regions such as tolerances, stability balls, and criticalities. Finally, following the approach in Chapter 4, this analysis is extended to eMST. The content of Chapter 5 is based on material published in Ref. [12].

As computing exact stability regions for optimal solutions to TSPs can become computationally intractable for large instances, Chapter 6 discusses computationally tractable methods to obtain over and under approximations of the stability regions of optimal solutions to symmetric non sequence-dependent TSPs. Upper and lower bounds on edge cost tolerances, approximate edge criticalities, approximate stability regions with respect to perturbations in vertex locations, safe radii and vertex criticalities are shown to be obtainable. The content of Chapter 6 is based on material published in Refs. [10, 13].

The results derived in this thesis are applicable to other combinatorial optimization problems such as sensor placement problems and runway scheduling problems. Chapter 7 outlines these applications that are detailed in Refs. [14–16].

A summary of the thesis and concluding remarks are provided in Chapter 8.

CHAPTER 2

Literature Survey

As discussed above, the problems being investigated touch upon multiple existing areas of study. Literature relevant to formulations of mission planning problems for unmanned aircraft, stability analysis for combinatorial optimization problems, and exact and approximate stability analysis of traveling salesman problems is now reviewed.

2.1 Traveling salesman problems

The traveling salesman problem is a combinatorial optimization problem and is a special case of the general routing problem [17]. Vehicle routing problems are usually stated either in terms of a set of required vertices on a graph that must be visited, or a set of required edges that must be traversed. The problem of visiting all vertices of a graph in minimum cost is the TSP.

2.1.1 Application to unmanned aircraft routing

The traveling salesman problem is often used as a prototypical example for many tactical planning problems for UAVs. Therefore, vehicle routing problems and traveling salesman problems have been studied extensively in the context of mission planning for unmanned aircraft. A wide variety of algorithms exist to solve traveling salesman

problems [18–25]. The problem of assigning and scheduling tasks for homogeneous teams of unmanned vehicles has been studied with a non-linear cost function [26], with a varying number of agents and dynamic tasks [27], as a patrolling problem with revisit deadlines [28], and as a patrolling and synchronization problem [29]. Multi-vehicle problems with heterogeneous teams have studied with static tasks [30] and dynamic tasks [31]. The problem of visiting neighborhoods rather than specific target locations is addressed for the single vehicle case [32] and for multiple vehicles [33].

Finally, an integrated approach to task and motion planning is presented in Ref. [34] that utilizes logical expressions to specify the tactical planning problem and a randomized tree search algorithm for motion planning to solve the mission planning problem in an integrated way. A problem that has received particular attention in the context of integrated mission planning is the Dubins traveling salesman problem, i.e., a variant of the traveling salesman problem in which the paths must be feasible for a Dubins vehicle [35]. The Dubins vehicle, i.e., a vehicle that can either travel in a straight line or turn with a given fixed turn radius, is often used to model the movement of a fixed-wing aircraft in the horizontal plane [36, 37]. Therefore, a common way to approach the problem of integrated task and motion planning for UAVs is to treat it as an instance of the Dubins TSP [38–40]. A two-layered approach that combines a heuristic approach to solving instances of TSPs with fast multi-query path planning algorithms has been suggested for task scheduling and motion planning for unmanned aircraft in obstacle rich 3D environments [1, 7].

Finally, this survey discusses multiple instances of UAV mission planning problems that can be cast as vehicle routing problems [41].

2.1.2 Sequence-dependent traveling salesman problems

In sequence-dependent traveling salesman problems, the cost of edge traversal depends on the sequence of vertices visited before traversing that edge. As motivated in

Chapter 1, this framework, among others, allows for the formulation of sequence-based loading constraints. Sequence-based loading ensures that no consignment is placed in such a way that it blocks the removal of items to be delivered earlier on the route [42, 43] and is sometimes referred to as a last-in-first-out constraint. The survey in Ref. [2] discusses additional publications relevant to this problem of which almost 60% were published after 2009. The specific case of a cargo aircraft routing problem subject to loading precedence constraints is discussed in Ref. [44].

2.1.3 Multi-objective traveling salesman problems

Multi-objective formulations of planning problems for unmanned aircraft reflect the fact that in many real world problems multiple, if not even competing, objectives exist. For example, in a monitoring mission one might seek to maximize the area covered while minimizing fuel consumption. The problem of multi-objective path planning for unmanned aircraft has been addressed using different solution approaches such as weighted-sums [4, 45] and a hierarchical decomposition framework [46]. One approach to solve multi-objective TSPs in the context of mission planning for UAVs is to task a human operator to interactively determine the preferences for multiple objectives [47]. The survey in Ref. [48] provides insight into recent developments in the area of multi-objective vehicle routing. Different types of multi-objective combinatorial optimization problems, their formulation, and methods of solving them are discussed in Ref. [5].

2.1.4 Time-varying traveling salesman problems

The above discussion suggests that the TSP and its variants have been widely studied and applied to capture real world problems. It is of interest to researchers and practitioners in the field. A great variety of methods exits to solve instances. Recently, the question of information quality and evolution of information in vehicle routing

problems arose [49].

Generally, two versions of time varying instances are considered. Traditionally, more attention has been directed towards problems, in which vertices are added and removed from the graph, for example to model the problem of a service vehicle that needs to service stochastic demands [31, 50].

This thesis focuses on instances where the traversal costs of edges are changing. Vehicle routing problems with stochastic edge costs have been investigated [51–53]. However, uncertainty in this type of problem is typically modeled as random processes and stochastic optimization techniques are employed to minimize the expected value of the objective function. This requires a priori knowledge of the nature of the random processes and does not account for cases where once the random variables are realized a better solution exists. Uncertain multi-objective traveling salesman problems have been formulated and solved in a similar fashion [54].

Simulation studies suggest that re-optimizing tours for time-varying instances of the TSP based on real-time traffic data can lead to shorter tours [55]. A stochastic variant of a TSP in which the salesman is allowed to observe outgoing edge realizations at each vertex before deciding what place to visit next is introduced in this context [56]. Finally, Ref. [57] provides a survey on recent developments in the area of dynamic vehicle routing, where routes are re-computed to adapt to changing problem data. In a setting where travel costs change with time, it is therefore of interest to study the properties of optimal solutions with respect to varying problem data to assess their optimality given a specific realization of the perturbations. Furthermore, this type of analysis allows for the assessment of robustness margins with respect to arbitrary changes in the problem data without making assumptions about perturbations.

2.2 Minimum spanning tree problems

The use of multiple UAVs to jointly perform a mission has been widely studied in the literature [58–61]. These missions typically require a level of communication between the UAVs to coordinate their execution. Furthermore, the specific use of UAVs to establish mobile ad-hoc communication networks has been suggested and different topology models and information routing approaches have been studied [62]. Minimum spanning trees [63,64] are frequently used methods to establish and optimize communication networks for mobile agents such as UAVs. Furthermore, MST have also been suggested as an optimal communication topology for commercial manned aircraft [65].

2.3 Sensitivity analysis of solutions to combinatorial optimization problems

Both the traveling salesman problem and the minimum spanning tree problem are combinatorial optimization problems. Sensitivity analysis for solutions to combinatorial optimization problems is concerned with the robustness of solutions to combinatorial optimization problems with respect to changes in the problem data. Combinatorial optimization problems are often formulated as integer problems and integer programming models, unlike linear programs, generally behave in an unstable and unpredictable manner under small changes in the initial data [6,66]. Therefore, sensitivity analysis for combinatorial optimization has been the subject of a growing body of literature. The purpose of sensitivity analysis is to determine how the optimality of a given optimal solution depends on the input data. Sensitivity analysis is a well-established topic in linear programming [67] and mixed integer programming [68]. Sensitivity analysis questions can be formulated in different ways. The approach

taken in thesis is typically referred to as posterior analysis [69]:

An optimal solution $x^\star$ is known for some nominal cost vector c^0. The question is then to determine the stability of $x^\star$ with respect to variations around c^0. Some common notions of stability are:

- The upper and lower tolerance of c_w at c^0, i.e., the supremum of cost increases of a cost vector entry c_w (resp. infimum of cost decreases) under which $x^\star$ remains optimal, provided all other cost vector entries remain unchanged.

- The stability region of $x^\star$ at c^0, i.e., the set of all perturbations Δc to c^0 under which $x^\star$ remains optimal.

- The stability radius of $x^\star$ at c^0, i.e., the radius of the largest ball B such that $x^\star$ remains optimal for all $\Delta c \in B$.

Computational issues of upper and lower tolerances in the context of sensitivity analysis in combinatorial optimization are discussed in Refs. [70–72]. Stability radii for optimal solutions to combinatorial optimization problems and easier to compute bounds are addressed in Ref. [73]. Recently, further progress in the theory of tolerances has been reached [74] and the theory of tolerances is extended from single tolerances to set tolerances in Ref. [75]. Finally, the annotated bibliography [68] and the more recent survey [69] provide an overview of the literature and the different approaches and notions of stability analysis for combinatorial optimization problems. The computational complexity of sensitivity analysis for combinatorial optimization problems depends on the problem at hand. For example, efficient algorithms to compute the edge weight tolerances for the MST problem are developed in Refs. [76–78]. Ref. [77] gives necessary and sufficient conditions on the weights of all graph edges for the optimality of a spanning tree.

2.3.1 Exact stability analysis for the TSP

The traveling salesman problem is a NP–hard combinatorial optimization problem. Several results exist indicating that analyzing the sensitivity of NP–hard problems is itself hard [69]. Specifically, several hardness results for 0/1 problems with linear objective function are proven in Ref. [8]. Computing the exact values of the tolerances for all edges in a TSP is NP–hard and can be achieved by solving auxiliary instances of the problem [79]. Furthermore, the topology of stability regions and subsets thereof are described in Ref. [79]. Edge cost tolerances are well defined with respect to the problem instance, i.e., the tolerances do not depend on the chosen optimal tour if multiple tours of similarly optimal cost exist. Furthermore, it is shown in Ref. [80] that the exact tolerance for every edge in case of additive cost functions can be computed by solving two instances of the TSP for each edge. However, the computation of tolerances and stability regions for the purpose of assessing the properties of solutions in the context of, for example, time-varying problems has not yet been a focus of the existing research. Regarding weighted-sum multi-objective formulations, a related notion to that of a stability region for perturbations to the weights is introduced in Ref. [81] for weighted-sum multi-objective linear programming, where percentage deviations from weights are considered. Criticality of elements in the problem data for weighted-sum multi-objective linear programs is discussed in Ref. [82]. To the best of the author's knowledge, stability of solutions to weighted-sum multi-objective traveling salesman problems has not yet been addressed in the literature.

2.3.2 Approximate stability analysis for the TSP

One method to obtain stability regions for solutions to traveling salesman problems relies on the enumeration of the set of all tours. This method does therefore not scale well with the cardinality of the set of vertices. One way to address this issue requires the pre-selection of a subset of tours with respect to which exact stability

regions are obtainable [9]. This can be of interest in real world applications where an expert a priori identifies and approves tours of interest. However, literature on systematically obtaining approximate stability regions is scarce and even determining an ϵ-approximation of the tolerances is NP–hard [79]. Exact edge cost tolerances for some and lower bounds on the edge cost tolerance for all other edges can be obtained by analyzing a set of k-best tours [83]. However, the k-best TSP problem itself is NP–hard and the quality of the approximation depends on the cardinality of the set of best tours and the instance of the problem. In Ref. [84], it is argued that the 1-tree relaxation of the TSP gives lower bounds of the tolerances for the TSP. These results on lower bounds are extended in Ref. [79]. Sensitivity information based on a 1-tree relaxation is used to improve the efficiency of an implementation of the Lin-Kernighan (LK) heuristic [18], which is an improvement heuristic for the TSP [85]. It employs two or three pairwise edge exchanges and is one of the most successful methods for generating near optimal solutions for the symmetric TSP. Ref. [86] analyzes the sensitivity of the LK heuristic and derives the tolerances of a tour with respect to pairwise edge exchanges to improve the LK heuristic.

2.4 Research directions

As the above discussion indicates, both the traveling salesman problem and the minimum spanning tree problem have been studied extensively in the literature and are often used to formulate UAV mission planning problems. Furthermore, theory regarding stability of solutions of combinatorial optimization problems and specifically theory regarding stability regions and tolerances for the symmetric non sequence-dependent TSPs is available. Also, sensitivity results for the minimum spanning tree problem are available. Based on this review, the following research directions have been identified and are addressed by the contributions listed in Section 1.5:

- **Stability of variants of traveling salesman problems:** While literature on stability analysis for symmetric non sequence-dependent TSP with respect to perturbations to the edge costs exists, other variants of the traveling salesman problem are more suitable to model certain type of UAV mission planning problems. This thesis therefore analyzes the stability of solutions to other variants of the traveling salesman problems such as sequence-dependent problems, Euclidean TSPs and perturbations to vertex locations rather than in the edge weights, and multi-objective formulations.

- **Robustness measures:** While stability regions and tolerances allow for a quantitative assessment of the robustness of a given solution, a qualitative assessment by, for example, a human operator might be difficult. This thesis presents several robustness measures such as safe radii and edge and vertex criticalities that ease the interpretation of the stability results by a human operator and allow for the identification of the most critical elements of a mission.

- **Approximate stability regions for TSPs:** The problem of obtaining under and over approximations of edge cost tolerances has been addressed in the literature. However, the problem of systematically obtaining tractable under and over approximations of stability regions has not been addressed. Approximate stability regions allow for robustness analysis with respect to a wider range of perturbations and tolerances can be easily computed once the stability region is known. Furthermore, a wider range of stability measures can be derived from stability regions than from tolerances alone.

- **Robustness of communication topologies:** MSTs have been identified as a feasible communication topology for multi-UAV missions. While sensitivity results for MSTs are readily available, this thesis focuses on the polyhedral description of stability regions and subsets thereof to study properties of MSTs

on graphs with time varying edge costs due to relative motion of the members of a team of UAVs.

CHAPTER 3

Preliminaries

This chapter formally defines the variants of the traveling salesman problem treated in this thesis. Furthermore, the concept of stability regions for solutions to traveling salesman problems is defined. Finally, the minimum spanning tree problem is formally introduced.

3.1 Traveling salesman problems

3.1.1 Variants of the traveling salesman problem

Let $G(V, E)$ be a graph with vertices V and edges E. The symmetric non sequence-dependent TSP (snTSP) on a fully connected undirected graph can be stated as follows:

Problem formulation 3.1.1 (snTSP)**.** *Given a fully connected undirected graph $G(V, E)$ with n vertices $\{v_1, \cdots, v_n\}$ and a symmetric edge cost matrix C, where c_{ij} denotes the cost of traveling from vertex v_i to vertex v_j on edge e_{ij}, find the* Hamiltonian *tour (*tour for short*) T^* in the set of all tours $\mathcal{T}$, where $T^*(m)$ denotes the vertex visited at the m-th step, such that $L(T^*) = \sum_{m=1}^{n} c_{T^*(m-1),T^*(m)}$ is minimal.*

The symmetric non sequence-dependent Euclidean TSP (eTSP) can then be stated as follows:

Problem formulation 3.1.2 (eTSP)**.** *Given a fully connected undirected graph* $G(V, E)$ *with* n *vertices* $\{v_1, \cdots, v_n\}$ *and a symmetric edge cost matrix* C*, where* c_{ij} *is the Euclidean distance between vertex* v_i *and vertex* v_j*, find the* Hamiltonian *tour (*tour for short*)* $T^\star$ *in the set of all tours* $\mathcal{T}$*, where* $T^\star(m)$ *denotes the vertex visited at the* m*-th step, such that* $L(T^\star) = \sum_{m=1}^{n} c_{T^\star(m-1),T^\star(m)}$ *is minimal.*

The asymmetric non sequence-dependent TSP (anTSP) on a fully connected graph can be stated as follows:

Problem formulation 3.1.3 (anTSP)**.** *Given a fully connected graph* $G(V, E)$ *with* n *vertices* $\{v_1, \cdots, v_n\}$ *and an edge cost matrix* C*, where* c_{ij} *denotes the cost of traveling from vertex* v_i *to vertex* v_j *on edge* e_{ij}*, find the tour* T^* *in the set of all tours* $\mathcal{T}$*, where* $T^*(m)$ *denotes the vertex visited at the* m*-th step, such that* $L(T^*) = \sum_{m=1}^{n} c_{T^*(m-1),T^*(m)}$ *is minimal.*

The weighted-sum multi-objective TSP (wsmoTSP) on a fully connected undirected graph can be stated as follows:

Problem formulation 3.1.4 (wsmoTSP)**.** *Given a fully connected undirected graph* $G(V, E)$*, a set of* t *symmetric edge cost matrices* U_k*, where* $u_{k,ij}$ *denotes the cost of traveling from vertex* v_i *to vertex* v_j *on edge* e_{ij} *with respect to the* k*-th cost matrix, and a set of non-negative weights* λ_k *such that* $\sum_{k=1}^{t} \lambda_k = 1$*, find the Hamiltonian tour* T^* *in the set of all tours* $\mathcal{T}$*, where* $T^*(m)$ *denotes the vertex visited at the* m*-th step, such that* $L(T^*) = \sum_{m=1}^{n} \sum_{k=1}^{t} \lambda_k u_{k,T^*(m-1),T^*(m)}$ *is minimal.*

This formulation is general enough to allow for different objective functions, such as distance traveled, minimum radar exposure, and minimum communication interference, as will be described in Section 4.7.3.

The symmetric sequence-dependent TSP (ssTSP) on a fully connected graph can then be stated as follows:

Problem formulation 3.1.5 (ssTSP)**.** *Let V be a set of n vertices $\{v_1, \ldots, v_n\}$. Let Q be a queue of vertices of fixed length $1 \leq \mu \leq n$ that operates in a "first in first out manner". The initial location of the agent is inserted into the queue at position $Q(1)$ while all other entries in Q are empty. When the agent moves to the next vertex, that vertex is inserted into the queue at position $Q(1)$ while the element previously at $Q(\mu)$ leaves the queue. Let v_j not belong to the queue and let v_i belong to the queue at location $Q(1)$, then $c_{ij}(Q)$ denotes the cost of traveling from v_i to v_j and $c_{ij}(Q) = c_{ji}(Q)$. Let T be a tour, such that $T(m)$ denotes the vertex visited at the m-th step of that tour and Q_m denotes the state of the queue at that step, i.e., the sequence of μ vertices in the queue. Find the tour $T^\star$ in the set of all tours $\mathcal{T}$, such that the cost associated with that tour, $L(T^*) = \sum_{m=1}^{n} c_{T^*(m-1),T^*(m)}(Q_m)$, is minimal.*

The asymmetric sequence-dependent TSP (asTSP) on a fully connected graph can then be stated as follows:

Problem formulation 3.1.6 (asTSP)**.** *Let V be a set of n vertices $\{v_1, \ldots, v_n\}$. Let Q be a queue of vertices of fixed length $1 \leq \mu \leq n$ that operates in a "first in first out manner". The initial location of the agent is inserted into the queue at position $Q(1)$ while all other entries in Q are empty. When the agent moves to the next vertex, that vertex is inserted into the queue at position $Q(1)$ while the element previously at $Q(\mu)$ leaves the queue. Let v_j not belong to the queue and let v_i belong to the queue at location $Q(1)$, then $c_{ij}(Q)$ denotes the cost of traveling from v_i to v_j. Let T be a tour, such that $T(m)$ denotes the vertex visited at the m-th step of that tour and Q_m denotes the state of the queue at that step, i.e., the sequence of μ vertices in the queue. Find the tour $T^\star$ in the set of all tours $\mathcal{T}$, such that the cost associated with that tour, $L(T^*) = \sum_{m=1}^{n} c_{T^*(m-1),T^*(m)}(Q_m)$, is minimal.*

Hence, for $\mu = 1$ the anTSP is recovered, while for $\mu = n$ the cost of returning to the initial location and completing the tour depends on the complete sequence of n vertices visited previously.

3.1.2 TSP stability analysis

First, edge cost tolerances and stability regions are defined for the non sequence-dependent variants of the traveling salesman problem. These two related concepts are defined as follows, where potential additive disturbances to the costs motivate stability analysis:

Definition 3.1.7 (Tolerance TSP)**.** *The additive upper tolerance Δc_{ij}^{+} (resp. lower tolerance Δc_{ij}^{-}) with respect to $T^{\star}$ is the supremum of cost increases of e_{ij} (resp. infimum of cost decreases of e_{ij}) under which $T^{\star}$ remains optimal, provided the other elements of C are unchanged.*

This definition generalizes to the case of sequence-dependent traveling salesman problems.

Definition 3.1.8 (Sequence-dependent TSP tolerance)**.** *Let $T^{\star}$ be an optimal tour and let v_j not belong to the queue Q and let v_i belong to the queue at location $Q(1)$, then $c_{ij}(Q)$ denotes the cost of traveling from v_i to v_j. The additive upper tolerance $\Delta c_{ij}(Q)^{+}$ (resp. lower tolerance $\Delta c_{ij}(Q)^{-}$) of e_{ij} with respect to $T^{\star}$ is the supremum of cost increases of $c_{ij}(Q)$ (resp. infimum of cost decreases of $c_{ij}(Q)$) under which $T^{\star}$ remains optimal, provided the other edge costs are unchanged.*

Finally:

Definition 3.1.9 (Stability region TSP)**.** *The stability region $\mathbf{\Delta}(T^{\star})$ corresponding to an optimal tour $T^{\star}$ for the traveling salesman problem is defined as the set of all edge cost changes for which that tour is optimal.*

Given an edge cost perturbation ΔC, the length $L(T)$ of a given tour T changes to $L(T(\Delta C))$. Hence, ΔC is not contained in the stability region $\mathbf{\Delta}(T^{\star})$ of $T^{\star}$ if there exists another tour in the set of all tours $\mathcal{T}$ on the graph $G(V, E)$ that is shorter.

Hence, the stability region of an optimal tour $T^\star$ to an instance can be expressed with respect to perturbations ΔC to the cost matrix C:

$$\forall \Delta C \in \mathbf{\Delta}(T^\star), \forall T' \in \mathcal{T} : L(T^\star(\Delta C)) \leq L(T'(\Delta C)). \tag{3.1}$$

3.2 Minimum spanning tree problems

3.2.1 Variants of the spanning tree problem

Problem formulation 3.2.1 (ST Problem)**.** *Given a fully connected undirected graph $G(V, E)$ with n vertices $\{v_1, \cdots, v_n\}$, find a subgraph that includes all of the vertices V of G that is a tree. This tree is a spanning tree ST of G.*

Hence, given a weighted graph, a minimum spanning tree can be defined:

Problem formulation 3.2.2 (MST Problem)**.** *Given a fully connected undirected graph $G(V, E)$ with n vertices $\{v_1, \cdots, v_n\}$ for which each edge $e_{ij} \in E$ has an associated edge cost $c_{ij} \in \mathbb{R}$, find a spanning tree of minimum total edge cost. This tree is a minimum spanning tree MST of G.*

Problem formulation 3.2.3 (eMST Problem)**.** *Given a fully connected undirected graph $G(V, E)$ with n vertices $\{v_1, \cdots, v_n\}$ and a symmetric edge cost matrix C, where c_{ij} is the Euclidean distance between vertex v_i and vertex v_j, find a spanning tree of minimum total edge cost. This tree is a Euclidean minimum spanning tree $eMST$.*

3.2.2 MST stability analysis

Reminiscent of the definitions of edge cost tolerances and the stability region for an optimal traveling salesman tour, edge cost tolerances and the stability region for a minimum spanning tree can be defined:

Definition 3.2.4 (Tolerance MST)**.** *The edge cost tolerance with respect to a MST is the supremum of cost increases of an edge (resp. infimum of cost decreases) under which that MST remains optimal, provided the other edge costs in the graph are unchanged.*

Definition 3.2.5 (Stability region)**.** *The stability region* $\mathbf{\Delta}(MST)$ *corresponding to a minimum spanning tree is defined as the set of all edge cost changes for which that tree is a minimum spanning tree.*

CHAPTER 4

Stability analysis for the traveling salesman problem

This chapter presents the exact stability analysis for solutions to non sequence-dependent traveling salesman problems and sequence-dependent traveling salesman problems with respect to perturbations in the edge costs. A description and the representation of the stability regions in half space representation are given. The derivation of edge cost tolerances from the stability regions is demonstrated and edge criticalities are defined. Furthermore, for non sequence-dependent eTSPs approximate stability regions with respect to perturbations in vertex locations, safe radii, and vertex criticalities are derived. Finally, stability regions for optimal solutions to non sequence-dependent wsmoTSPs in the space of weight changes with respect to a given set of tours are given.

4.1 Problem formulation

The underlying problem in this chapter can be formulated as follows: Given a set of tours $\mathcal{T}$ for an instance of the TSP and letting $T^\star$ denote the best tour within $\mathcal{T}$, define the stability region of $T^\star$ with respect to $\mathcal{T}$ and determine an expression to test whether arbitrary disturbances cause another tour in $\mathcal{T}$ to be better than $T^\star$.

To solve this problem, methods for the symmetric non sequence-dependent TSP

are presented first and then generalized to the asymmetric sequence-dependent TSP.

4.2 Symmetric single objective TSPs

Solving the TSP can be understood as choosing the shortest tour $T^\star$ from the set of all possible tours for an instance of the TSP. In this section, only symmetric non sequence-dependent TSPs are considered. This class of TSP is formally stated in Problem Formulation 3.1.1. For an edge $e_{ij} = e_{ji}$, the cost of traveling along that edge is $c_{ij} = c_{ji}$. Note that edges e_{ii} are not included in the set of all edges E, hence $|E| = \frac{n(n-1)}{2}$. Then, let $c \in \mathbb{R}^{|E|}$ be a column vector containing all edge costs in lexicographical ordering. Hence, the index of a vector element c_w is related to edge $e_{ij} = e_{ji}$ for all $i \neq j$ and $i < j$ by the following relationship:

$$w = n(i-1) - \frac{(i-1)i}{2} + j - i. \tag{4.1}$$

All cases where $i > j$ can be treated using (4.1) by exploiting the symmetry of the problem. For clarity of presentation entries of the edge cost vector c are denoted by either their single index w as c_w or by the tuple of indices $\{ij\}$ as c_{ij} where appropriate, and w is related to $\{ij\}$ through (4.1).

To facilitate the study of stability with respect to changes to the edge costs, let Δc be a vector of perturbations in the edge costs defined in a similar fashion. The length $L(T)$ of a given tour T changes to $L(T(\Delta c))$ if the edge costs are perturbed by Δc. Hence, a vector Δc is not contained in the stability region $\mathbf{\Delta}(T^\star)$ of $T^\star$ if there exists another tour in the set of all tours $\mathcal{T}$, i.e., Hamiltonian cycles on the graph $G(V, E)$, that is shorter. Hence, the stability region of an optimal tour $T^\star$ to an instance can be expressed with respect to perturbations Δc to the cost vector c:

$$\forall \Delta c \in \mathbf{\Delta}(T^\star), \forall T' \in \mathcal{T} : L(T^\star(\Delta c)) \leq L(T'(\Delta c)). \tag{4.2}$$

Furthermore, the tours in the set of all possible tours are enumerated and a subset of tours $\mathcal{T}$ with an induced enumeration is defined, i.e., the r-th element in $\mathcal{T}$ is the r-th element found when searching for elements of $\mathcal{T}$ in the set of all possible tours.

Definition 4.2.1 (x)**.** *Let x be a column vector and let its dimension be the cardinality of $\mathcal{T}$. Then for each element in $\mathcal{T}$ there exists a vector x that is associated with it in the following way: All entries in x are binary and $\sum_{r=1}^{|\mathcal{T}|} |x_r| = 1$. Thus, there exists only one non-zero entry x_r at position r. The position r of the non-zero entry x_r then associates x with tour T_r.*

Definition 4.2.2 (h)**.** *Let h be a column vector of length $|E|$. A vector h then identifies the edges $e_{ij} \in T$ in the following way: For all edges $e_{ij} \in T$, the corresponding entry h_w, where w is computed using (4.1), is one. All other entries are zero.*

Definition 4.2.3 (H)**.** *Let H be a matrix of the following form: The r-th row of H is vector h_r^T, which identifies the edges contained in tour $T_r \in \mathcal{T}$.*

Then, the problem of finding the best tour in $\mathcal{T}$ can be formulated as follows:

$$\begin{aligned} \underset{x}{\text{minimize}} \quad & c^T H^T x \\ \text{subject to} \quad & \sum_{r=1}^{|\mathcal{T}|} x_r = 1 \\ & x_r \geq 0,\ r = 1, \ldots, |\mathcal{T}|, \\ & x_r \in \mathbb{Z},\ r = 1, \ldots, |\mathcal{T}|. \end{aligned} \tag{4.3}$$

This formulation is different from the classical ILP formulation of the TSP as for example given in Ref. [87] by constraining and explicitly enumerating the set of candidate tours $\mathcal{T}$. Let $q = Hc$ and substitute in (4.3). Then, the cost coefficients q_r are linear combinations of the elements of the edge cost vector c, where q_r represents the cost of the corresponding tour T_r. This yields the problem in canonical form with a single equality constraint:

$$
\begin{aligned}
\underset{x}{\text{minimize}} \quad & q^T x \\
\text{subject to} \quad & \overrightarrow{1} x = 1 \\
& x_r \geq 0,\ r = 1, \ldots, |\mathcal{T}|, \\
& x_r \in \mathbb{Z},\ r = 1, \ldots, |\mathcal{T}|,
\end{aligned}
\tag{4.4}
$$

where $\overrightarrow{1}$ is a row vector of ones of appropriate length.

Proposition 1. *Every solution x of the optimization problem* (4.4) *identifies a cheapest tour in $\mathcal{T}$ through the scheme given in Definition 4.2.1. Conversely, every cheapest tour $T^\star$ in $\mathcal{T}$ is associated with a solution of optimization problem* (4.4) *through the same scheme.*

Proof. Sufficiency: Let x be a solution of optimization problem (4.4), then x identifies a tour through the scheme in Definition 4.2.1. That tour is a cheapest tour. To prove that claim let us assume that another tour is strictly cheaper. Then, that tour is associated with another x and that other x gives a strictly better cost in optimization problem (4.4) because that other tour is strictly cheaper. Therefore, x cannot be a solution of optimization problem (4.4). This contradiction completes the proof of sufficiency.

Necessity: Let $T^\star$ be a cheapest tour in $\mathcal{T}$. This tour is associated with an x through the scheme of Definition 4.2.1. That x is a solution to optimization problem (4.4). To prove that claim, let us assume that there is another x that gives a strictly lower cost. Then, that other x is associated with another tour that is strictly cheaper than $T^\star$. Therefore, $T^\star$ cannot be a cheapest tour. This contradiction completes the proof. □

4.2.1 LP relaxation of the 0-1 ILP formulation

The computational complexity of computing tolerances for a large class of 0-1 programming and combinatorial optimization problems (including the TSP) is known to be as hard as the optimization problem itself [8]. However, given two conditions, the optimal solution to the linear programming (LP) relaxation of an ILP is guaranteed to optimally solve the ILP [87]. These conditions are that the constraint matrix of the ILP is totally unimodular, and that the right hand side of the constraint is integer [87].

Definition 4.2.4 (Totally unimodular)**.** *An integer matrix $A \in \mathbb{Z}^{m \times n}$ is totally unimodular if each square submatrix S of A has $det(S) \in \{0, \pm 1\}$.*

Equation (4.4) satisfies these two conditions. Therefore, stability analysis is applied to the linear programming relaxation of optimization problem (4.4):

$$\begin{aligned} \underset{x}{\text{minimize}} \quad & q^T x \\ \text{subject to} \quad & \vec{1} x = 1 \\ & x_r \geq 0, \ r = 1, \ldots, |\mathcal{T}|, \\ & x_r \in \mathbb{R}, \ r = 1, \ldots, |\mathcal{T}|. \end{aligned} \tag{4.5}$$

Note that the search space of optimization problem (4.4) is a subset of the search space of optimization problem (4.5). Therefore, optimization problem (4.5) is a relaxation of optimization problem (4.4).

Theorem 4.2.5 ([87])**.** *Let A be a totally unimodular matrix and let b be an integral vector. Then the polyhedron $P := \{x | Ax \leq b\}$ is integral.*

Theorem 4.2.6 ([88])**.** *Given a linear program in standard form where A is an $m \times n$ matrix of rank m, i) if there is a feasible solution, there is a basic feasible solution, ii) if there is an optimal feasible solution, there is an optimal basic feasible solution.*

Theorems 4.2.5 and 4.2.6 guarantee that the optimal solution to optimization problem (4.5) solves optimization problem (4.4).

The following lemma establishes the converse.

Lemma 4.2.7. *Every optimal solution to problem* (4.4) *is an optimal solution to problem* (4.5).

Proof. Let x be an optimal solution to problem (4.4). Then x is feasible for problem (4.5), because problem (4.5) is a relaxation of problem (4.4). Assume x is not optimal for problem (4.5), then there exists an $\hat{x}$ that is feasible for problem (4.5) and strictly better than x. Theorem 4.2.6 guarantees that the optimal solution of problem (4.5) happens at a vertex. Therefore, there must exist a vertex $\overline{x}$ that is better than $\hat{x}$. That vertex $\overline{x}$ is feasible for problem (4.4), because it is a vertex, and is strictly better than x, because it is better than $\hat{x}$, which was itself strictly better than x. Therefore, x cannot be an optimal solution of problem (4.4). This contradiction completes the proof. □

4.2.2 Stability region based on $\mathcal{T}$

The LP relaxation (4.5) is in canonical form. Therefore, the stability region of the solution $x^\star$ to optimization problem (4.5) can be computed using the method given in Ref. [67] for linear programs.

When there exist alternative optimal solutions to this problem, then there exists a set of optimal solutions in $\mathcal{T}$ with cardinality greater than one. This chapter is not concerned with solving (4.4), but with analyzing the stability of one optimal tour $T^\star$ that is associated with one x through the scheme in Definition 4.2.1. That tour could either be given by a human operator or, for example, obtained through the use of the k-opt heuristic. The stability region of that tour can be computed based on the LP relaxation.

Let there be a disturbance to cost vector c characterizing the specific instance of the TSP, which results in an additive disturbance edge cost vector Δc. This affects the objective function coefficients q as follows:

$$\Delta q = H \Delta c. \tag{4.6}$$

This equation establishes the relationship between perturbations to the cost vector c of optimization problem (4.3) and perturbations to the vector of objective function coefficients of optimization problem (4.5). Then, to analyze stability, the reduced cost vector $\overline{q}$ for optimization problem (4.5) is utilized [67]:

$$\overline{q} = \overrightarrow{1}^{T} q_r - q, \tag{4.7}$$

where q_r is the unperturbed objective function coefficient, i.e., the r-th entry in q, and r is the position of the non-zero entry of the optimal solution vector $x^\star$. Let H_r denote the row of H, where r is defined likewise. Then, let:

$$\overline{H} = \overrightarrow{1}^{T} H_r - H. \tag{4.8}$$

In order to maintain $x^\star$ as optimal solution to optimization problem (4.5), it is necessary and sufficient for the perturbation vector Δc to satisfy inequality [67]:

$$\overline{H} \Delta c \leq -\overline{q}. \tag{4.9}$$

In other words: By design of the equality constraint and from the fact that the solutions of interest are 0-1 integer feasible: For any chosen optimal solution, $\overline{H}$ has the following structure: The row corresponding to the optimal solution is all zeros. The other rows of $\overline{H}$ are structured as follows:

- Entries corresponding to edges that are contained in the chosen optimal tour

and in the tour corresponding to the specific row are zero.

- Entries corresponding to edges that are contained in the chosen optimal tour but not in the tour corresponding to the specific row are 1.

- Entries corresponding to edges that are not contained in the chosen optimal tour but in the tour corresponding to the specific row are -1.

Thus, the number of -1 and $+1$ within one row is always identical, as for every removed edge from a tour, another edge must be added.

This gives the following: Note that, as per Theorems 4.2.5 and 4.2.6, every optimal solution to problem (4.5) is an optimal solution to problem (4.4).

Proposition 2. *The stability region of every optimal integral solution to problem* (4.5) *is equal to the stability region of that solution as an optimal solution to problem* (4.4)*.*

Proof. Sufficiency: Let x be an integral optimal solution to problem (4.5). Then by Theorems 4.2.5 and 4.2.6, x is also an optimal solution to problem (4.4). Let Δc be an arbitrary perturbation to the data of problem (4.5) in the stability region of x, then x is an optimal integral solution of problem (4.5) perturbed by Δc. By Theorems 4.2.5 and 4.2.6, x also solves the perturbed version of problem (4.4). Therefore, Δc belongs to the stability region of x as an optimal solution to problem (4.4). Therefore, the stability region of x as an optimal solution to problem (4.5) is a subset of the stability region of x as an optimal solution to problem (4.4). This completes the sufficiency part of the proof.

Necessity: Let x be an optimal solution to problem (4.4). Then by Lemma 4.2.7, x is also an optimal solution to problem (4.5). Let Δc be an arbitrary perturbation to the data of problem (4.4) in the stability region of x, then x is an optimal solution of problem (4.4) perturbed by Δc. By Lemma 4.2.7, x also solves the perturbed version of problem (4.5). Therefore, Δc belongs to the stability region of x as a

solution to problem (4.5). Therefore, the stability region of x as an optimal solution to problem (4.4) is a subset of the stability region of x as an optimal solution to problem (4.5). This completes the proof. □

Inequality (4.9) therefore defines the stability region of the optimal solution $x^\star$ and its associated optimal tour $T^\star$, such that for any edge cost perturbation vector Δc that satisfies (4.9), $T^\star$ remains the optimal tour in $\mathcal{T}$. Hence, evaluating (4.9) gives a polynomial time method to determine whether an optimal tour $T^\star$ remains optimal in $\mathcal{T}$ after a cost change Δc occurs. Note that (4.9) describes a polyhedron in the space of cost changes.

4.2.3 Edge cost tolerances

Using (4.9), the edge cost tolerances with respect to $\mathcal{T}$ can be computed as follows: To compute the tolerance for an arbitrary edge $e_{ij} \in T$, where $T \in \mathcal{T}$, with associated edge cost vector entry c_w, set $\Delta c_k = 0$ for all $k \neq w$. This immediately yields the tolerance Δc_w by identifying the most restrictive inequality resulting by row-wise evaluation of (4.9). Note, that for any edge e_{ij}, only the upper tolerance Δc_{ij}^+ or the lower tolerance Δc_{ij}^- is finite. Both tolerances can never be finite at the same time [84]. Intuitively, if an edge is in the best tour, decreasing the cost of that edge decreases the cost of all tours that utilize that edge by the same amount. Hence, the original best tour remains the best. Similarly, if an edge is not part of the optimal tour and the cost of that edge increases, the cost of all tours utilizing that edge increases by the same amount. There, that edge can never be part of the optimal tour.

4.2.4 Edge criticality

The stability region of an optimal tour can be understood as a margin of optimality of that tour with respect to arbitrary disturbances in edge costs and the edge tolerance

as the margin of optimality with respect to a disturbance of the cost of a single edge. Once the stability region of an optimal tour and the edge cost tolerances are known, it might be of interest to identify edges that are critical. Critical edge here refers to an edge for which the margin of optimality of the optimal tour with respect to disturbances to the cost of that edge is smaller than the margin of optimality with respect to disturbances in the cost of other edges. Hence, a high criticality of an edge indicates that the optimal tour is more susceptible to cost changes in that edge. Let Δc^+_{min} denote the minimum upper edge cost tolerance for any edge and let Δc^-_{max} be the maximum lower edge cost tolerance for any edge.

Definition 4.2.8 (Δc^+_{min}, Δc^-_{max})**.** *Let:*

$$\Delta c^+_{min} = \min_{ij} \Delta c^+_{ij} \tag{4.10}$$

$$\Delta c^-_{max} = \max_{ij} \Delta c^-_{ij} \tag{4.11}$$

Then, χ_{ij} is a dimensionless parameter that characterizes the criticality of an edge and can be defined as follows:

Definition 4.2.9 (χ_{ij})**.** *For $1 \leq i, j \leq n$, the criticality of edge e_{ij} is defined as:*

$$\begin{cases} \chi_{ij} = \frac{\Delta c^+_{min}}{\Delta c^+_{ij}} & \Delta c^+_{min} \neq 0 \wedge |\Delta c^+_{ij}| < \infty, \\ \chi_{ij} = -\frac{\Delta c^-_{max}}{\Delta c^-_{ij}} & \Delta c^-_{max} \neq 0 \wedge |\Delta c^-_{ij}| < \infty. \end{cases} \tag{4.12}$$

Note that for a minimal upper tolerance equal to zero the criticality of edges with respect to cost increase is not defined and similarly, if the maximum lower tolerance is equal to zero, the criticality of edges with respect to cost decreases is not defined. Furthermore, a negative criticality χ_{ij} indicates that edge e_{ij} is not part of the optimal tour and hence only cost decreases in that edge, if all other edge costs are held constant, can influence the optimal solution. Similarly, a positive criticality

χ_{ij} indicates that edge e_{ij} is part of the optimal tour and hence only cost increases in that edge, if all other edge costs are held constant, can influence the optimal solution.

4.2.5 Vertex location stability

All the above discussion focuses on robustness with respect to perturbation in the edge costs. In the eTSP as defined in Problem Formulation 3.1.2, the cost of an edge is the Euclidean distance between the two vertices covered by that edge. In unmanned aircraft operations the exact location of the targets might not be precisely known. Hence, the robustness of a tour with respect to the locations of the vertices is of interest. Furthermore, if only limited resources for intelligence are available, insight into which locations need to be known most precisely to guarantee optimality of a given tour is valuable. Therefore, the following section studies stability regions of optimal solutions to eTSPs with respect to perturbations to the vertex locations.

Let p_1 and p_2 be the locations of two vertices v_1 and v_2 in an instance of an eTSP. Hence, the cost c_{12} of the edge between v_1 and v_2 is given by the Euclidean distance between these two vertices:

$$c_{12} = \|p_1 - p_2\|_2 = ((p_1 - p_2)^T (p_1 - p_2))^{\frac{1}{2}}. \tag{4.13}$$

Let $p_{1,0}$, $p_{2,0}$, $c_{12,0}$ denote the nominal location and the nominal distance between the vertices. Then, a Taylor series expansion about these nominal values yields:

$$c_{12} \approx c_{12,0} + \frac{p_{1,0}^T - p_{2,0}^T}{c_{12,0}} \delta p_1 + \frac{p_{2,0}^T - p_{1,0}^T}{c_{12,0}} \delta p_2. \tag{4.14}$$

Thus, a first order approximation of the relationship between a disturbance in the

vertex locations and the edge costs is given by:

$$\begin{aligned}\Delta c_{12} &\approx \frac{p_{1,0}^T - p_{2,0}^T}{c_{12,0}}\Delta p_1 + \frac{p_{2,0}^T - p_{1,0}^T}{c_{12,0}}\Delta p_2, \\ &= \begin{bmatrix}\alpha_{12} & -\alpha_{12}\end{bmatrix}\begin{bmatrix}\Delta p_1 \\ \Delta p_2\end{bmatrix}.\end{aligned} \tag{4.15}$$

Using (4.15) and the scheme in (4.1), define the following matrix that captures the relationship between small perturbations to the locations of each vertex and the change in the edge costs:

$$A = \begin{bmatrix} \alpha_{12} & -\alpha_{12} & & & & 0 \\ & & \alpha_{13} & -\alpha_{13} & & \\ & & & \ddots & \ddots & \\ 0 & & & & \alpha_{n-1n} & -\alpha_{n-1n} \end{bmatrix}. \tag{4.16}$$

Thus, the cost change vector Δc for all edge costs can be expressed as:

$$\Delta c = A\Delta p. \tag{4.17}$$

Finally, substituting into (4.9) gives a first order approximation of the stability region of an optimal solution to an eTSP with respect to the vertex location disturbance vector in half space representation:

$$\overline{H}A\Delta p \leq -\overline{q}. \tag{4.18}$$

4.2.6 Vertex criticality

However, as these stability regions are obtained through linearization assuming small perturbations, the notion of a safe radius associated with each vertex is introduced to

be more conservative. The minimal perturbation in the L2 norm sense, $\Delta p_{w,min}$, in the location of a single vertex v_w that lies on the boundary of the linearized stability region can be computed as follows:

$$\begin{aligned} \Delta p_{w,min} = \underset{\Delta p_w}{\operatorname{argmin}} \quad & \|\Delta p_w\|_2 \\ \text{subject to} \quad & \overline{H} A \Delta p = -\overline{q}, \\ & \Delta p_k = 0, \ \forall k \neq w. \end{aligned} \tag{4.19}$$

Definition 4.2.10 ($r_{w,safe}$)**.** *Let $r_{w,safe}$ be the radius of the largest circle centered at the nominal location of vertex v_w that is fully contained in the stability region associated with vertex v_w with respect to perturbations of the location of v_w obtained through linearization assuming that all other vertices are located at their nominal locations.*

Hence, $r_{w,safe}$ can be computed as:

$$r_{w,safe} = \|\Delta p_{w,min}\|_2. \tag{4.20}$$

The unit vector $\frac{\Delta p_{w,min}}{\|\Delta p_{w,min}\|_2}$ gives the direction in which the least magnitude in change in location for vertex v_w can be tolerated before the current best tour becomes sub-optimal, assuming all other vertices remain at their nominal locations.

To ease interpretation by a human operator, a vertex criticality measure is introduced as follows: Let ξ_w denote the criticality of a vertex v_w. Furthermore, let $r_{min,safe}$ denote the smallest of all safe radii:

$$r_{min,safe} = \min_w r_{w,safe}. \tag{4.21}$$

Then the criticality of vertex v_w can be computed as follows:

$$\xi_w = \frac{r_{min,safe}}{r_{w,safe}}. \tag{4.22}$$

The criticality of vertices provides a human operator with a relative measure of how robust the optimal tour is with respect to perturbations to the location of that vertex. Hence, it is more important to have high confidence in the estimates of vertex locations with high criticality than for those with low criticality. Furthermore, in a game scenario, where an opponent tries to prevent the operator from choosing an optimal tour for the UAV by moving targets, that opponent can cause more harm to optimality by moving vertices with high criticality. This notion of vertex criticality and its interpretation is analogous to the notion of edge criticality in Section 4.2.4. Note that, if $\exists w : r_{w,safe} = 0$, vertex criticalities cannot be defined.

4.3 Multi-objective traveling salesman problems

Stability regions and robustness measures for symmetric non sequence-dependent TSPs are been derived above. In UAV mission planning multiple objectives might exist with respect to which a mission plan should be optimized. These types of problems are often cast as weighted-sum multi-objective optimization problem. This section presents the stability analysis for solutions to symmetric weighted-sum multi-objective non sequence-dependent traveling salesman problems.

4.3.1 Stability analysis with respect to changing weights

Consider a wsmoTSP as defined in Problem Formulation 3.1.4. Let $u_{k,ij}$ denote the cost of traveling on edge e_{ij} with respect to the k-th objective function. Then the

weighted cost of edge traversal from vertex i to vertex j given the weights λ_k is:

$$c_{ij} = \sum_{k=1}^{t} \lambda_k \cdot u_{k,ij}. \tag{4.23}$$

Using the scheme in (4.1), let u_k be a column vector containing all traversal costs with respect to the k-th objective. Let:

$$U = \begin{bmatrix} | & | & & | \\ u_1 & u_2 & \cdots & u_t \\ | & | & & | \end{bmatrix}. \tag{4.24}$$

Then the cost vector containing all edge costs with respect to the weighted objectives is given by:

$$c = U \cdot \lambda, \tag{4.25}$$

where λ is a column vector of weights. Using matrix H as defined in Section 4.2, the vector containing the costs of all tours in the set of tours $\mathcal{T}$ is given by:

$$q = Hc. \tag{4.26}$$

Using vector $\overline{q}$ (see (4.7)) and matrix $\overline{H}$ (see (4.8)) as defined in Section 4.2, the stability region with respect to a perturbation $\Delta\lambda$ is given by the intersection of the polyhedron:

$$\overline{H}U\Delta\lambda \leq -\overline{q} \tag{4.27}$$

and the normalization constraint:

$$\sum_{k=1}^{t} \Delta\lambda_k = 0. \tag{4.28}$$

The stability region is a polytope in the space of weight changes.

Given the nominal weights λ and the stability region, the question arises what the minimal perturbation in weights is that can cause the solution to become suboptimal. $\Delta\lambda_{crit}$ is therefore computed as the follows:

$$\begin{aligned} \Delta\lambda_{crit} = \underset{\Delta\lambda}{\operatorname{argmin}} \quad & \|\Delta\lambda\|_2 \\ \text{subject to} \quad & \overline{H}U\Delta\lambda = -\overline{q} \\ & \sum_{k=1}^{t} \Delta\lambda_k = 0. \end{aligned} \tag{4.29}$$

$\Delta\lambda_{crit}$ can be interpreted in different ways. $\|\Delta\lambda_{crit}\|_2$ gives a safe margin where any perturbation that is smaller than $\|\Delta\lambda_{crit}\|_2$ in the L2 norm sense is guaranteed to not alter the optimal solution. The unit vector $\frac{\Delta\lambda_{crit}}{\|\Delta\lambda_{crit}\|_2}$ defines a critical direction and helps to identify the weights out of the set of all weights and their associated objective functions that affect the optimal solution the most in terms of the notion of stability defined above.

4.3.2 Stability analysis with respect to changing objectives

Similar to the analysis of stability regions for solutions to single objective TSPs, stability regions of solutions in the cost space of all objectives for a wsmoTSP can be obtained assuming fixed weights. Using the notation introduced above, the stability region is given by the convex polyhedron:

$$\overline{H}\Delta U \cdot \lambda \leq -\overline{q}. \tag{4.30}$$

Given an optimal tour $T^\star$, all perturbation matrices ΔU for which (4.30) is satisfied, are contained in the stability region associated with $T^\star$.

4.3.3 Stability analysis with respect to simultaneously changing objectives and weights

Finally, stability regions for simultaneous changes in the objectives as well as the weights can be obtained. Using the product rule for finite differences, the stability region in terms of perturbations to P and λ is given by:

$$\overline{H}(\Delta U \cdot \lambda + U \cdot \Delta\lambda + \Delta U \cdot \Delta\lambda) \leq -\overline{q}. \tag{4.31}$$

Neglecting higher-order terms, a first order approximation is given by the convex polyhedron:

$$\overline{H}(\Delta U \cdot \lambda + U \cdot \Delta\lambda) \leq -\overline{q}. \tag{4.32}$$

4.4 Generalization to shortest paths

The above results for solutions to snTSPs and wsmoTSPs can be applied to shortest path problems. Given an undirected complete graph $G(V, E)$ with source vertex v_s, target vertex v_t, and cost c_{ij} for each edge e_{ij}, consider the linear program with variables h_{ij}:

$$\begin{aligned} \underset{ij \in E}{\text{minimize}} \quad & c_{ij} h_{ij} \\ \text{subject to} \quad & h \geq 0, \\ & \forall i : \sum_j h_{ij} - \sum_j h_{ji} = \begin{cases} 1, & \text{if } i = s; \\ -1, & \text{if } i = t; \\ 0, & \text{otherwise.} \end{cases} \end{aligned} \tag{4.33}$$

The edge cost c_{ij} might be computed as the convex combination of multiple costs as outlined in (4.23). Hence, single and weighted-sum multi-objective shortest path

problems can be addressed. Feasible solutions to optimization problem (4.33) are zero one vectors h that denote whether a certain edge is contained in a path. Therefore, the optimal solution to optimization problem (4.33) identifies the edges contained in the shortest path from v_s to v_t [89]. Using the the scheme in (4.1) to convert the indices to a single index, explicitly enumerating the set of solutions, and the introduction of a vector x that is associated with a path in the set of paths similar to Definition 4.2.1 lead to the problem of choosing the shortest path in a set of paths in the form of optimization problem (4.4). Hence, the methods for stability analysis with respect to perturbations in the edge costs and to perturbations in the vertex locations can be directly applied to single objective and multi-objective shortest path problems.

4.5 Asymmetric single objective TSP

So far symmetric variants of the TSP have been considered. The asymmetric TSP is a variant of the TSP, where the edge cost matrix C is not symmetric. Such a problem formulation can be utilized for example, if the effect of wind shall be captured in a UAV planning problem. For example, the cost incurred for edge traversal with headwind is greater than or equal to the cost of traversal of the same edge in the opposite direction with tail wind. The stability results derived above are directly applicable to the asymmetric TSP.

Proposition 3. *The asymmetric TSP can be re-formulated as an integer linear programming problem* (4.4)*.*

Proof. Consider a n-vertex TSP for which the cost c_{ij} of traveling from vertex v_i to vertex v_j is not necessarily equal to the cost c_{ji}. The data for optimization problem (4.4) is obtained through transformation of the data of the asymmetric TSP as follows.

First, let $c \in \mathbb{R}^{n(n-1)}$ be a column vector containing all travel costs c_{ij} for all $i \neq j$

in lexicographical ordering. Hence, the index of a vector element c_w is related to edge e_{ij} for all $i \neq j$ by the following relationship:

$$w = n(i-1) + j - 1 - \left\lfloor \frac{n(i-1)+j-1}{n+1} \right\rfloor . \tag{4.34}$$

Then, enumerate the tours in the set of all possible tours and define a subset of tours $\mathcal{T}$ with an induced enumeration, i.e., the r-th element in $\mathcal{T}$ is the r-th element found when searching for elements of $\mathcal{T}$ in the set of all possible tours. Furthermore, let x be a vector associated to a tour in $\mathcal{T}$ using Definition 4.2.1. Finally, similarly to Definition 4.2.2, let h be a column vector of length $n(n-1)$ that identifies the edges e_{ij} contained in a tour T, where the indices of the entries being equal to one are computed using (4.34). All other entries are zero. Then, similarly to Definition 4.2.3, a matrix H can be constructed, where the r-th row of H is vector h_r^T, which identifies the edges contained in tour $T_r \in \mathcal{T}$. Hence, the cost vector for optimization problem (4.4), q, is given by $q = Hc$. Finally, using an argument similar to Proposition 1, the optimal solution $x^\star$ of optimization problem (4.4), $x^\star$, identifies a best tour $T^\star$ in $\mathcal{T}$ that solves the asymmetric TSP. □

Therefore, the stability region for the best tour $T^\star \in \mathcal{T}$ can be computed using the method given in Section 4.2.2 and (4.9). Hence, evaluating (4.9) gives a polynomial time method to determine whether an optimal tour $T^\star$ remains optimal in $\mathcal{T}$ after a cost change Δc occurs. Again, this stability region is a polyhedron. Edge cost tolerances can be computed using the method outlined in Section 4.2.3. Finally, the edge criticality for the asymmetric TSP can be defined as given in Definition 4.2.9.

4.6 Sequence-dependent TSP

In this section the stability region for a solution to the asymmetric sequence-dependent TSP is analyzed.

4.6.1 Stability regions

Proposition 4. *The asymmetric sequence-dependent TSP can be re-formulated as an integer linear programming problem* (4.4).

Proof. Consider a n-vertex asymmetric sequence-dependent TSP. The data for optimization problem (4.4) is obtained through transformation of the data of the asymmetric sequence-dependent TSP as follows.

First, enumerate the tours in the set of all possible tours and define a subset of tours $\mathcal{T}$ with induced enumeration, i.e., the r-th element in $\mathcal{T}$ is the r-th element T_r found when searching for elements of $\mathcal{T}$ in the set of all possible tours.

Let $Q_{r,m}$ denote the state of the queue of cities after having completed $m-1$ steps of the r-th tour in $\mathcal{T}$, i.e., the sequence of cities in the queue after $m-1$ steps. Let $c_{r,m} \in \mathbb{R}^{n(n-1)}$ be a vector containing the edge costs $c_{ij}(Q_{r,m})$ for all vertex pairs v_i, v_j, i.e., the traversal costs of all edges at the m-th step when pursuing tour T_r:

$$c_{r,m} = [c_{12}(Q_{r,m}), \dots c_{n(n-1)}(Q_{r,m})]^T, \tag{4.35}$$

where the k-th entry in $c_{r,m}$ is associated to the vertex pair v_i, v_j through (4.34). Additionally, let $c_m \in \mathbb{R}^{n(n-1)|\mathcal{T}|}$ be a vector containing all edge costs at the m-th step for all tours in $\mathcal{T}$:

$$c_m = [c_{1,m}^T, \dots, c_{|\mathcal{T}|,m}^T]^T. \tag{4.36}$$

Let $h_{r,m} \in \mathbb{Z}^{n(n-1)|\mathcal{T}|}$ be a vector that identifies the edge e_{ij} used at the m-th step when following the r-th tour T_r using the following scheme: It contains a single non-zero entry equal to one at the y-th location, where y is computed as follows:

$$y = (r-1)n(n-1) + k, \tag{4.37}$$

and k is computed using (4.34). Let $h_r \in \mathbb{Z}^{n^2(n-1)|\mathcal{T}|}$ be a vector that identifies all

edges contained in the r-th tour:

$$h_r = [h_{r,1}^T, \ldots, h_{r,n}^T]^T. \tag{4.38}$$

Furthermore, let H be a matrix, where the r-th row of H is h_r^T.

Moreover, let $c \in \mathbb{R}^{n^2(n-1)|\mathcal{T}|}$ be the cost vector concatenating the costs of all edges at all steps for all tours:

$$c = [c_1^T, \ldots, c_m^T, \ldots, c_n^T]^T. \tag{4.39}$$

The cost q_r of the r-th tour T_r in $\mathcal{T}$ is then given by:

$$q_r = \sum_{m=1}^{n} c_{r,m}^T h_{r,m}. \tag{4.40}$$

Hence, the cost vector q for optimization problem (4.4) containing the cost of all tours in $\mathcal{T}$ can be written as:

$$q = Hc. \tag{4.41}$$

Let vector x be associated to a tour in $\mathcal{T}$ using Definition 4.2.1. Then, again by similar argument to Proposition 1, the solution $x^\star$ to optimization problem (4.4) identifies a cheapest tour in $\mathcal{T}$ that solves the asymmetric sequence-dependent TSP.

□

The stability region for the best tour $T^\star \in \mathcal{T}$ for the sequence-dependent asymmetric TSP can therefore be computed using the method given in Section 4.2.2 and (4.9). Hence, evaluating (4.9) gives a polynomial time method to determine whether an optimal tour $T^\star$ remains optimal in $\mathcal{T}$ after a cost change Δc occurs. Again, that stability region is a polyhedron. Note that the above proof uses redundant data for legibility and ease of notation. Edge cost tolerances can be computed using the method outlined in Section 4.2.3.

A proof that the optimization version of the asymmetric sequence-dependent TSP

is NP–hard is now provided. The proof is in the form of reducing the associated decision version of the symmetric non sequence-dependent TSP that is NP–complete [90] to the associated decision version of the asymmetric sequence-dependent TSP. The decision version of the symmetric non sequence-dependent TSP can be stated as follows:

Problem formulation 4.6.1 (Decision snTSP)**.** *Given a value $J_0 \in \mathbb{R}$, a set V of n cities $\{v_1, \cdots, v_n\}$ and a symmetric edge cost matrix c, where c_{ij} denotes the cost of traveling from vertex v_i to vertex v_j on edge e_{ij}, decide whether there exists a* Hamiltonian *tour, (*tour for short*) T, where $T^\star(m)$ denotes the vertex visited at the m-th step, such that $J(T) = \sum_{m=1}^{n} c_{T^\star(m-1),T^\star(m)} < J_0$.*

The decision version of the asymmetric sequence-dependent TSP can then be stated as follows:

Problem formulation 4.6.2 (Decision asTSP)**.** *Let $J_0 \in \mathbb{R}$, V be a set of n cities $\{v_1, \ldots, v_n\}$, Q be a queue of cities of fixed length $1 \leq \mu \leq n$ that operates in a "first in first out manner". The initial location of the agent is inserted into the queue at position $Q(1)$ while all other entries in Q are empty. When the agent moves to the next vertex, that vertex is inserted into the queue at position Q(1) while the element previously at $Q(\mu)$ leaves the queue. Let v_j not belong to the queue and let v_i belong to the queue at location $Q(1)$, then $c_{ij}(Q)$ denotes the cost of traveling from v_i to v_j. Let T be a tour, such that $T(m)$ denotes the vertex p visited at the m-th step of that tour and Q_m denotes the state the queue at that step, i.e., the sequence of μ cities in the queue. Decide whether there exists a tour T such that the cost associated with that tour, $J(T) = \sum_{m=1}^{n} c_{T^\star(m-1),T^\star(m)}(Q_m) < J_0$.*

Proposition 5. *The decision version of the asymmetric sequence-dependent TSP is NP–hard.*

Proof. A problem P is NP–hard if an NP–complete problem is reducible to P [90]. The decision version of the snTSP can be reduced to the decision version of the asTSP as follows: Let subscript sn denote inputs to the decision version of the symmetric non-sequence-dependent TSP and let subscript as denote inputs to the decision version of the asymmetric sequence-dependent TSP. Then set: $J_{0,sn} = J_{0,as}$, $V_{sn} = V_{as}$, $\mu_{as} = 1$, $\forall i, j : c_{ij,sn} = c_{ij,as}(Q)$. The solution to the decision version of the asTSP with these inputs solves the decision version of the snTSP. Hence the decision version of the asTSP is NP–hard. □

Corollary 4.6.3. *The asymmetric sequence-dependent TSP is NP–hard.*

Proof. This follows from Proposition 5. □

Corollary 4.6.4. *The symmetric sequence-dependent TSP can be re-formulated as an integer linear programming problem* (4.4)*.*

Proof. This follows from Propositions 3 and 4. □

Therefore, the stability region for the best tour $T^\star \in \mathcal{T}$ for the symmetric sequence-dependent TSP can be computed using the method given in Section 4.2.2 and (4.9). Hence, evaluating (4.9) gives a polynomial time method to determine whether an optimal tour $T^\star$ remains optimal in $\mathcal{T}$ after a cost change Δc occurs. Again, this stability region is a polyhedron. Edge cost tolerances can be computed using the method outlined in Section 4.2.3.

4.6.2 Edge criticality

Similarly to the edge criticality for the non sequence-dependent symmetric and asymmetric TSP, an edge criticality with respect to a certain optimal tour for the sequence-dependent TSP can be formulated. Let $\Delta c^{\star +}$ be a vector containing the upper edge cost tolerances for all edges for all steps when following the optimal tour. Similar in

structure to (4.35), it is given by:

$$\Delta c^{\star +} = [\Delta c^{+T}_{r^\star,1} \dots \Delta c^{+T}_{r^\star,n}]^T, \tag{4.42}$$

where $r^\star$ is the index of the best tour. The vector $\Delta c^{\star -}$ of all lower edge cost tolerances is defined similarly.

Let $\Delta c^{\star +}_w$ denote the minimal upper tolerance an edge in $\Delta c^{\star +}$, where k is the index of edge e_{ij} computed either using (4.1) for symmetric problems or (4.34) for asymmetric problems. The maximal lower tolerance $\Delta c^{\star -}_w$ of edge w is defined similarly.

Then, let $\Delta c^{\star +}_{min}$ denote the minimum upper edge cost tolerance for any edge given the optimal tour and let $\Delta c^{\star -}_{max}$ be the maximum lower edge cost tolerance for any edge given the optimal tour.

Definition 4.6.5 (Δc^{*+}_{min} , Δc^{*-}_{max})**.** *Let:*

$$\Delta c^{\star +}_{min} = \min_i \Delta c^{\star +}_i, \tag{4.43}$$

$$\Delta c^{\star -}_{max} = \max_i \Delta c^{\star -}_i. \tag{4.44}$$

Then, $\chi^\star_w$ a dimensionless parameter that characterizes the criticality of edge e_w with respect to the optimal tour, where w is computed using either (4.1) or (4.34) depending on whether the problem is symmetric or asymmetric:

Definition 4.6.6 (χ_w)**.** *The criticality of edge e_w is defined as:*

$$\begin{cases} \chi^\star_w = \frac{\Delta c^{\star +}_{min}}{\Delta c^{\star +}_w} & \Delta c^{\star +}_{min} \neq 0 \wedge |\Delta c^{\star +}_w| < \infty \\ \chi^\star_w = -\frac{\Delta c^{\star -}_{max}}{\Delta c^{\star -}_w} & \Delta c^{\star -}_{max} \neq 0 \wedge |\Delta c^{\star -}_w| < \infty \end{cases} \tag{4.45}$$

This definition resembles the definition of criticality for the non sequence-dependent TSP variants in Definition 4.2.9. Note that, while the edge costs in the non sequence-

dependent variants do not depend on the optimal tour $T^\star$, in the sequence-dependent variants the edge costs depend on the optimal tour. This is accounted for by the introduction of the upper tolerance vector in (4.42) and the similarly constructed lower tolerance vector that are defined with respect to the optimal tour. Edge criticality for the sequence-dependent TSP is computed with respect to those tolerances.

4.6.3 Application of the k-opt heuristic to the sequence-dependent TSP

The sequence-dependent TSP is NP–hard as shown in Corollary 4.6.3. Hence, it is expedient to use heuristic methods to solve intractably large instances of it. The k-opt heuristic is a widely and successfully used improvement heuristic for the TSP [91]. Let the k-neighborhood $\mathcal{T}_k$ of a tour T be the set of all tours obtained by permutation of any k cities in the tour. Without loss of generality, let v_1 be the initial location of the vehicle. The k-opt heuristic is an iterative method that goes from one iterate tour to the next by doing the following: (a) construct the k-neighborhood of the tour, (b) select as the next iterate the best tour in the k-neighborhood obtained in (a), where the cost q_r of each tour $T_r \in \mathcal{T}_k$ is evaluated using (4.40) with $T_r(0) = v_1$. Hence, the k-opt heuristic terminates at a so-called k-opt tour that is guaranteed to be optimal in its k-neighborhood.

4.6.4 Application to tours obtained by the k-opt heuristic

Based on the above analysis, the stability of solutions obtained using the k-opt heuristic with respect to the k-neighborhood can be obtained as follows: Given a k-optimal tour $T^\star$, construct its k-neighborhood $\mathcal{T}_k$ and let $\mathcal{T}$ be $\mathcal{T}_k \cup T^\star$. Then, (4.9) yields the exact stability region of $T^\star$ with respect to $\mathcal{T}_k \cup T^\star$.

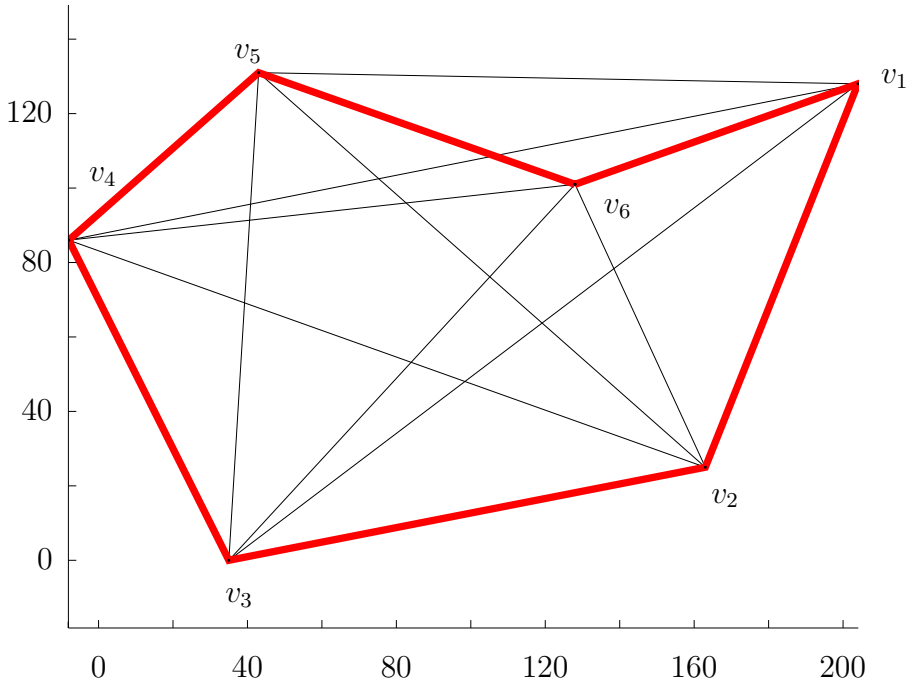

Figure 4.1: **Optimal solution for 6-vertex TSP:** The optimal tour to this 6-vertex TSP is indicated by the thick, red line.

4.7 Examples

4.7.1 Symmetric non sequence-dependent TSP

The following section demonstrates the application of stability analysis to the solution of a non sequence-dependent symmetric Euclidean 6-vertex TSP based on the example in Ref. [3]. An unmanned aircraft is used to query multiple unattended ground sensors at multiple locations repeatedly. A traditional approach to obtain optimized flight patterns in this case is to pose this problem as a symmetric non sequence-dependent TSP, in which the unmanned aircraft is required to visit each unattended ground sensor only once, starting from any sensor and returning to the original place of departure. The locations of the unattended ground sensor are enumerated v_1 through v_6, and are shown in Fig. 4.1. The unperturbed edge costs are the Euclidean distances between these locations. The optimal tour is $T^\star = (v_1, v_2, v_3, v_4, v_5, v_6, v_1)$.

Fig. 4.2 depicts the stability region for changes in the edge costs c_{12}, c_{15}, c_{34} ob-

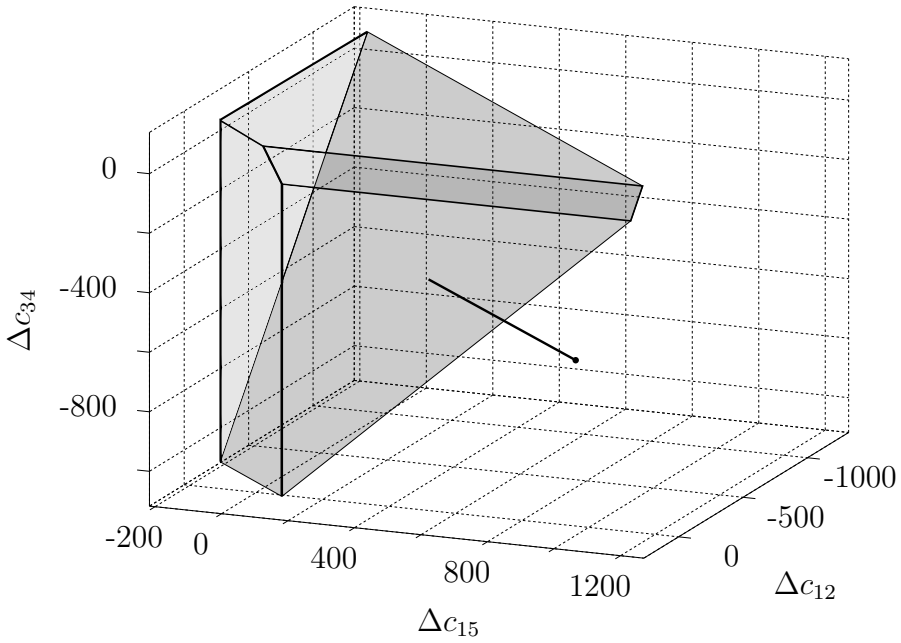

Figure 4.2: **Stability region for 6-vertex TSP**: The stability region of the optimal solution for perturbations in edges $e_{1,2}$, $e_{1,5}$, and $e_{3,4}$ is given. It extends to infinity in the direction of the black line.

tained through evaluation of (4.9), assuming that all other edge costs are held constant. A disturbance of $\Delta c_{12} = 50$ and $\Delta c_{15} = -50$ lies outside the stability region of $T^\star$ as indicated in Fig. 4.3. The new optimal solution for that disturbance is $\hat{T}^* = (v_1, v_6, v_2, v_3, v_4, v_5, v_1)$ as shown in Fig. 4.4.

The TSP edge criticality plot in Fig. 4.5 visualizes the criticality for each edge with respect to $T^\star$. The thickness of the edges (from thin to thick), and the color of the edges (from yellow to red) correspond to the criticality of that edge (from less critical to more critical). The numerical value of the edge criticality for each edge is indicated next to it. The criticality plot can be interpreted in multiple ways:

- If the problem data, i.e., here the travel times, are based on models or for example gathered data, it is more important to have high confidence in the estimates for edges with high criticality than for edges with low criticality.

- In a game scenario, where an opponent tries to prevent the agent from per-

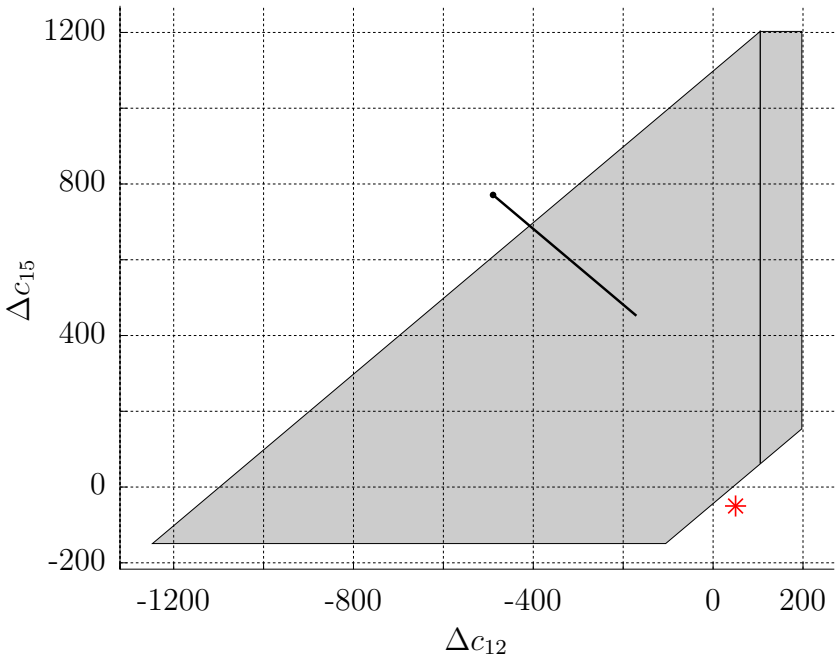

Figure 4.3: **Stability region for perturbed 6-vertex TSP:** The applied perturbation as indicated by the red star is outside of the stability region.

forming an optimal tour, that opponent can cause more harm to optimality by targeting edges with high criticality.

- Likewise, the agent should assign resources, if possible, to reenforce the critical edges.

Hence, decision makers can use the criticality plot to allocate resources to enhance the performance of the system.

4.7.2 Vertex location

For the eTSP, the concepts introduced in Section 4.2.5 regarding robustness of the shortest tour with respect to vertex location perturbations are demonstrated in this section. Consider the example depicted in Fig. 4.6 that is based upon scenarios in Ref. [3]. An unmanned aircraft is used to query multiple unattended ground sensors at multiple locations repeatedly. A traditional approach to obtain optimized flight

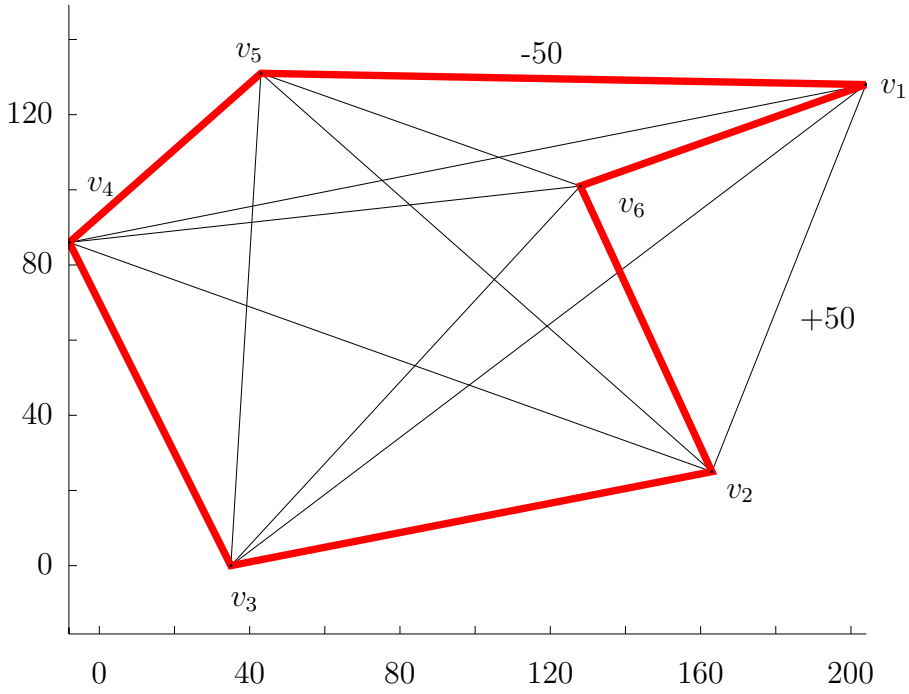

Figure 4.4: **Optimal solution for perturbed 6-vertex TSP:** The optimal tour to the perturbed 6-vertex TSP after the edge cost c_{15} has been decreased and the edge cost c_{12} has been increased is indicated by the thick, red line.

patterns in this case is to pose this problem as a symmetric TSP, in which the unmanned aircraft is required to visit each unattended ground sensor once, starting from any sensor and returning to the original place of departure, resulting in a tour. The locations of the unattended ground sensor are enumerated v_1 through v_6. Assuming uncertainty in the exact location of the unattended ground sensors, Fig. 4.6 depicts the safe radii associated with each of the targets, i.e., the circles centered at each location v_i have radius $r_{i,safe}$. The thickness of the circle boundaries (from thin to thick), and the color of the circle (from yellow to red) correspond to the criticality of that location (from less critical to more critical).

The red polyhedron containing vertex v_6 depicts the stability region of that vertex with respect to perturbations of the location of that vertex based on the linearization described in Section 4.2.5. Furthermore, the relationship between the stability region of a vertex and the associated safe radius can be seen. The plotted safe radii agree

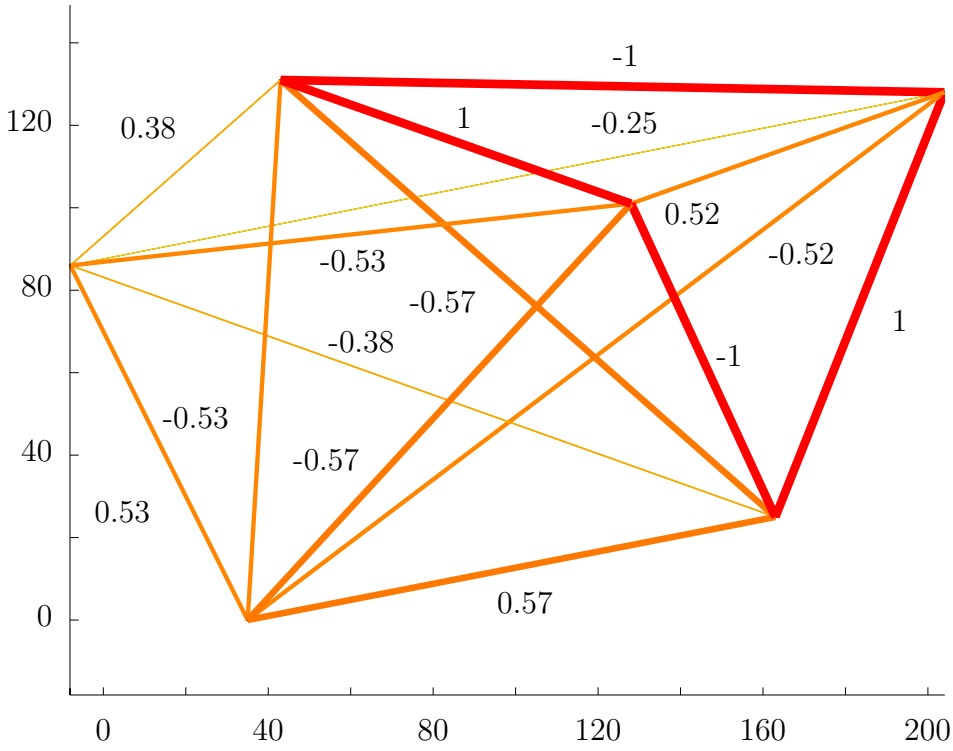

Figure 4.5: **Edge criticalities:** The thickness of the edges (from thin to thick), and the color of the edges (from yellow to red) correspond to the criticality of that edge (from less critical to more critical). The numerical value of the edge criticality for each edge is indicated next to each edge.

with the intuition that vertex v_6 has the smallest safe radius as the path (v_5, v_1, v_6, v_2) becomes shorter than (v_5, v_6, v_1, v_2) for small perturbations in the location of v_6.

4.7.3 Weighted-sum multi-objective traveling salesman problems

This section demonstrates the application of stability analysis to the solution of a 6-vertex wsmoTSP based on the examples in Ref. [3] and Ref. [4]. An unmanned aircraft is used to query multiple unattended ground sensors at multiple locations repeatedly. The locations of the unattended ground sensor are enumerated v_1 through v_6. Hostile radar sites as well as hostile communication jamming devices are present within the area of operation and need to be avoided while keeping the mission time short and

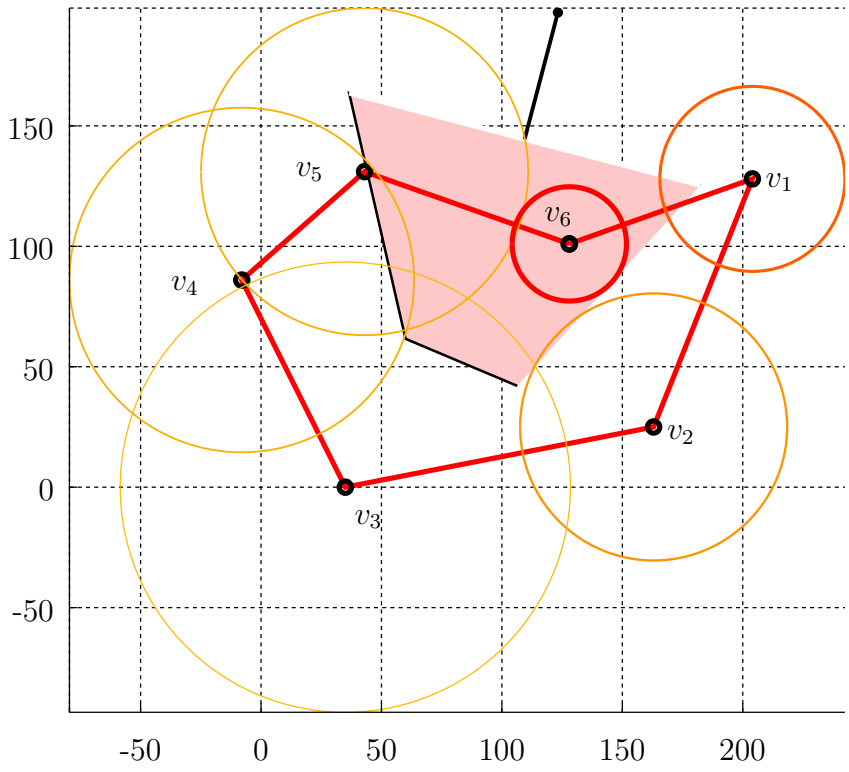

Figure 4.6: **Vertex criticalities:** This figure depicts the concepts of vertex stability for the shortest tour for the single objective Euclidean TSP based on the example in Ref. [3]. The circles centered at each location v_i have radius $r_{i,safe}$. The thickness of the circle boundaries (from thin to thick), and the color of the circle (from yellow to red) correspond to the criticality of that location (from less critical to more critical). The polyhedron about vertex v_6 depicts the linearized stability region of that vertex with respect to perturbations of the location of that vertex based upon the linearization described in Section 4.2.5.

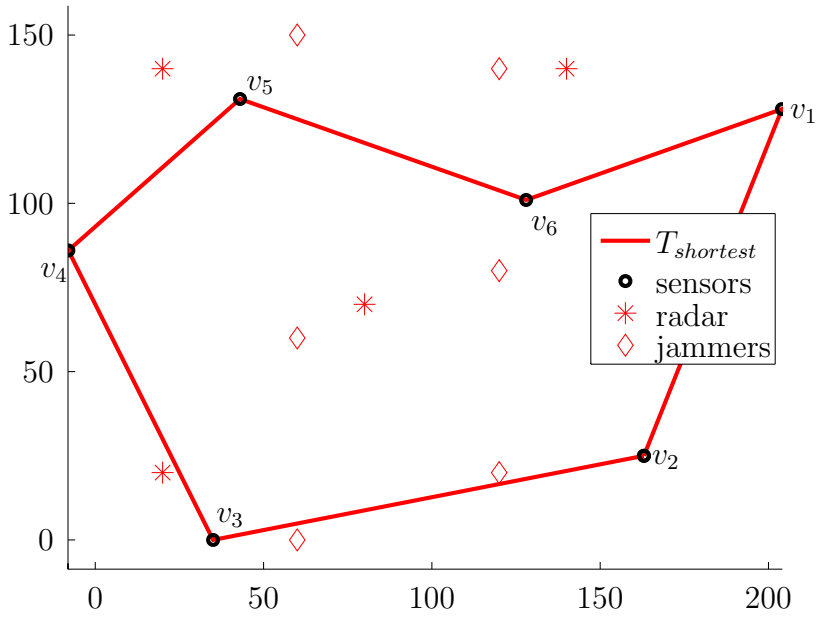

Figure 4.7: **Multi-objective TSP - shortest tour:** This figure depicts the shortest tour for the single objective Euclidean TSP as also given in Ref. [3]. While short, this tour leads the aircraft close to the radar and jamming sites along edges e_{23} and e_{34}.

the flown path fuel efficient.

In this section, three different objectives are considered:

4.7.3.1 Minimum length

Fuel consumption is related to the distance traveled. The length of an edge is the Euclidean distance between the two vertices that are connected by that edge. Hence, the cost of traveling from vertex v_i at location p_i to vertex v_j at location p_j is given by:

$$u_{E,ij} = \|p_i - p_j\|_2. \tag{4.46}$$

The shortest tour, $T^{\star}_{Euclidean} = (v_1, v_2, v_3, v_4, v_5, v_6, v_1)$, is depicted in Fig. 4.7. However, as can be seen in the figure, this tour leads the aircraft very close to the radar sites and communication jamming devices along edges e_{34} and e_{23}.

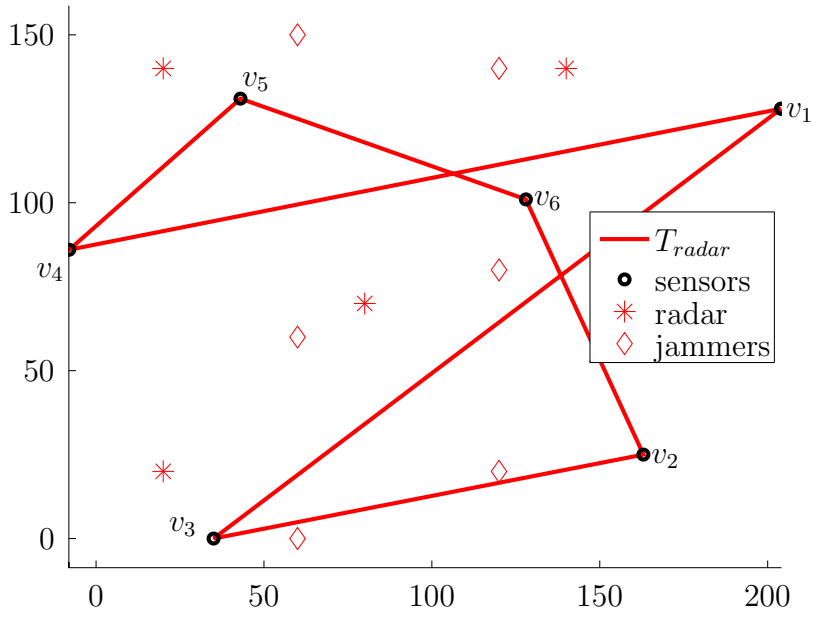

Figure 4.8: **Multi-objective TSP - minimum radar exposure tour:** This figure depicts the optimal tour for the single objective minimum radar exposure TSP. This tour leads the aircraft close to the communication jamming sites along edge e_{23}.

4.7.3.2 Minimum radar exposure

Given a set of radar sources Π, the threat cost due to radar $c_{R,ij}$ associated with an edge e_{ij} is calculated based on radar exposure of a vehicle traveling along that edge. To simplify the calculation of radar exposure, it is assumed that the vehicle's radar signature is uniform in all directions and is proportional to d_π^{-4}, where d_π represents the distance from the vehicle to radar site π. In order to calculate the threat cost along a given edge, the integration of the cost along the edge is required. Instead of integrating costs for every edge the three point approximation given in Ref. [45] is applied. Let $g_{ij} = p_j - p_i$ and let O_{ij} be a set of points associated with edge e_{ij}:

$$O_{ij} = \{p_i + \frac{1}{6}g_{ij}, p_i + \frac{1}{2}g_{ij}, p_i + \frac{5}{6}g_{ij}\}. \tag{4.47}$$

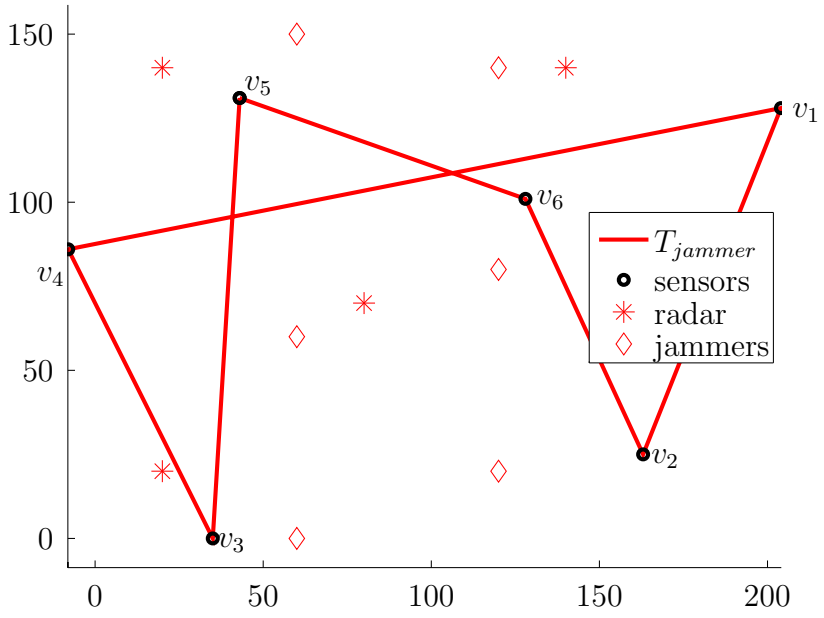

Figure 4.9: **Multi-objective TSP - minimum communication disturbance tour:** This figure depicts the optimal tour for the single objective minimum communication disturbance TSP. This tour leads the aircraft close to the radar site along edge e_{34}.

Then the cost of edge e_{ij} due to radar exposure to all radar sites $\pi_k \in \Pi$ is given by:

$$u_{R,ij} = \frac{\gamma_R \|g_{ij}\|_2}{3} \sum_{k=1}^{|\Pi|} \sum_{w=1}^{|O_{ij}|} \frac{1}{\|\pi_k - b_w\|_2^4}, \tag{4.48}$$

where $\gamma_R = 10$ is a constant scaling factor. Fig. 4.8 depicts the minimum radar exposure tour $T^\star_{Radar} = (v_1, v_4, v_5, v_6, v_2, v_3, v_1)$. The tour avoids close encounters with the radar sites, but is longer than the shortest tour and leads the aircraft close to to the adversarial communication jamming sites along edge e_{23}.

4.7.3.3 Minimum communication interference

The presence of a set of adversarial communication jamming devices Ξ is assumed whose efficiency decreases proportionally with d_ξ^{-4}, where d_ξ represents the distance from the vehicle to jammer location ξ. Using the same three point approximation as above for the path integral, the cost associated with an edge e_{ij} due to to the presence of all jammers $\xi_k \in \Xi$ is given by:

$$u_{R,ij} = \frac{\gamma_R \|g_{ij}\|_2}{3} \sum_{k=1}^{|\Xi|} \sum_{w=1}^{|O_{ij}|} \frac{1}{\|\xi_k - b_w\|_2^4}, \tag{4.49}$$

where $\gamma_J = 10$ is a constant scaling factor. Fig. 4.9 depicts the minimum communication jammer exposure tour $T^\star_{Jammer} = (v_1, v_4, v_3, v_5, v_6, v_2, v_1)$. The tour does not include edge e_{23} that would lead the aircraft close to two jamming sites. However, it leads the aircraft close to the radar site along edge e_{34}.

4.7.3.4 Weighted-sum approach

Fig. 1.6 shows the optimal tour $T^\star_{Weighted}$ for the weighted-sum objective for the following choice of weights: $\lambda_{Euclidean} = 0.1$, $\lambda_{Radar} = 0.5$, and $\lambda_{,Jammer} = 0.4$. Fig. 4.10 depicts the stability region of that optimal tour with respect to changes in the weights. The diamond indicates the chosen set of weights and the star indi-

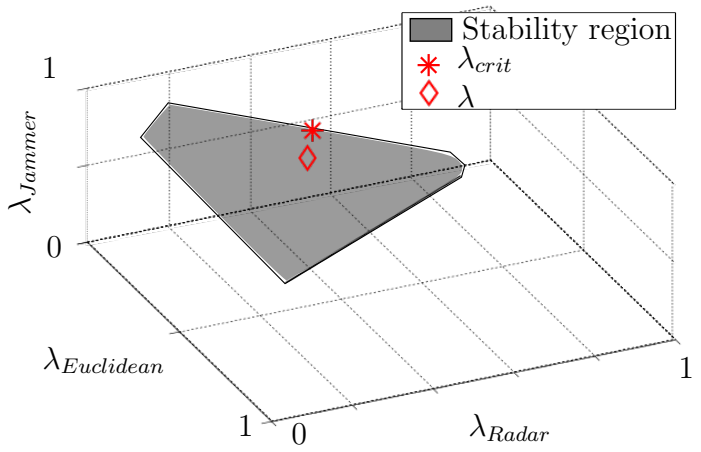

Figure 4.10: **Multi-objective TSP - stability region:** This figure depicts the stability region indicated by the grey polytope associated with the optimal tour depicted in Fig. 1.6 with respect to changes in the weights. The diamond indicates the chosen weights and the star depicts the smallest change in weights that causes that tour to become suboptimal.

cates $\lambda + \Delta\lambda_{crit}$, i.e., the smallest perturbation in weights that would lead to another tour being optimal with respect to the weighted objective as defined in (4.29), where $\Delta\lambda_{crit,Euclidean} = -0.1$, $\Delta\lambda_{crit,Radar} = 0.05$, and $\Delta\lambda_{crit,Jammer} = 0.05$. From the figure, the range of weights for which the tour in Fig. 1.6 is optimal can be seen. By considering the direction and magnitude of the most critical perturbation, it can be seen that only slightly increasing the aversion to radar exposure and communication interference will change the tour, while a stronger emphasis on a shorter tour will not change the solution for small weight changes. Hence, fine tuning the weights is only of interest or might result in a different tour if the radar and jamming objectives should be prioritized higher, but not if shorter tour length would be desirable.

4.7.4 Sequence-dependent TSP

In the following section, two examples for two different problems that can be formulated as sequence-dependent problems are presented that exhibit different characteristics based on the nature of their sequence-depence.

4.7.4.1 Cargo plane

Consider the motivating example from Section 1.3.2. A cargo aircraft starting at location v_1 visits three locations and delivers one distinct piece of cargo at each location. The goal is to find a minimum time route. The travel time for an edge is assumed to be the length of that edge in time units. The best tour is $T^\star = (v_1, v_2, v_3, v_4, v_1)$ as shown in Fig. 1.5 and the cost of that tour is $q^\star = 7.1004$. The cargo is stacked according to this itinerary in the cargo aircraft to minimize time when unloading. Hence, the cargo for location v_4 is at the bottom of the stack and the load for location v_2 at the top. If the aircraft deviates from the originally optimal tour, any cargo on top of the cargo for that location must be unloaded and reloaded back into the aircraft. The unloading and loading operation is assumed to consume one time unit, where solely unloading the cargo on top of the stack is assumed to not add additional time. Hence, if the aircraft follows the original route, the time to complete the route is only the travel time. If the aircraft, however, deviates from the original tour and first visits location v_4, an additional cost for unloading and reloading the freight for locations v_2 and v_3 of two time units is added. Therefore, this is a sequence-dependent TSP.

Using the method detailed above, the stability region for the optimal tour in this scenario with respect to cost changes in the edges connecting location v_2 and location v_3 when being used as the second edge within any possible tour is depicted in Fig. 4.11. This could, for example, be interpreted as additional travel time due to poor weather occurring during a time window on the flightpath that connects location v_2 and v_3

in both directions. Notice that, as this is an asymmetric instance of the TSP, only a limited cost increase in edge e_{23} can be tolerated for $T^\star$ to remain optimal, as $e_{23} \in T^\star$. Conversely, as $e_{32} \notin T^\star$, $T^\star$ becomes suboptimal if the cost for e_{32} falls below a threshold.

Fig. 4.11 depicts the stability region for this problem with respect to sequence-dependent edge cost disturbances to e_{23} and e_{32}. These disturbances are applied assuming that e_{23} and e_{32} are the second step of the tour and that there is a sequence-dependent penalty for deviating from the previous tour. For comparison, the stability region for the same perturbations, however, without the sequence-dependent penalty for deviating from the tour is given in Fig. 4.12. The stability region is not the same as before. The sequence-dependent additive cost translates the stability region, because $T^\star$ is more robust to cost changes, as the sequence-dependent additive costs penalize deviating from $T^\star$. However, the shape of the stability region is preserved, as all tours are affected equally.

In this example, the cost data is sequence-dependent, however, the disturbances to the cost due to poor weather to the edges are independent of the sequence in which locations are visited, and all the tours are affected equally.

4.7.4.2 Intelligent adversary

Consider the 4-vertex TSP in Fig. 4.13. An unmanned aircraft, flying at constant velocity, starting at location v_1, is tasked to gather intelligence regarding three suspects at locations v_2, v_3, and v_4 in minimum time, where the distance between the locations of the suspects is the Euclidean distance. Nominally, the best tour to visit the suspects is $T^\star = (v_1, v_2, v_3, v_4, v_1)$. However, the suspects adjacent to each other can communicate with each other through the links indicated by the arrows with the radio tower symbol in the figure. Note that, there is no communication link between v_2 and v_4. If the unmanned aircraft visits two suspects in succession that can commu-

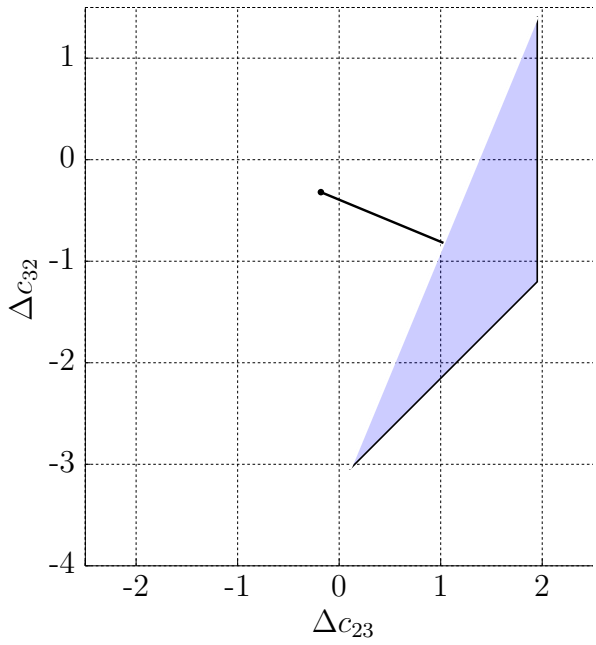

Figure 4.11: **Stability region for sequence-dependent TSP:** The stability region for the sequence-dependent TSP with respect to cost changes in c_{23} or c_{32} if visited at the second step of the tour affecting all tours equally.

nicate with each other, the suspects are assumed to detect a pattern and to alert the third suspect. That suspect then camouflages, which requires the aircraft to loiter above the location instead of just flying by to gather the data about the remaining suspect. If, however, after visiting the first suspect the aircraft visits the suspect that has no communication link to the first no warning is given to the third remaining suspect.

The problem of finding a minimum time tour to visit all three suspects can be formulated as a sequence-dependent TSP. The stability region of the nominal optimal tour with respect to cost increases due to the third suspect camouflaging if alerted identifies the range of cost increases for which the nominal tour remains optimal. Notice that, by using the diagonal edges, alerting the third suspect can be avoided.

In this example, the nature of the sequence-dependence is different from the previous example. Here, the travel cost depends on the sequence in which the locations are visited as in the previous example, but also the change in edge costs are sequence-

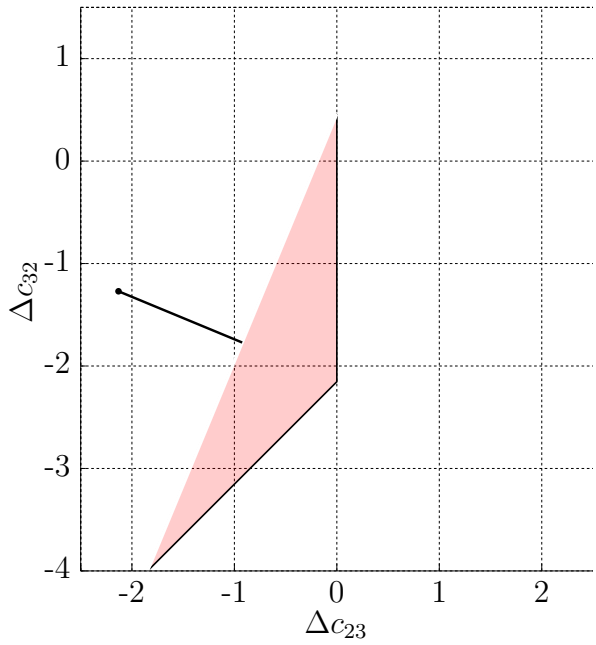

Figure 4.12: **Stability region for sequence-dependent TSP:** The stability region for the sequence-dependent TSP with respect to cost changes in c_{23} or c_{32} without the sequence-dependent penalty for deviating from the tour is depicted.

dependent and only affect tours that include that specific sequence of locations.

Fig. 4.14 depicts the stability region for perturbations in edges e_{23} and e_{34} for the sequence independent 4-vertex TSP. In contrast, the stability region for $\Delta c_{(v_1,v_2,v_3),34}$ and $\Delta c_{(v_1,v_4,v_3),32}$, i.e., the sequence-dependent case is given in Fig. 4.15. Again, the stability region for the sequence-dependent TSP is not equal to the stability region of the sequence independent problem. However, in this example, the stability region is not only translated compared to the non sequence-dependent problem, but also the shape of the stability region is different due to the sequence-dependent effect on the edges.

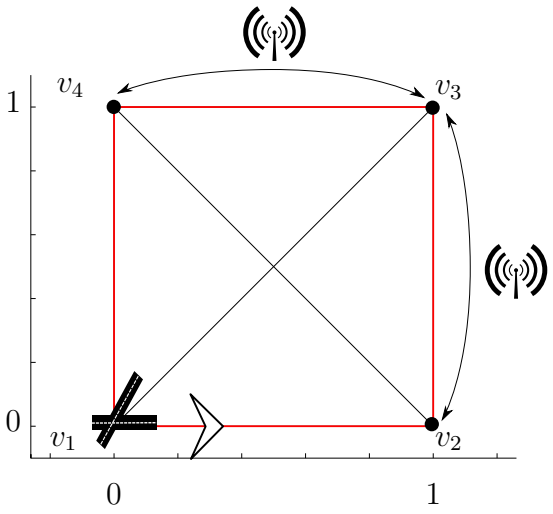

Figure 4.13: **Sequence-dependent TSP with intelligent adversary:** The scenario for the sequence-dependent TSP instance with communicating adversaries is shown.

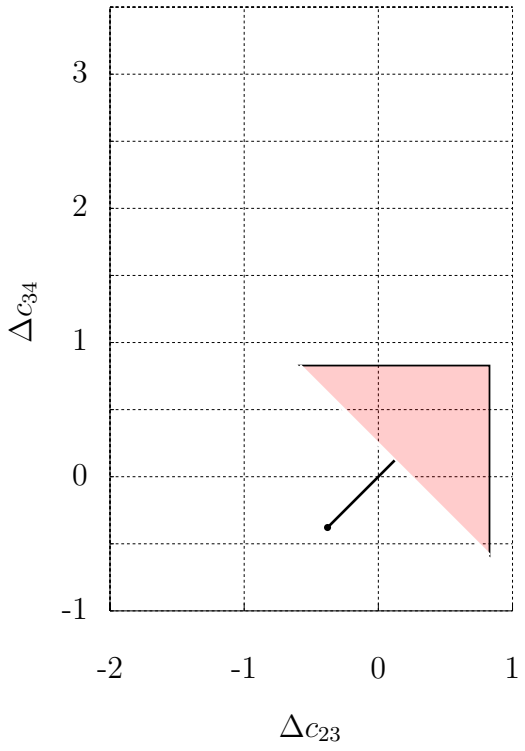

Figure 4.14: **Stability region without communication:** The stability region of the optimal tour is given for the case that the adversaries do not communicate. The problem is therefore not sequence-dependent.

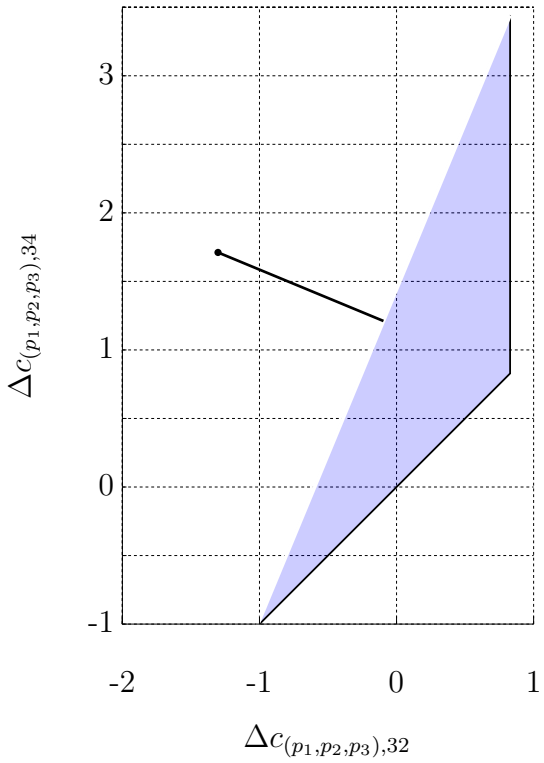

Figure 4.15: **Stability region with communication:** The stability region of the optimal tour is given for the case that the adversaries can communicate. The problem is sequence-dependent.

CHAPTER 5

Stability analysis for the minimum spanning tree problem

This chapter presents the exact stability analysis for solutions to minimum spanning tree problems with respect to perturbations in the edge costs. A description and a representation of the stability regions in half space representation are given. The derivation of edge cost tolerances from the stability regions is demonstrated and edge criticalities are defined. Furthermore, for eMSTs, the derivation of approximate stability regions with respect to perturbations in vertex locations, safe radii, and vertex criticalities are given. These are derived from the stability regions with respect to edge cost perturbations.

5.1 Problem formulation

The problem addressed in this chapter can be formulated as follows: Given a MST for a weighted graph, find the stability region of that MST and determine an expression to test whether arbitrary perturbations to the edge weights cause another spanning tree of that graph to be better than the current MST.

To solve this problem, necessary and sufficient conditions for the optimality of a MST from the literature [77] are exploited to obtain a half-space representation of the stability region of a MST. Using a small perturbation analysis, approximate stability

regions for eMSTs are derived for vertex location perturbations.

5.2 Stability regions of a MST

Let $\mathcal{ST}$ denote the set of all spanning trees for a graph. A naive approach to obtaining the stability region of a MST as defined in Problem Formulation 3.2.2 relies on total enumeration of all spanning trees of a graph. However, as $|\mathcal{ST}| = n^{n-2}$ this becomes intractable for reasonably sized problems. Another approach could be based on performing sensitivity analysis of the linear programming relaxation of the integer programming formulation of the MST problem. However, linear programming formulations of MST problems grow exponentially in size with the number of vertices. Building upon Lemma 1 in Ref. [77], a different approach is presented in the subsequent paragraphs.

Let MST be a minimum spanning tree on G, and let F denote the set of edges such that $\forall f \in F : f \notin \text{MST}$.

It is known that for a spanning tree of minimum total edge weight, the following must hold:

Lemma 5.2.1 ([77]). *MST is a minimum spanning tree of G if and only if, for each non-tree edge f, the weight of f is at least as large as the weight of any edge on the (unique) simple path in MST joining the ends of f. (In what follows we shall denote the path in MST joining the ends of f by MST(f).)*

Re-writing Lemma 5.2.1 as a set of inequalities yields:

$$\forall f : c(f) \geq c(e), \forall e \in \text{MST}(f). \tag{5.1}$$

The set of inequalities (5.1) provides necessary and sufficient conditions for the optimality of a spanning tree MST. To introduce perturbations to the weight of an edge

$c(e)$, let $\Delta c(e)$ denote a deviation in the edge weight of edge e. Then, the stability region of a MST with respect to changes in the edge weights is given by the following corollary:

Corollary 5.2.2. *Given perturbations $\Delta c(e)$ to the edge weights, MST remains a minimum spanning tree of G if and only if the following inequality is satisfied for each non-tree edge f:*

$$c(f) + \Delta c(f) \geq c(e) + \Delta c(e), \forall e \in MST(f), \tag{5.2}$$

where $c(e)$ and $c(f)$ denote the unperturbed weights of the respective edges.

Clearly, the stability region of a MST is a convex polyhedron in the space of weight changes and obtaining its half-space representation in matrix form is therefore desirable. Then, let the set E_f associated with a non-tree edge $f \in F$ denote the set of edges that are contained in the path MST(f) with an induced enumeration, i.e., the m-th element in E_f is the m-th element found when searching for elements of E_f in the set E, the set of all edges of the graph.

Hence, for each edge $f \in F$, the set of inequalities given by (5.2) can be written in matrix form:

$$U_f \cdot (c + \Delta c) \leq A_f \cdot (c + \Delta c), \tag{5.3}$$

where the q-th row of matrix U_f is vector u_q^T:

$$u_q = \begin{bmatrix} 0 & \dots & 0 & -1 & 0 & \dots & 0 \end{bmatrix}^T, \tag{5.4}$$

and the index of the non-zero entry in u_q is computed using (4.1) such that $\{i, j\}$ are the indices of the vertices $\{v_i, v_j\}$ covered by f. Furthermore, the q-th row of matrix A_f is vector a_q^T:

$$a_q = \begin{bmatrix} 0 & \dots & 0 & -1 & 0 & \dots & 0 \end{bmatrix}^T, \tag{5.5}$$

where the index of the non-zero entry is computed using (4.1) such that $\{i, j\}$ are the indices of the vertices $\{v_i, v_j\}$ covered by $E_f(q)$, i.e., the q-th edge in set E_f.

Then, concatenating all matrices U_f and A_f as follows:

$$U = \begin{bmatrix} U_1^T & U_2^T & \dots & U_{|F|}^T \end{bmatrix}^T, \tag{5.6}$$

and

$$A = \begin{bmatrix} A_1^T & A_2^T & \dots & A_{|F|}^T \end{bmatrix}^T, \tag{5.7}$$

yields:

$$U \cdot (c + \Delta c) \leq A \cdot (c + \Delta c). \tag{5.8}$$

Furthermore, let:

$$\overline{U} = U - A, \tag{5.9}$$

and:

$$\overline{q} = A \cdot c - U \cdot c. \tag{5.10}$$

Finally:

$$\overline{U} \cdot \Delta c \leq \overline{q}. \tag{5.11}$$

This gives the desired description of the stability region of a MST in its half-space representation in matrix form.

5.3 Properties of the MST stability region

In the following paragraphs, the dimensions of the elements in (5.11) are analyzed:

- $\Delta c \in \mathbb{R}^{|E|}$, where $|E| = \frac{1}{2} \cdot n \cdot (n-1) \approx O(n^2)$.
- $\overline{U} \in \mathbb{Z}^{\beta \times |E|}$, where β is bounded by:

  $\beta \leq (n-1)[\frac{1}{2} \cdot (n-1) \cdot (n-2)] \approx O(n^3)$, where $(n-1)$ is the number of edges

contained in the MST and $[\frac{1}{2} \cdot (n-1) \cdot (n-2)] = |F|$.

- Finally, $q \in \mathbb{R}^{\beta}$.

Hence, the number of elements to be stored for (5.11) is of order $O(n^5)$ and therefore polynomial in n, the cardinality of the set of vertices. Furthermore, the stability region of a MST is a convex polyhedron in the $|E|$ dimensional space of edge weight perturbations with at most $(n-1)[\frac{1}{2} \cdot (n-1) \cdot (n-2)] \approx O(n^3)$ facets.

By exploiting the sparsity of $\overline{U}$, representations of the stability region that scale more favorably with the size of the graph could be developed. [77] gives an efficient algorithm to construct the sets E_f.

5.4 Perturbations in a single edge

From the development of stability regions above, multiple measures of sensitivity can be derived. First, let us consider the robustness of the MST with respect to changes in the weight of a single edge. The edge weight tolerance is the supremum of weight increases of an edge (resp. infimum of weight decreases) under which a given MST remains optimal, provided the other edge weights in the graph are unchanged. This definition is analogous to the definition of edge cost tolerances in the context of TSPs in the previous chapter. Using (5.11), the edge weight tolerances can be computed using the same method as described above: To compute the tolerance for an arbitrary edge e_{ij}, with associated edge weight vector entry c_w, set $\Delta c_k = 0$ for all $k \neq w$. This immediately yields the tolerance Δc_w by identifying the most restrictive inequality resulting by row-wise evaluation of (5.11). Note, that for any edge e_{ij}, only the upper tolerance Δc_{ij}^{+} or the lower tolerance Δc_{ij}^{-} is finite. Intuitively, if an edge is in the MST, decreasing the weight of that edge decreases the weight of all spanning trees that contain that edge by the same amount. Hence, the original MST remains optimal. Similarly, if an edge is not part of the MST and the weight of that edge

increases, the weights of all spanning trees that contain that edge increase by the same amount and can therefore not be lower than the weight of the MST that does not contain that edge. An alternative way of computing tolerances for MSTs that does not require the construction of the stability region is given in Ref. [77].

The stability region of a MST can be understood as a margin of optimality of that MST with respect to arbitrary disturbances in edge weights and the edge tolerance as the margin of optimality with respect to a disturbance of the weight of a single edge. Once the stability region of a MST and the edge weight tolerances are known, it might be of interest to identify edges that are critical. Critical edge here refers to an edge for which the margin of optimality of the MST with respect to disturbances to the weight of that edge is smaller than the margin of optimality with respect to disturbances in the weight of other edges. Hence, a high criticality of an edge indicates that the MST is more susceptible to weight changes in that edge. Again, the notion of edge criticality and the development is analogous to Section 4.2.4. Let Δc^+_{min} denote the minimum upper edge weight tolerance for any edge and let Δc^-_{max} be the maximum lower edge weight tolerance for any edge.

Definition 5.4.1 (Δc^+_{min}, Δc^-_{max})**.** *Let:*

$$\Delta c^+_{min} = \min_{ij} \Delta c^+_{ij}, \tag{5.12}$$

$$\Delta c^-_{max} = \max_{ij} \Delta c^-_{ij}. \tag{5.13}$$

Then, χ_{ij} is a dimensionless parameter that characterizes the criticality of an edge and can be defined as follows:

Definition 5.4.2 (χ_{ij})**.** *For $1 \leq i, j \leq n$, the criticality of edge e_{ij} is defined as:*

$$\begin{cases} \chi_{ij} = \frac{\Delta c^+_{min}}{\Delta c^+_{ij}} & \Delta c^+_{min} \neq 0 \wedge |\Delta c^+_{ij}| < \infty, \\ \chi_{ij} = -\frac{\Delta c^-_{max}}{\Delta c^-_{ij}} & \Delta c^-_{max} \neq 0 \wedge |\Delta c^-_{ij}| < \infty. \end{cases} \tag{5.14}$$

For a minimal upper tolerance equal to zero, the criticality of edges with respect to weight increases is not defined and similarly, if the maximum lower tolerance is equal to zero, the criticality of edges with respect to weight decreases is not defined. Furthermore, a negative criticality χ_{ij} indicates that edge e_{ij} is not part of the MST and hence only weight decreases in that edge, if all other edge weights are held constant, can influence the optimal solution. Similarly, a positive criticality χ_{ij} indicates that edge e_{ij} is part of the MST and hence only weight increases in that edge, if all other edge weights are held constant, can influence the optimal solution.

5.5 Stability balls

The tolerances discussed above are defined with respect to perturbations in the weight of a single edge. However, other subsets of the stability region are also of interest in sensitivity analysis. This paragraph discusses the stability ball, i.e., the largest inscribed ball in the stability region that is centered at the origin. Hence, the stability ball provides sensitivity information with respect to simultaneous changes in the weights of multiple edges. The radius of the stability ball can be computed as follows:

$$\begin{aligned} \Delta r_{crit} = \underset{\Delta c}{\operatorname{argmin}} \quad & \|\Delta c\|_2 \\ \text{subject to} \quad & \overline{U} \cdot \Delta c = \overline{q}. \end{aligned} \tag{5.15}$$

Δr_{crit} can be interpreted in different ways. $\|\Delta r_{crit}\|_2$ gives a safe margin where any perturbation that is smaller than $\|\Delta r_{crit}\|_2$ in the L2-norm sense is guaranteed to not alter the optimal solution. The unit vector $\frac{\Delta r_{crit}}{\|\Delta r_{crit}\|_2}$ defines a critical direction and helps to identify the edge weights that the optimal solution is most susceptible to. This definition and interpretation is analogous to the notion of critical weights changes in Section 4.3.1 for solutions to wsmoTSP.

5.6 Approximate stability regions for eMST

For the eMST, the weight of a graph edge is the Euclidean distance between two vertices. In unmanned aircraft operations, the relative locations of the aircraft in a team vary over time. Hence, the robustness of a eMST with respect to the locations of the vertices is of interest. Therefore, the following sections studies stability regions of optimal solutions to eMST as stated in Definition 3.2.3 with respect to perturbations to the vertex locations. Following the same derivation as in Section 4.2.5, a first order approximation of the stability region of an optimal solution to an eMST with respect to the vertex location disturbance vector is given through substitution of the linearized relationship in (4.17) between vertex location perturbations Δp and the edge weight perturbations Δc into (5.11) by the polyhedron:

$$\overline{U} \cdot A \cdot \Delta p \leq \overline{q}. \tag{5.16}$$

5.7 Perturbations in the location of a single vertex for eMST

Similarly to the derivation of vertex location stability regions for eTSP, stability regions with respect to vertex location perturbations for the eMST are obtained through linearization assuming small perturbations. The notion of a safe radius can be introduced to be more conservative. The minimal perturbation in the L2 norm sense, $\Delta p_{w,min}$, in the location of a single vertex v_w that lies on the boundary of the

linearized stability region is computed as follows:

$$\begin{aligned} \Delta p_{w,min} = \underset{\Delta p_w}{\operatorname{argmin}} \quad & \|\Delta p_w\|_2 \\ \text{subject to} \quad & \overline{H} A \Delta p = -\overline{q}, \\ & \Delta p_k = 0, \ \forall k \neq w. \end{aligned} \tag{5.17}$$

Definition 5.7.1 ($r_{w,safe}$)**.** *Let $r_{w,safe}$ be the radius of the largest circle centered at the nominal location of vertex v_w that is fully contained in the stability region associated with vertex v_w with respect to perturbations of the location of v_w obtained through linearization assuming that all other vertices are located at their nominal locations.*

Hence, $r_{w,safe}$ can be computed as:

$$r_{w,safe} = \|\Delta p_{w,min}\|_2. \tag{5.18}$$

The unit vector $\frac{\Delta p_{w,min}}{\|\Delta p_{w,min}\|_2}$ gives the direction in which the least magnitude in change in location for vertex v_w can be tolerated before another spanning tree is better, assuming all other vertices remain at their nominal locations.

To ease interpretation by a human operator, a vertex criticality measure is defined as follows: Let ξ_w denote the criticality of a vertex v_w. Furthermore, let $r_{min,safe}$ denote the smallest of all safe radii:

$$r_{min,safe} = \min_w r_{w,safe}. \tag{5.19}$$

Then the criticality of vertex v_w can be computed as follows:

$$\begin{cases} \xi_w = \frac{r_{min,safe}}{r_{w,safe}} & r_{w,safe} > 0, \\ \xi_w = \infty & \text{otherwise.} \end{cases} \tag{5.20}$$

This definition is equivalent to the definition for eTSPs above. Note that, if $\exists w$: $r_{w,safe} = 0$, vertex criticalities cannot be defined.

5.8 Example

Recall the motivating UAV communication network example in Section 1.3.4. Three UAVs survey an area of interest by following elliptical flight paths counterclockwise at a speed that results in the same period for each orbit. Fig 5.1 depicts the trajectory $v_{i,inertial}(t)$ of each aircraft with respect to an inertial frame. The initial location $v_{i,inertial}(0)$ of aircraft i at time 0 and its flight path azimuth are indicated by the black arrows.

While performing this mission all aircraft must maintain communication links between each other such that each aircraft can receive data from any other aircraft by means of single or multi hop communication while minimizing the transmission power. The transmission power to establish a connection between any pair of aircraft is inversely proportional to a power of the Euclidean distance between these aircraft. An optimal communication topology with respect to the cumulative transmission power in this case is a minimum spanning tree on the communication graph, where the UAVs correspond to the vertices of that graph and the weight of an edge of that graph corresponds to the distance between the two vertices covered by that edge. Specifically, this MST is an Euclidean MST (eMST), where the edge weight c_{ij} is the Euclidean distance between the vertices v_i and v_j. The initial MST T_0 is depicted by the dotted lines connecting the black arrows in Fig 5.1.

As the aircraft follow their flight paths, their relative positions with respect to each other change. This results in changing weights of the edges of the communication graph over time. Fig 5.2 depicts the stability region of T_0 with respect to changes in the edge weights and Fig 5.3 shows the projection of that stability region onto

the $\Delta c_{23}/\Delta c_{13}$ plane. The black solid lines in Figs. 5.2, 5.3 depict the trajectory of the edge weight changes starting at the origin in the direction of the black arrow as the aircraft perform one complete orbit. Upon reaching point a, indicated by the + symbol, the trajectory exits the stability region of T_0. Hence, T_0 is not a minimum spanning tree anymore. In Fig 5.1, the corresponding positions of the three aircraft along their trajectories are indicated and the new minimum spanning tree is shown. As the aircraft reach the respective locations denoted b along the flight path, the trajectory of weight changes in Figs. 5.2, 5.3 re-enters the stability region of T_0. Hence, as shown in Fig 5.1, the optimal communication topology changes and T_0 is a minimum spanning tree again for the remainder of the period.

This example is chosen to be small in order to allow for a visualization of the complete stability region in the space of edge weight changes. However, as shown in Section 5.3, the demonstrated methods scale favorably with the number of aircraft. Similarly, the stability region does not depend on the trajectories of the aircraft but only on the initial locations and therefore the chosen elliptical flight paths are representative for a wide range of possible trajectories.

Finally, Fig 5.4 demonstrates the concepts developed in Sections 5.6 and 5.4. First, an approximation of the stability region in the space of location changes of the UAV is obtained through linearization about the initial locations as described in Section 5.6. This results in a six dimensional stability region. For visualization purposes, the following frame is chosen: Its origin 0_{team} is collocated with the location of UAV 1 $v_{1,inertial}(t)$ and the abscissa of the frame is parallel to the vector $v_{2,inertial}(t) - v_{1,inertial}(t)$. The ordinate of the team frame completes a right hand frame. Fig 5.4 depicts the trajectories of the UAVs with respect to the team frame. UAV 1 and UAV 2 are stationary with respect to that frame. Hence, a two-dimensional cut through the stability region in the space of location changes suffices to visualize the trajectories of the UAVs with respect to the stability region as any relative movement

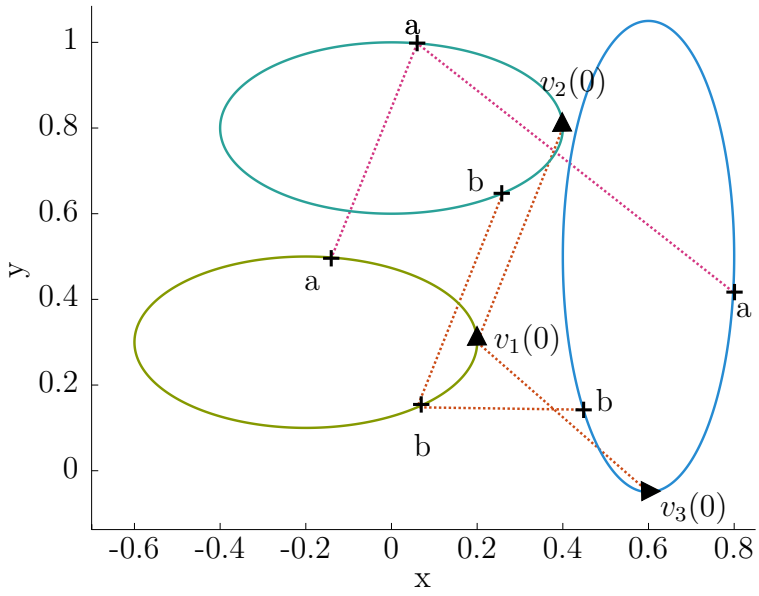

Figure 5.1: **Communication topology planning in inertial frame:** The initial locations and flight path azimuths of the 3 aircraft $v_i(0)$ with respect to the inertial frame are indicated by the black arrows. The elliptical flights paths are also shown. Furthermore, the MSTs at the initial locations and for the UAVs at the locations denoted a and b along their respective trajectories are depicted by the dotted lines.

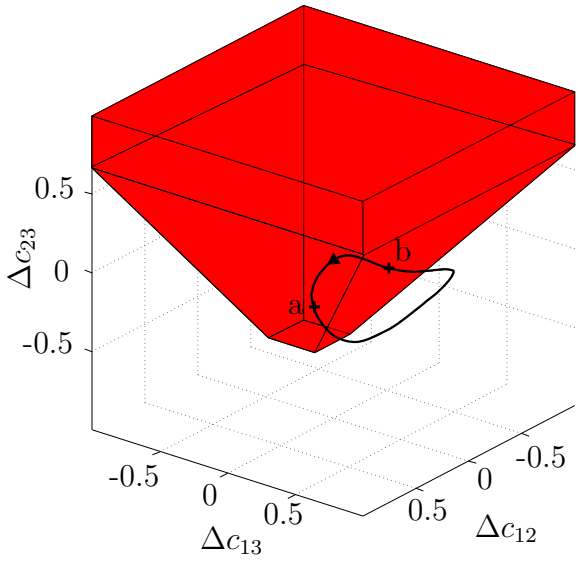

Figure 5.2: **Stability region of the initial MST:** The stability region of spanning tree T_0 with respect to changes in the edge weights is depicted. The black solid line shows the trajectory of the edge weight changes starting at the origin in the direction of the black arrow as the aircraft perform one complete orbit leaving the stability region at point a and re-entering it at point b. For visualization purposes, this figure shows the intersection of the stability region with a cube of 2 units edge length centered at the origin.

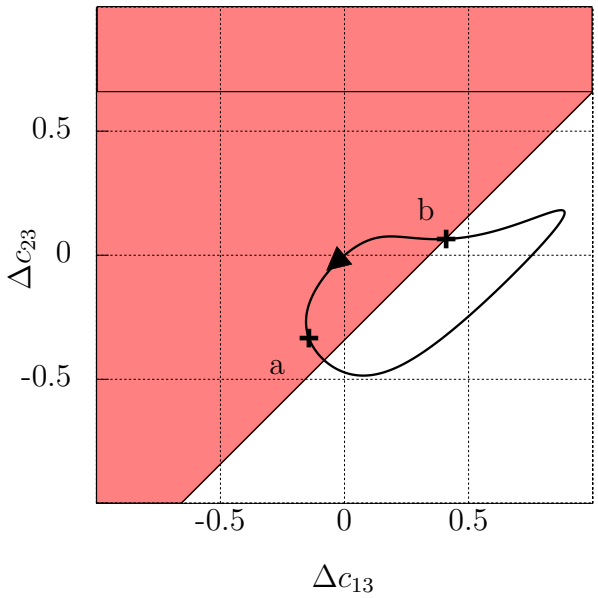

Figure 5.3: **Projection of the stability region of the initial MST:** The projection of the stability region of spanning tree T_0 with respect to changes in the edge weights onto the $\Delta c_{23}/\Delta c_{13}$ plane is shown. The black solid line shows the trajectory of the edge weight changes starting at the origin in the direction of the black arrow as the aircraft perform one complete orbit, leaving the stability region at point a and re-entering it at point b.

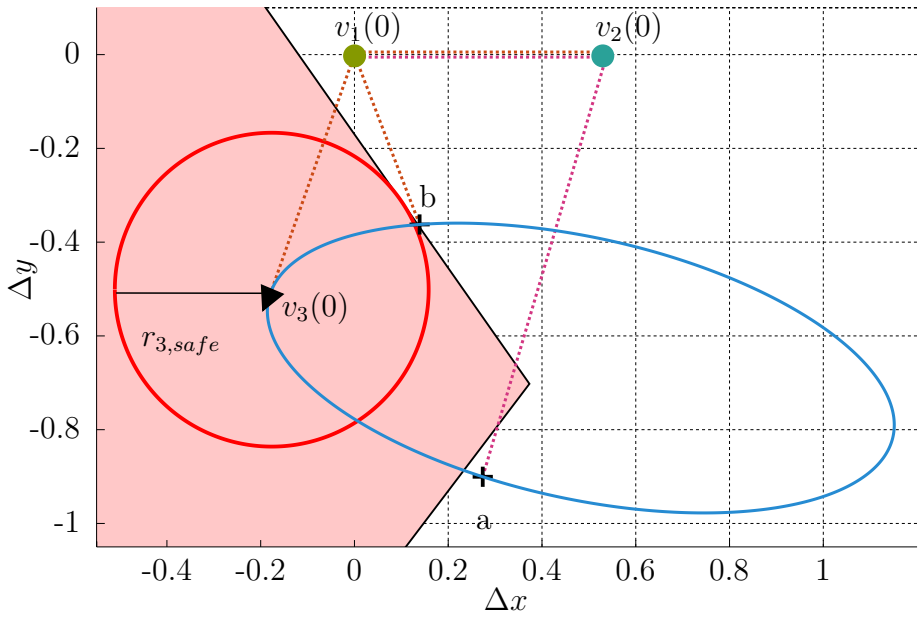

Figure 5.4: **Stability region of initial MST in non inertial frame:** The trajectories of the aircraft are depicted with respect to a right-hand frame whose origin 0_{team} is collocated with $v_{1,inertial}(t)$ and whose abscissa is parallel to the vector $v_{2,inertial}(t) - v_{1,inertial}(t)$. The ordinate of the team frame completes a right hand frame. The red polyhedron depicts a cut through the linearized stability region with respect to location changes of UAV 3, Δv_3, offset by $p_{3,inertial}(0) - p_{1,inertial}(0)$. The red circle is centered at $p_{3,team}(0)$ with radius $r_{3,safe}$. Points a and b along the trajectory of UAV 3 indicate where T_0 becomes suboptimal and regains optimality respectively. The dotted lines depict the respective minimum spanning trees.

is completely captured by the trajectory of UAV 3. The red polyhedron depicts the cut through the linearized stability region with respect to location changes of UAV 3, Δv_3, offset by $p_{3,inertial}(0) - p_{1,inertial}(0)$. The red circle is centered at $p_{3,team}(0)$ with radius $r_{3,safe}$ as defined in Section 5.4. Again, points a and b along the trajectory of UAV 3 indicate where T_0 becomes suboptimal and regains optimality respectively and the dotted lines depict the respective minimum spanning trees.

CHAPTER 6

Approximate stability analysis for the traveling salesman problem

This chapter addresses the problem of approximate stability analysis for solutions to symmetric non sequence-dependent traveling salesman problems. Over and under approximations of the stability region of optimal solutions are given. Upper and lower bounds on edge cost tolerances and approximate edge criticalities are derived from the approximate stability regions. For the special case of the eTSP, approximate stability regions with respect to perturbations in vertex locations are shown to be obtainable from the approximate stability region in edge cost perturbations. Based on these, approximate safe radii and vertex criticalities are defined.

6.1 Intractability of exact stability analysis

Chapter 4 gives a method to compute stability regions of an optimal tour with respect to an arbitrary set of tours. If that set of tours is chosen to be $\mathcal{T}$, the set of all tours, the method in Chapter 4 gives the exact stability region of the optimal tour. From that exact stability region, exact edge cost tolerances can be derived as shown in Section 4.2.3. However, this approach to obtaining exact edge cost tolerances for instances of the symmetric non sequence-dependent TSP becomes intractable for large instances. This thesis only considers complete graphs and therefore $|\mathcal{T}| = \frac{(n-1)!}{2}$. In

a fully connected graph, there exist $2\frac{(n-2)!}{2} = (n-2)!$ tours $T' \in \mathcal{T} : e_{ij} \in T'$ and $\frac{(n-1)!}{2} - (n-2)! = \frac{(n-3)(n-2)!}{2}$ tours $T \in \mathcal{T} : e_{ij} \notin T$. Hence, computing Δc_{ij}^{+} for an edge $e_{ij} \in T^{\star}$ requires the evaluation of $\frac{(n-3)(n-2)!}{2}$ inequalities. Computing Δc_{ij}^{-} for an edge $e_{ij} \notin T^{\star}$ requires the evaluation of $(n-2)!$ inequalities. The edge cost tolerance problem for the TSP is NP–hard [79] and it is not possible to check in polynomial time whether an optimal TSP tour is still optimal after an arbitrary change in the cost of a single edge occurs unless $P = NP$ [8]. Even determining an ϵ-approximation Δc_{w}^{+} given $0 \leq \epsilon \leq 1$ of the tolerances such that $(1-\epsilon)\Delta c_{w}^{+} \leq \Delta c_{w}^{+} \leq \Delta c_{w}^{+}$ for all edges is not possible in polynomial time. ϵ-approximations of lower tolerances are likewise not obtainable in polynomial time unless $P = NP$ [8]. The method in Chapter 4 for obtaining the exact stability region of an optimal tour relies on total enumeration of all tours in $\mathcal{T}$. Hence, obtaining exact stability regions following that method becomes computationally prohibitive as n becomes large. Indeed, it is not possible to check in polynomial time whether an optimal TSP tour is still optimal after the cost of an arbitrary set of edges has been changed unless $P = NP$ [8]. This result is closely related to the problem of finding the stability region of an optimal tour.

Let $\lambda \in \mathbb{R}^{|E|}$ be vector, where $\sum_{i=1}^{|E|} \lambda_i = 1$ and $\forall i : \lambda_i \geq 0$. Let $r_{\lambda} \in \mathbb{R}$ be a scalar such that r_{λ} is the solution to the following optimization problem:

Problem formulation 6.1.1 (Directed stability problem)**.** *Given a fully connected undirected graph $G(V, E)$, an edge cost vector c, a shortest tour $T^{\star}$, and a vector $\lambda \in \mathbb{R}^{|E|}$, find r_{λ} such that:*

$$
\begin{aligned}
r_\lambda = \underset{r,y}{\text{maximize}} \quad & r \\
\text{subject to} \quad & yr\lambda \in \mathbf{\Delta}(T^\star), \\
& (1-y)r\lambda \in \mathbf{\Delta}(T^\star), \\
& y \in \{0,1\}, \\
& r_\lambda \geq 0.
\end{aligned}
\tag{6.1}
$$

The stability decision problem for the TSP along a given direction can be stated as follows:

Problem formulation 6.1.2 (Directed stability decision problem)**.** *Given a fully connected undirected graph $G(V,E)$, an edge cost vector c, a shortest tour $T^\star$, a vector $\lambda \in \mathbb{R}^{|E|}$, and a scalar $B \in \mathbb{R}$, is r_λ at most B?*

This is a generalization of the tolerance decision problem that is NP–complete [79]. Therefore, the directed stability decision problem for the TSP along a given direction λ is NP–hard. Hence, determining the exact value r_λ along a given direction is at least as hard as the decision problem and therefore is NP–hard [90]. Finally, the problem of obtaining the stability region for the TSP is NP–hard, as it is a generalization of the problem of determining the exact value r_λ along a given direction and hence at least as hard as that problem. The results in Refs. [8, 79] also imply that an ϵ-approximation of the stability region is not obtainable by a polynomial time method, where an ϵ-approximation of the stability region would allow for the computation of ϵ-approximate tolerances using the method in Section 4.2.3.

Hence, this chapter focuses on computationally tractable stability region approximations. Methods for over and under approximation without tightness guarantees in the ϵ sense but rather heuristic reasoning regarding the approximation quality are given.

6.2 Problem formulation

The problems addressed in this chapter can be formulated as follows:

- Given an instance of the TSP, and letting $T^\star$ denote the best tour within $\mathcal{T}$, find an efficient method to obtain an over approximation of the stability region of $T^\star$ with respect to $\mathcal{T}$ such that for any perturbation to the edge costs outside of that over approximation there exists a better tour than $T^\star$ in $\mathcal{T}$.
- Given an instance of the TSP, and letting $T^\star$ denote the best tour within $\mathcal{T}$, find an efficient method to obtain an under approximation of the stability region of $T^\star$ with respect to $\mathcal{T}$ such that for any perturbation to the edge costs within that under approximation there does not exist a better tour than $T^\star$ in $\mathcal{T}$.

6.3 Over approximation

This section develops a general method to over approximate the stability regions of an optimal tour $T^\star$, gives heuristic guidelines on how to obtain a good over approximation, and presents one specific way of obtaining an over approximation of the stability region of an optimal tour that follows the guidelines for obtaining a good over approximation.

6.3.1 Over approximation by subsets

Define the following sets:

- Let $\mathcal{T}'$ denote a subset of $\mathcal{T}$ that does not contain $T^\star$, i.e., $\mathcal{T}' \subseteq \mathcal{T} \setminus T^\star$.
- Let W denote the set of edges that are contained in $T^\star$ and not contained in at least one tour in $\mathcal{T}'$, i.e., $W = \{\{e : e \in T^\star\} \cap \{e : \exists T \in \mathcal{T}', e \notin T\}\}$.

- Let M denote the set of edges that are not contained in $T^\star$ and contained in at least one tour in $\mathcal{T}'$, i.e., $M = \{\{e : e \notin T^\star\} \cap \{e : \exists T \in \mathcal{T}', e \in T\}\}$.

Let Δc" be a vector of cost changes to edges that are contained in the sets W or M, i.e., $\forall i : e_i \notin W \cup M, \Delta c_i" = 0$. Then, let $\mathbf{\Delta}"(T^\star)$ denote the stability region of $T^\star$ with respect to cost changes only in edges contained in W or M, assuming all other edge costs remain unchanged:

$$\forall \Delta c" \in \mathbf{\Delta}"(T^\star), \forall T' \in \mathcal{T}, L(T^\star(\Delta c")) \leq L(T'(\Delta c")). \tag{6.2}$$

Then, by considering only the subset of tours $\mathcal{T}'$:

$$\forall \Delta c" \in \overline{\mathbf{\Delta}"}(T^\star), \forall T' \in \mathcal{T}', L(T^\star(\Delta c")) \leq L(T'(\Delta c")), \tag{6.3}$$

an over approximation of $\mathbf{\Delta}"(T^\star)$ is obtained.

Proposition 6. $\mathbf{\Delta}"(T^\star) \subseteq \overline{\mathbf{\Delta}"}(T^\star)$.

Proof. Let $\Delta c" \notin \overline{\mathbf{\Delta}"}(T^\star)$. $\implies \exists T' \in \mathcal{T}' : L(T'(\Delta c")) < L(T^\star(\Delta c")) \implies \Delta c" \notin \Delta"(T^\star)$. This completes the proof by contrapositive. □

Hence, using any subset $\mathcal{T}'$, an over approximation of the stability region with respect to changes in the costs of specific edges can be obtained using the method outlined in Section 4.2 by only considering the subset.

6.3.2 Heuristic guidelines

As discussed in Section 6.1, giving guarantees on the tightness of approximation in the sense of an ϵ-approximation as introduced above is hard. Trivially, letting $\mathcal{T}' = \mathcal{T} \setminus T^\star$ gives the exact stability region. However, this becomes intractable for larger instances. This section provides heuristic guidelines on how to choose a subset $\mathcal{T}'$ that gives a good approximation of the stability region:

1. "Coverage": As shown in Proposition 6, an approximate stability region constructed using the method only allows for cost changes that are contained in either M or W. Hence, a good set $\mathcal{T}'$ should be chosen such that the resulting sets of edges M and W satisfy $M \cup W = E$. Intuitively, if $e \in T^\star$, then e must not be contained in at least one tour in $\mathcal{T}'$ as otherwise a cost increase of that edge does not affect optimality of $T^\star$ with respect to $\mathcal{T}'$ as the length of all tours in the subset increase by the same amount. Similarly, if $e \notin T^\star$, then e must be contained in at least one tour in $\mathcal{T}'$ as otherwise a cost decrease of that edge does not affect optimality of $T^\star$ with respect to $\mathcal{T}'$ as the decrease in cost of that edge does not affect the length of any tour in $\mathcal{T}'$ while $L(T^\star)$ remains unchanged.

2. "Tightness": Each tour included in $\mathcal{T}'$ adds an inequality to the halfspace representation of the approximate stability region. For a good approximation these inequalities need to be tight. The tightness of the inequalities depends on the length difference between the tour that gives the inequality and $L(T^\star)$. Hence, all tours included in $\mathcal{T}'$ should be short tours.

6.3.3 Over approximation by $\mathcal{T}_2$

Let the 2-neighborhood of a tour T be the set of all tours obtained by permutation of any two cities in the tour T. Specifically, let $\mathcal{T}_2$ denote the 2-neighborhood of the optimal tour $T^\star$. $\mathcal{T}' = \mathcal{T}_2$ gives an over approximation of the stability region of $T^\star$ and $\mathcal{T}_2$ fulfills both criteria given above for a good set of tours:

1. Coverage of $\mathcal{T}_2$ is ascertained by the following two lemmas, where the nomenclature is clarified in Fig. 6.1:

   Lemma 6.3.1. $\forall e, \exists T \in \mathcal{T}_2 : e \in T$.

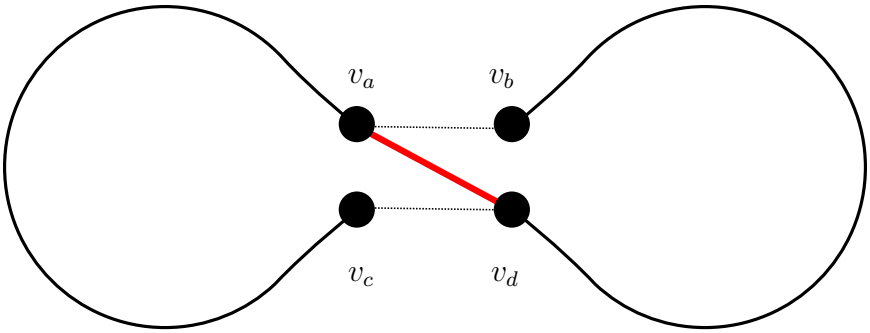

Figure 6.1: **An optimal tour:** This figure depicts an optimal tour $T^\star$ that contains vertices v_a, v_b, v_c, v_d.

Proof. Assume $\forall T \in \mathcal{T}_2, \exists e_{ad}$: $e_{ad} \notin T \implies \exists v_b$ adjacent to v_a and v_c adjacent to v_d such that $e_{a,b} \in T^\star$ and $e_{c,d} \in T^\star$. Deleting $e_{a,b}$ and $e_{c,d}$ from $T^\star$ and adding e_{bc} and e_{ad} gives a tour T' and $T' \in \mathcal{T}_2$. □

Lemma 6.3.2. $\forall e, \exists T \in \mathcal{T}_2 : e \notin T$.

Proof. First, consider edges that are contained in $T^\star$: Assume $\forall T \in \mathcal{T}_2, \exists e_{ab} \in T^\star : e_{ab} \in T$. Then, pick an arbitrary $e_{cd} \in T^\star$. Deleting e_{ab} and e_{cd} from $T^\star$ and adding e_{cb} and e_{ad} gives a tour T' and $T' \in \mathcal{T}_2$. Second, consider edges that are not contained in $T^\star$: Assume $\forall T \in \mathcal{T}_2, \exists e_{ad} \notin T^\star$, s.t. $e_{a,d} \notin T$. However, $\exists v_b$ adjacent to v_a and v_c adjacent to v_d such that $e_{ab} \in T^\star$ and $e_{cd} \in T^\star$. Deleting e_{ab} and e_{cd} from $T^\star$ and adding e_{cb} and e_{ad} gives a tour T' and $T' \in \mathcal{T}_2$.

□

Hence, $M \cup W = E$.

2. Tightness of the inequalities that result from considering $\mathcal{T}_2$ cannot be guaranteed. Indeed, $\mathcal{T}_2$ is not a set of best tours for almost all instances. However, tours in the 2-neighborhood of $T^\star$ are typically good tours. In the literature [75], it has been observed that many good tours share a significant amount of edges which has led to the study of backbones of TSP tours. This supports the notion

of permuting the least possible number of edges starting with the optimal tour to create a set of good tours. Specifically, for an instance of the TSP, the length of a tour $T \in \mathcal{T}_2$ can be computed as follows: $L(T) = L(T^\star) - c_i - c_j + c_k + c_l$, where $e_i, e_j \in T^\star \setminus T$ and $e_k, e_l \in T \setminus T^\star$. Let:

$$c_{min} = \min_{c_{ij} \in T^\star} c_{ij}, \tag{6.4}$$

$$c_{min_2} = \min_{c_{ij} \in T^\star \setminus c_{min}} c_{ij}. \tag{6.5}$$

Similarly, let

$$c_{max} = \max_{c_{ij} \notin T^\star} c_{ij}, \tag{6.6}$$

$$c_{max_2} = \max_{c_{ij} \notin T^\star \setminus c_{max}} c_{ij}. \tag{6.7}$$

Then, the maximal difference in tour length between $T \in \mathcal{T}_2$ and $T^\star$ can be bounded by:

$$\Delta L \leq -c_{min} - c_{min_2} + c_{max} + c_{max_2}. \tag{6.8}$$

Hence, for instances where edge lengths are of similar order of magnitude, tours in the two neighborhood of the optimal tour are good tours. Conversely, an over approximation of the stability region based on $\mathcal{T}_2$ is likely to be better if the difference $\Delta c = \max c(e) - \min c(e)$ between the maximum cost edge and the minimum cost edge in the graph is small.

An alternative approach of selecting a set of tours by choosing $\mathcal{T}'$ to be the k-best tours in $\mathcal{T}$ has been studied in Ref. [83] in the context of over approximating edge cost tolerances. While satisfying the tightness requirement, this approach does not guarantee coverage. Furthermore, solving the k-best TSP is computationally hard, whereas the 2-neighborhood can be constructed efficiently in post-processing after obtaining $T^\star$. As $|\mathcal{T}_2| = O(n^2)$, this approach scales favorable with n.

6.3.4 Over approximation of edge cost tolerances

An over approximation and hence an upper bound on the upper tolerance and a lower bound on the lower tolerance for edge cost tolerances with respect to $\mathcal{T}$ can be computed as follows: Consider the over approximation of the stability region of $T^\star$ obtained by considering $\mathcal{T}_2$ given in half-space representation. Using the method outlined in Section 4.2.3, the desired approximate tolerances can be computed by identifying the most restrictive inequalities for each edge.

6.4 Under approximation

This section develops a general method to under approximate the stability regions of an optimal tour $T^\star$ based on a relaxation. Let Z^* be the optimal solution to a relaxation of the traveling salesman problem on $G(V, E)$. Then, its length is $L(Z^\star)$, and $L(Z^\star) \leq L(T^\star)$ because it is a relaxation. Let $\mathcal{Z}$ denote the set of all feasible solutions to that relaxation or the traveling salesman problem on that graph. The cost of a feasible solution to the relaxed problem changes to $L(Z(\Delta c))$ if the edge costs of the graph are perturbed by Δc. Let $\mathbf{\Delta}(Z^\star)$ denote the stability region of $Z^\star$:

$$\forall \Delta c \in \mathbf{\Delta}(Z^\star), \forall Z' \in \mathcal{Z}, L(Z^\star(\Delta c)) \leq L(Z'(\Delta c)). \tag{6.9}$$

Then, introduce the following sets of edges:

- Let P denote the set of edges that are contained in $T^\star$ and $Z^\star$: $P = \{e : e \in T^\star \cap e \in Z^\star\}$.
- Let Q denote the set of edges that are only contained in $T^\star$: $Q = \{e : e \in T^\star \cap e \notin Z^\star\}$.
- Let R denote the set of edges that are only contained in $Z^\star$: $R = \{e : e \in Z^\star \cap e \notin T^\star\}$.

- Let S denote the set of edges that are contained in neither $T^\star$ nor $Z^\star$. $S = \{e : e \notin T^\star \cap e \notin Z^\star\}$.

Let $L(A)$ denote the sum of the costs of the edges $e \in A$ for an arbitrary set of edges A. Note that $L(T^\star) = L(P) + L(Q)$ and $L(Z^\star) = L(P) + L(R)$. Let $L(A(\Delta c))$ denote the sum of the costs of edges that are contained in set A under cost perturbation Δc. Let $\Delta\tilde{c}$ be a vector of cost changes to edges that are in P or S, i.e., $\forall i : e_i \notin P \cup S, \Delta\tilde{c}_i = 0$. Hence, only edges that are either contained in both $T^\star$ and $Z^\star$, or in neither are perturbed. Let $\tilde{\mathbf{\Delta}}(T^\star)$ denote the stability region of $T^\star$ with respect to cost changes only in edges contained in P or S, assuming all other edge costs remain unchanged:

$$\forall \Delta\tilde{c} \in \tilde{\mathbf{\Delta}}(T^\star), \forall T' \in \mathcal{T}, L(T^\star(\Delta\tilde{c})) \leq L(T'(\Delta\tilde{c})). \tag{6.10}$$

Let $\tilde{\mathbf{\Delta}}(Z^\star)$ denote the stability region of $Z^\star$ with respect to cost changes only in edges contained in P or S, assuming all other edge costs remain unchanged:

$$\forall \Delta\tilde{c} \in \tilde{\mathbf{\Delta}}(Z^\star), \forall Z' \in \mathcal{Z}, L(Z^\star(\Delta\tilde{c})) \leq L(Z'(\Delta\tilde{c})). \tag{6.11}$$

Let $\tilde{\mathbf{\Delta}}'(Z^\star)$ denote a subset of $\tilde{\mathbf{\Delta}}(Z^\star)$, such that:

$$\forall \Delta\tilde{c} \in \tilde{\mathbf{\Delta}}'(Z^\star), \forall Z' \in \mathcal{Z},$$
$$L(Z^\star(\Delta\tilde{c})) + (L(T^\star) - L(Z^\star)) \leq L(Z'(\Delta\tilde{c})) \tag{6.12}$$

Note that $(L(T^\star) - L(Z^\star)) \geq 0$, because $Z^\star$ is a relaxation. The following is then claimed:

Proposition 7. $\tilde{\mathbf{\Delta}}'(Z^\star) \subseteq \tilde{\mathbf{\Delta}}(T^\star)$.

Proof. 1. Let $\Delta\tilde{c} \notin \tilde{\mathbf{\Delta}}(T^\star)$.

2. $\exists T'(\Delta\tilde{c}) \in \mathcal{T}$ such that $L(T'(\Delta\tilde{c}))$ is minimal.

3. $L(T^\star(\Delta\tilde{c})) > L(T'(\Delta\tilde{c}))$ because of step 1.

4. $L(P(\Delta\tilde{c})) + L(Q) > L(T'(\Delta\tilde{c}))$. Note that $L(Q) = L(Q(\Delta\tilde{c}))$. Similarly, $L(R) = L(R(\Delta\tilde{c}))$.

5. Let $Z'(\Delta\tilde{c})$ be the optimal solution to the relaxed problem under perturbation $\Delta\tilde{c}$.

6. $L(P(\Delta\tilde{c})) + L(Q) > L(T'(\Delta\tilde{c})) \geq L(Z'(\Delta\tilde{c}))$ because it is a relaxation.

7. $L(P(\Delta\tilde{c})) + L(Q) + L(R) - L(R) > L(Z'(\Delta\tilde{c}))$.

8. $L(P(\Delta\tilde{c})) + L(R) + L(Q) - L(R) > L(Z'(\Delta\tilde{c}))$.

9. $L(Z^\star(\Delta\tilde{c})) + L(Q) - L(R) > L(Z'(\Delta\tilde{c}))$.

10. $L(Z^\star(\Delta\tilde{c})) + L(P) + L(Q) - L(P) - L(R) > L(Z'(\Delta\tilde{c}))$.

11. $L(Z^\star(\Delta\tilde{c})) + (L(T^\star) - L(Z^\star)) > L(Z'(\Delta\tilde{c}))$.

12. $\Delta\tilde{c} \notin \tilde{\mathbf{\Delta}}'(Z^\star)$ because of step 11.

This completes the proof by contrapositive. □

The following observations can be made. The notions of coverage and tightness discussed above for over approximations are also applicable in the case of under approximations. Here, coverage is directly related to the cardinality of sets Q and R. If both, Q and R, are empty, $T^\star$ and $Z^\star$ contain the same set of edges. Therefore, the under approximation in this case is valid for perturbations in all edges in E. The notion of tightness is reflected by the term $(L(T^\star) - L(Z^\star))$, i.e., the closer the value of the optimal solution to the traveling salesman problem to the value of the optimal solution to the relaxed problem, the better the under approximation obtained from the relaxation. A similar observation regarding the tightness of approximation is made in Ref. [79] for the special case of obtaining approximate tolerances for the traveling salesman problem from relaxations.

The following sections discuss the minimum 1-tree relaxation of the TSP and methods to obtain the stability region of a minimum 1-tree (M1T).

6.4.1 The M1T relaxation

A 1-tree is a spanning tree with an additional edge:

Definition 6.4.1 ($1T_k$)**.** *Let $G(V, E)$ be a fully connected undirected graph consisting of a vertex set V of cardinality $|V| = n$ and an edge set E. Each edge $e_{ij} \in E$ has an associated edge weight $c(e) \in \mathbb{R}$. Let $v_k \in V$ be an arbitrarily chosen vertex. Let $G_1(V_{MST_k}, E_{MST_k})$ denote the subgraph of $G(V, E)$, where $V_{MST_k} = V \setminus v_k$ and $E_{MST_k} = \{\{u, v\} \in E : u, v \in V_{MST_k}\}$. Let $E_k = E \setminus E_{MST_k}$. For any $e_1, e_2 \in E_k$: $e_1 \neq e_2$, and spanning tree ST on $G_1(V_{MST_k}, E_{MST_k})$, the set $1T = ST \cup \{e_1, e_2\}$ is a 1-tree in G.*

Given a weighted graph, a minimum 1-tree can be defined:

Definition 6.4.2 (Minimum 1-tree)**.** *A minimum 1-tree $M1T_k$ on the graph G is a 1-tree on G such that the sum of the weights of the edges contained in any other 1-tree on G is not greater than the sum of the weights of the edges contained in $M1T_k$ for a given vertex v_k.*

The M1T problem is a well known relaxation of the TSP and was first studied by Held and Karp in Ref. [92]. Note that every tour is a 1-tree, but the converse is not true. Hence, the M1T problem is a relaxation of the TSP. In Ref. [84], it is argued that the 1-tree relaxation of the TSP gives lower bounds of the tolerances for the TSP. The following sections explore approximate stability regions that can be obtained from the 1-tree relaxation.

6.4.2 Derivation of stability regions for M1T

Based on the following necessary and sufficient optimality condition for a M1T, a polyhedral description of the stability region of a M1T in half-space form is derived in the following paragrahs:

Proposition 8 (Optimality 1-tree [92])**.** *A 1-tree* $1T$ *is a minimum 1-tree* $M1T_k$ *in* G *if and only if* e_1 *and* e_2 *are the shortest edges incident to vertex* v_k *and* MST_k *is a minimum spanning tree in* $G_1(V_{MST_k}, E_{MST_k})$*.*

The problem of choosing the two shortest vertices incident to v_k is a combinatorial optimization problem. Let $M2E_k$ denote the solution to that problem. The stability region $\mathbf{\Delta}(M1T_k)$ of a minimum 1-tree $M1T_k$ can be composed of the stability region of MST_k on G_1, i.e., $\mathbf{\Delta}(MST_k)$, and the stability region $\mathbf{\Delta}(M2E_k)$ of $M2E_k$ with respect to weight changes of all edges incident to v_k.

Corollary 6.4.3 ($\mathbf{\Delta}(M1T_k)$)**.**

$$\mathbf{\Delta}(M1T_k) = \mathbf{\Delta}(MST_k) \cap \mathbf{\Delta}(M2E_k). \tag{6.13}$$

Proof. This follows from Proposition 8 □

The stability region of a MST has been discussed in detail in Chapter 5. To use Corollary 6.4.3 to obtain the stability region of a M1T, the following paragraph derives $\mathbf{\Delta}(M2E_k)$ in half-space representation.

6.4.2.1 Stability region $E2_k$

Let $E_k = E \setminus E_{MST_k}$ denote the set of edges incident to v_k. Let $ME2_k$ be the two least weight edges in E_k. Finally, let $\overline{ME2_k} = E_k \setminus ME2_k$. Then, a solution $ME2_k$ is optimal if and only if:

$$\forall f \in \overline{ME2_k} : c(f) \geq c(e), \forall e \in ME2e_k. \tag{6.14}$$

The set of inequalities (6.14) provides necessary and sufficient conditions for the optimality of a solution $ME2_k$ and is reminiscent of (5.1) for minimum spanning trees. Hence, similar steps are carried out to obtain the stability region in half-space representation. To introduce perturbations to the weight of an edge $c(e)$, let $\Delta c(e)$ denote a deviation in the edge weight of edge e. Then, the stability region of a solution $ME2_k$ with respect to changes in the edge weights is given by the following corollary:

Corollary 6.4.4. *Given perturbations $\Delta c(e)$ to the edge weights, $ME2_k$ remains optimal if and only if, for each edge $f \in \overline{ME2_k}$, the following inequality is satisfied:*

$$c(f) + \Delta c(f) \geq c(e) + \Delta c(e), \forall e \in ME2_k, \tag{6.15}$$

where $c(e)$ and $c(f)$ denote the unperturbed weights of the respective edges.

Hence, for each edge $f \in \overline{ME2_k}$, the set of inequalities given by (6.15) can be written in matrix form:

$$U_f^{E2_k} \cdot (c + \Delta c) \leq A_f^{E2_k} \cdot (c + \Delta c), \tag{6.16}$$

where the q-th row of matrix $U_f^{E2_k}$ is vector u_q^T:

$$u_q = \begin{bmatrix} 0 & \dots & 0 & -1 & 0 & \dots & 0 \end{bmatrix}^T, \tag{6.17}$$

and the index of the non-zero entry in u_q is computed using (4.1) such that $\{i, j\}$ are the indices of the vertices $\{v_i, v_j\}$ covered by f.

Furthermore, the q-th row of matrix $A_f^{E2_k}$ is vector a_q^T:

$$a_q = \begin{bmatrix} 0 & \dots & 0 & -1 & 0 & \dots & 0 \end{bmatrix}^T, \tag{6.18}$$

where the index of the non-zero entry is computed using (4.1) such that $\{i, j\}$ are the indices of the vertices $\{v_i, v_j\}$ covered by $ME2_k(q)$, i.e., the q-th edge in set $ME2_k$.

Then, concatenating all matrices $U_f^{E2_k}$ and $A_f^{E2_k}$ as follows:

$$U^{E2} = \begin{bmatrix} {U_1^{E2_k}}^T & {U_2^{E2_k}}^T & \dots & {U_{|\overline{ME2_k}|}^{E2_k}}^T \end{bmatrix}^T, \tag{6.19}$$

and

$$A^{E2_k} = \begin{bmatrix} {A_1^{E2_k}}^T & {A_2^{E2_k}}^T & \dots & {A_{|\overline{ME2_k}|}^{E2_k}}^T \end{bmatrix}^T, \tag{6.20}$$

yields:

$$U^{E2_k} \cdot (c + \Delta c) \leq A^{E2_k} \cdot (c + \Delta c). \tag{6.21}$$

Furthermore, let:

$$\overline{U}^{E2_k} = U^{E2_k} - A^{E2_k}, \tag{6.22}$$

and:

$$q^{E2_k} = A^{E2_k} \cdot c - U^{E2_k} \cdot c. \tag{6.23}$$

Finally:

$$\overline{U}^{E2_k} \cdot \Delta c \leq \overline{q}_{E2_k}. \tag{6.24}$$

This gives the desired description of the stability region of a solution $ME2_k$ in its half-space representation in matrix form.

6.4.3 Stability regions for M1T in half-space representation

Using the method in Chapter 5 for minimum spanning trees, the stability region of MST_k on the subgraph $G_1(V_{MST_k}, E_{MST_k})$, where k denotes an arbitrary vertex $v_k : v \in V \cap v \notin E_{MST_k}$, is given by:

$$\overline{U}^{T1_k} \cdot \Delta c \leq \overline{q}^{T1_k}. \tag{6.25}$$

Hence, using corollary 6.4.3, the stability region of a minimum 1-tree $\mathbf{\Delta}(M1T_k)$ using the notation given above can be written as:

$$\begin{bmatrix} \overline{U}^{T1_k} \\ \overline{U}^{ME2_k} \end{bmatrix} \cdot \Delta c \leq \begin{bmatrix} \overline{q}^{T1_k} \\ \overline{q}^{E2_k} \end{bmatrix}, \tag{6.26}$$

where k denotes the choice vertex $v_k \in V$. Finally, for ease of notation, the matrix $\overline{U}^{M1T_k}$ and vector $\overline{q}^{M1T_k}$ are introduced such that:

$$\overline{U}^{M1T_k} \cdot \Delta c \leq \overline{q}^{M1T_k}. \tag{6.27}$$

6.4.4 Properties of stability regions of M1T

Given a graph with n vertices, G_1 has $|V_{MST_k}| = n - 1$ vertices, $|E_{MST_k}| = \frac{(n-1)(n-2)}{2}$ edges, and $|E_k| = n - 1$. The stability region of an optimal pair of edges $ME2_k$ is given by $2 \cdot (n-1-2) \approx O(n)$ inequalities. Furthermore, the stability region of MST_k is a convex polyhedron in the $|E_{MST_k}|$ dimensional space of edge weight perturbations with at most $((n-1)-1)[\frac{1}{2} \cdot ((n-1)-1) \cdot ((n-1)-2)] = \frac{n^3}{2} - \frac{7n^2}{2} + 8n - 6 \approx O(n^3)$ facets. Finally, the stability region of $M1T_k$ is a convex polyhedron in the $|E|$ dimensional space of edge weight perturbations with at most $\frac{n^3}{2} - \frac{7n^2}{2} + 10n - 12 = O(n^3)$ facets.

6.4.5 Under approximation of a TSP stability using the M1T stability region

Utilizing $\mathbf{\Delta}(M1T_k)$ given by (6.27) to obtain an under approximation of the stability region $\mathbf{\Delta}(T^\star)$ of an optimal tour $T^\star$ requires the following two additional steps as given in Section 6.4:

1. Let:

$$\overline{q}'^{M1T_k} = \max(\overline{q}^{M1T_k} - \overrightarrow{1} \cdot (L(T^\star) - L(M1T_k), \overrightarrow{0}), \tag{6.28}$$

where the max operator is applied element wise and $\overrightarrow{1}$ and $\overrightarrow{0}$ are column vectors of ones and zeros of appropriate length. This yields the intermediate polyhedron

$$\overline{U}^{M1T_k} \cdot \Delta c \leq \overline{q}'^{M1T_k}. \tag{6.29}$$

2. The sets P_k, Q_k , R_k, and S_k as defined in Sec. 6.4 need to be determined. To obtain a representation with respect to the cost vector c rather than the vector of restricted cost changes $\Delta\tilde{c}_k$, two inequalities are added for each edge $e_w \notin P_k \cup S_k$ to the half-space representation of the form:

$$\begin{aligned} -\Delta c_w &\leq 0, \\ \Delta c_w &\leq 0. \end{aligned} \tag{6.30}$$

These inequalities can be expressed in vector form and appended to (6.29), yielding:

$$\tilde{U}^{M1T_k} \cdot \Delta c \leq \tilde{q}'^{M1T_k}. \tag{6.31}$$

Eq. (6.31) gives $\tilde{\mathbf{\Delta}}'(M1T_k)$. As shown above $\tilde{\mathbf{\Delta}}'(M1T_k) \subseteq \tilde{\mathbf{\Delta}}(T^\star)$, where $\tilde{\mathbf{\Delta}}(T^\star)$ is the stability region of the optimal tour $T^\star$ for cost changes in edges that are contained in P_k or S_k. With respect to the concept of coverage for under approximations

introduced in Section 6.4, it is interesting to note that an optimal tour usually has many edges in common with a minimum 1-tree. As reported in Ref. [85], an optimal tour normally contains between 70% and 80% of the edges of a minimum 1-tree on that graph.

6.4.6 Under approximation of a TSP stability region by unions of M1T stability regions

As the selection of vertex v_k when obtaining $\tilde{\mathbf{\Delta}}'(M1T_k)$ is arbitrary, $\forall k, \tilde{\mathbf{\Delta}}'(M1T_k) \subseteq \tilde{\mathbf{\Delta}}(T^\star)$ and the following holds:

$$\bigcup_{k=1}^{|V|} \tilde{\mathbf{\Delta}}'(M1T_k) \subseteq \tilde{\mathbf{\Delta}}'(T^\star). \tag{6.32}$$

One can obtain $|V| = n$ sets of inequalities that each give an under approximation of the stability region of the optimal tour $T^\star$ with respect to edges that are contained in the respective sets P_k or S_k. As outlined in Sec. 6.4, tightness and coverage are metrics that can help assess the quality of an under approximation. By considering the union of all $\tilde{\mathbf{\Delta}}'(M1T_k)$, one can potentially assess optimality with respect to a wider range of affected edges as the sets P_k and S_k vary. Furthermore, if only a small set of edges is affected by cost changes, they might be contained in P_k or S_k for multiple k and hence, with respect to that specific cost perturbation, a tighter under approximation of the stability region might be achievable.

6.4.7 Under approximation of edge cost tolerances

Using (6.31), an under approximation and hence a lower bound on the upper tolerance and an upper bound on the lower tolerance for edge cost tolerances with respect to $\mathcal{T}$ can be computed as follows: Consider an under approximation of the stability region of $T^\star$ given in half-space representation (6.31). Using the method outlined

in Section 4.2.3, the desired approximate tolerances can be computed by identifying the most restrictive inequalities for each edge. Similarly, when using (6.32), an under approximation of edge cost tolerances for edges can be obtained from each of the under approximations. Then, vertex v_k can be chosen for each edge such that the magnitude of the resulting under approximation of the edge cost tolerance is maximized and a tighter under approximation may be achievable.

6.5 Approximate vertex location stability based on approximate stability regions for eTSPs

Section 4.2.5 derives approximate stability regions of solutions to eTSPs with respect to perturbations in the vertex locations derived from stability regions with respect to edge cost perturbations through the relationship given in (4.17). Using this relationship approximate stability regions with respect to vertex location perturbations can also be obtained from approximate stability regions with respect to edge cost perturbations.

The method described in Section 4.2.5 is directly applicable to an over approximation of the stability region of an optimal tour in half space representation, as for example derived in Sec. 6.3.3 based on the 2-neighborhood. Similarly, the application of the method described in Section 4.2.5 to an under approximation of the stability region obtained by considering $M1T_k$ as defined in Sec. 6.4.5 is possible by substituting (4.17) into (6.31). Again, by considering all choices of k one can obtain multiple approximate stability regions with respect to vertex location perturbations.

6.6 Criticalities

Chapter 4 defines edge criticalities based on the exact edge cost tolerances in Section 4.2.4. Furthermore, vertex criticalities are derived from stability regions with respect to vertex location perturbations for instances of eTSPs in Section 4.2.6. The following paragraphs present analogous concepts based on approximate stability regions.

6.6.1 Approximate edge criticality based on approximate tolerances

Edge criticality is a dimensionless parameter that allows for the comparison of the upper and lower cost tolerances of edges in an intuitive manner. A high criticality of an edge indicates that the optimal tour is more susceptible to cost changes in that edge given that the cost of all other edges is held constant. Assume that over/under approximations of the edge cost tolerances are available (For example through the method described in Section 6.3.4/Section 6.4.7). Let $\tilde{\Delta}c_{ij}^{+}$ denote approximate upper edge cost tolerances and let $\tilde{\Delta}c_{ij}^{-}$ denote approximate lower edge cost tolerances. Then, define $\tilde{\Delta}c_{min}^{+}$ to be the minimum upper bound/lower bound on the upper edge cost tolerance for any edge and let $\tilde{\Delta}c_{max}^{-}$ be maximum lower bound/upper bound on the lower edge cost tolerance for any edge.

Definition 6.6.1 ($\tilde{\Delta}c_{min}^{+}$, $\tilde{\Delta}c_{max}^{-}$)**.** *Let:*

$$\tilde{\Delta}c_{min}^{+} = \min_{ij} \tilde{\Delta}c_{ij}^{+}, \tag{6.33}$$

$$\tilde{\Delta}c_{max}^{-} = \max_{ij} \tilde{\Delta}c_{ij}^{-}. \tag{6.34}$$

Then, $\tilde{\chi}_{ij}$ is a dimensionless parameter that characterizes the approximate criticality of an edge and can be defined as follows:

Definition 6.6.2 ($\tilde{\chi}_{ij}$)**.** *For $1 \leq i, j \leq n$, the criticality of edge e_{ij} is defined as:*

$$\begin{cases} \tilde{\chi}_{ij} = \frac{\tilde{\Delta}c^{+}_{min}}{\tilde{\Delta}c^{+}_{ij}} & \tilde{\Delta}c^{+}_{min} \neq 0 \wedge |\tilde{\Delta}c^{+}_{ij}| < \infty, \\ \tilde{\chi}_{ij} = -\frac{\tilde{\Delta}c^{-}_{max}}{\tilde{\Delta}c^{-}_{ij}} & \tilde{\Delta}c^{-}_{max} \neq 0 \wedge |\tilde{\Delta}c^{-}_{ij}| < \infty. \end{cases} \tag{6.35}$$

Note that for a minimal approximate upper tolerance equal to zero the criticality of edges with respect to cost increase is not defined and similarly, if the maximum approximate lower tolerance is equal to zero, the criticality of edges with respect to cost decreases is not defined. The interpretation is similar to Section 4.2.4. A negative approximate criticality $\tilde{\chi}_{ij}$ indicates that edge e_{ij} is not part of the optimal tour and hence only cost decreases in that edge, if all other edge costs are held constant, can influence the optimal solution. Similarly, a positive approximate criticality $\tilde{\chi}_{ij}$ indicates that edge e_{ij} is part of the optimal tour and hence only cost increases in that edge, if all other edge costs are held constant, can influence the optimal solution.

As there exist cases for which edge criticalities cannot be defined, approximate edge criticalities based on over approximations of the edge cost tolerances seem more practicable.

6.6.2 Approximate vertex criticality based on approximate stability regions

For eTSPs the notion of of vertex criticalities and safe radii introduced in Sec. 4.2.6 based on the linearized exact stability region of $T^{\star}$ with respect to vertex location perturbations are defined. Similarly, one can obtain approximate vertex criticalities and safe radii based on the linearized approximate stability region of $T^{\star}$ with respect to vertex location perturbations as defined in Section 6.5.

Given k approximations of the stability region with respect to vertex perturbations derived from either k over approximations of the stability region with respect

to edge cost perturbations or k under approximations of the stability region with respect to edge cost perturbations, $\Delta p_{w,min,k}$ associated with vertex v_w is computed for each approximation k using (4.19). Note, over and under approximations cannot be considered simultaneously. Then, the approximate safe radius is given by:

$$\tilde{r}_{w,safe} = \max_{k}(\|\Delta p_{w,min,k}\|_2). \tag{6.36}$$

Furthermore, let $\tilde{r}_{w,safe}$ denote the smallest of all approximate safe radii:

$$\tilde{r}_{min,safe} = \min_{w} \tilde{r}_{w,safe}. \tag{6.37}$$

Finally, the approximate criticality of vertex v_w can be computed as follows:

$$\tilde{\xi}_w = \frac{\tilde{r}_{min,safe}}{\tilde{r}_{w,safe}}. \tag{6.38}$$

Note that, if $\exists w : \tilde{r}_{w,safe} = 0$, vertex criticalities cannot be defined.

As there exist cases for which vertex criticalities cannot be defined, approximate vertex criticalities based on approximations of the stability region with respect to vertex perturbations derived from over approximations of the stability region with respect to edge cost perturbations seem more practicable.

6.7 Examples

The following sections demonstrate the application of the methods discussed above to instances of a 6-vertex eTSP.

6.7.1 Assessment of approximations by ellipsoids

First, a method to assess properties of approximations of stability regions is presented. Means to compare the stability region with approximations of it are necessary. Stability regions are polyhedra in the space of cost changes. However, comparing polyhedra is a computationally challenging problem. This section focuses on giving a qualitative assessment rather than a rigorous numerical analysis. Therefore, the following computationally tractable approach is chosen to compare polyhedra.

The largest inscribed ellipsoid contained in each polyhedron is computed. The problem of finding the largest inscribed ellipsoid in a polyhedron can be formulated as a convex optimization problem [93]. Given a polyhedron $P = \{\Delta c : \overline{H}\Delta c \leq \overline{q}\}$, the largest inscribed ellipsoid $E = \{Bu + d | \|u\|_2 \leq 1\}$ is the solution to the following problem:

$$\begin{aligned} \underset{B,d}{\text{maximize}} \quad & \log\det B \\ \text{subject to} \quad & ||B \cdot \overline{h}_i||_2 + \overline{h}_i^T d \leq \overline{q}_i,\ i = 1, \ldots, m, \\ & B \succ 0. \end{aligned} \tag{6.39}$$

where $\overline{h}$ denote rows of matrix $\overline{H}$.

The size of the two resulting ellipsoids is then compared. A frequently used measure of size of ellipsoids is the sum of the squared semi-axis lengths, which is given by the trace of $(B^T B)$ [94]. The matrix $(B^T B)$ is often called the shape matrix of the ellipsoid. Let r denote the length of a semi-axis of the ellipsoid. Then, the following holds:

$$\sum_{i=1} r_i^2 = \text{trace}(B^T B). \tag{6.40}$$

Let $\hat{r}$ denote the length of the semi-axis of the largest inscribed ellipsoid in the approximate stability region, and let r be the length of the semi-axis of the largest inscribed ellipsoid in the actual stability region. The following quantity ϕ is defined

to compare the approximate stability region with the actual stability region:

$$\phi = \frac{\sum_i \hat{r}_i^2 - \sum_i r_i^2}{\sum_i r_i^2}. \tag{6.41}$$

The larger ϕ, the more dissimilar the polyhedra. The closer to zero, the more similar the polyhedra. As the stability region associated with a tour is not a closed set, only a closed subset of the stability region is considered for comparison. The polyhedron $P_{normalize} = \{\Delta c : -c \leq \Delta c \leq c\}$ is defined. Given the polyhedron P_{stab} representing the actual stability region and the polyhedron P_{approx} representing the approximate stability region, the largest inscribed ellipsoids are found for the polyhedra resulting from the intersection $P_{stab} \cap P_{normalize}$ and $P_{approx} \cap P_{normalize}$. ϕ is then computed to assess the similarity of $P_{stab} \cap P_{normalize}$ and $P_{approx} \cap P_{normalize}$.

6.7.2 Over approximation by subsets of tours

This method is now used to assess over approximations of the stability region of an optimal tour $T^\star$ by consideration of a subset of tours $\mathcal{T}'$. Recall that each tour can be represented as a vector h of zeros and ones as given in Definition 4.2.2. Let h_r denote the vector representation of the r-th tour and let $h^\star$ be the vector representation of the optimal tour $T^\star$. The relatedness ω_r of a tour T_r with the optimal tour $T^\star$ is defined as:

$$\omega_r = \frac{\langle h_r, h^\star \rangle}{\|h^\star\|_1}. \tag{6.42}$$

Let $\mathcal{T}_{related}$ denote the set $\mathcal{T} \setminus T^\star$ in which the tours are enumerated such that the following holds: $\forall T_r \in \mathcal{T}_{related}, \omega_r \leq \omega_{r+1}$. Hence, by choosing the first $|\mathcal{T}_2|$ tours from $\mathcal{T}_{related}$ as a subset $\mathcal{T}'$, $\mathcal{T}' = \mathcal{T}_2$.

Finally, let $\mathcal{T}_{related,sorted}$ denote the set of tours in which tours are enumerated with respect to the following criterion $\zeta_r = [\omega_r, L(T_r)]$ that is evaluated in lexicographic

order. Then it holds that $\forall T_r \in \mathcal{T}_{related,sorted}, \zeta_r \leq \zeta_{r+1}$. In other words, tours are first ordered by their relatedness and then by their length.

100 random instances of a 6-vertex eTSP are generated, where the coordinates of each vertex are sampled from a uniform distribution on the unit square $[0, 1] \times [0, 1]$. Fig. 6.2 depicts ϕ over k, where $k = |\mathcal{T}'|$, i.e., the cardinality of the subset of tours $\mathcal{T}'$ used to construct an over approximation of the stability region. Four different subset generation methods are compared:

1. Let $\mathcal{T}'$ be a set of k randomly selected tours.

2. Let $\mathcal{T}'$ be the set of k-best solutions.

3. Let $\mathcal{T}'$ be the set of the first k tours in $\mathcal{T}_{related}$.

4. Let $\mathcal{T}'$ be the set of the first k tours in $\mathcal{T}_{related,sorted}$.

The black vertical line at $k = 9$ indicates $k = |\mathcal{T}_2|$, i.e., the value for which the first k tours in $\mathcal{T}_{related}$ and $\mathcal{T}_{related,sorted}$ are equal to the two neighborhood of $T^\star$. The following observations can be made from the figure. All four approximation methods achieve better approximation quality the larger the value of k. The random set selection performs worst with respect to the chosen metric. The k-best approach is better. The approaches based on the relatedness of tours perform best and show a rapid convergence to $\phi \approx 0$, i.e., the value for which the approximation and the actual stability region are indistinguishable with respect to the chosen metric. Indeed, this is achieved for $k = 9$, i.e., the value for k for which $k = |\mathcal{T}_2|$ and $\mathcal{T}' = \mathcal{T}_2$. Obtaining over approximations based on the two neighborhood of an optimal tour was suggested in Section 6.3.3 as it satisfies the heuristic guidelines for choosing a subset choice technique outlined in Section 6.3.2.

Fig. 6.3 depicts ϕ over k for Euclidean 6-vertex TSP depicted in Fig. 4.1.

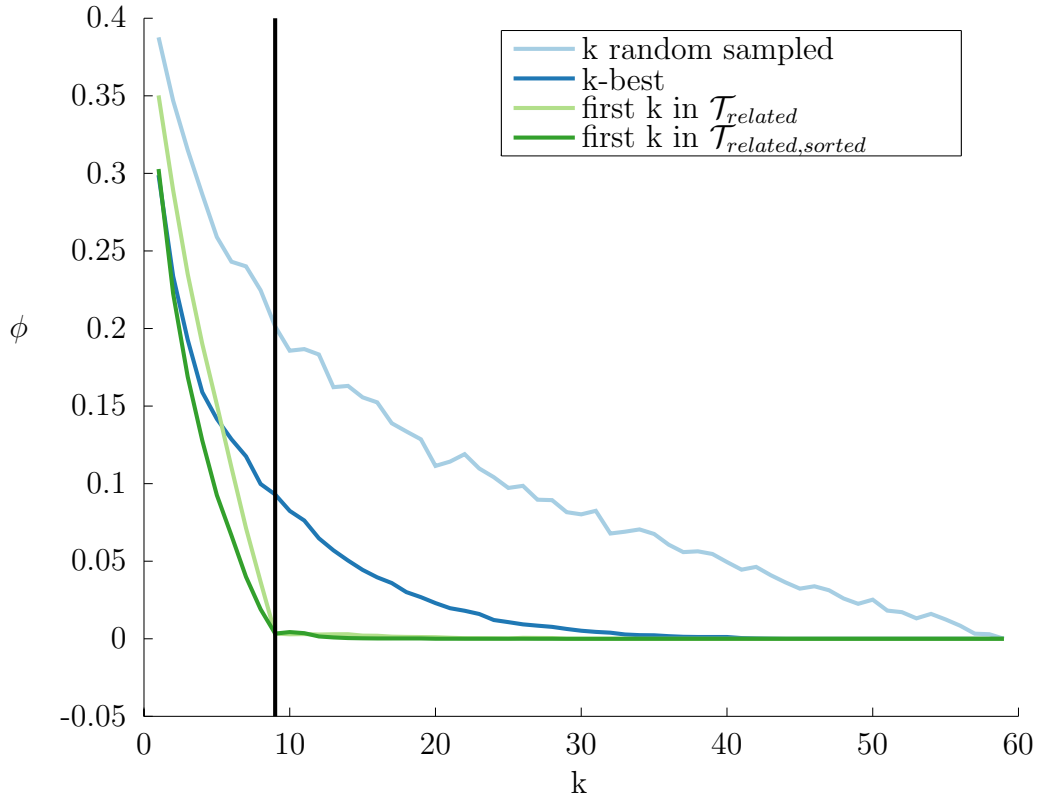

Figure 6.2: **Average approximation quality:** This figure depicts depicts ϕ versus k for 100 random instances of a 6-vertex eTSP, where the coordinates of each vertex are sampled from a uniform distribution on the unit square $[0,1] \times [0,1]$. $k = |\mathcal{T}'|$, i.e., the cardinality of the subset of tours $\mathcal{T}'$ used to construct an over approximation of the stability region and ϕ is the similarity measure defined in (6.41). Four different subset generation methods are compared.

6.7.3 Under approximation by M1Ts

Section 6.4.6 introduces the use of the M1T relaxation to obtain under approximations of the stability region of a solution to the traveling salesman problem. Specifically, the use of the union of stability regions of multiple $M1T_k$ is suggested, where multiple trees can be generated by choice of vertex v_k. The choice of vertex v_k defines the subgraph $G_1(V_{MST_k}, E_{MST_k})$ and the set of edges E_k. Fig. 6.4 depicts the M1Ts (in red) on the graph for the symmetric Euclidean 6-vertex TSP in Section 4.7.1. The complete graph for this problem is shown in Fig. 4.1. In each of the subfigures in

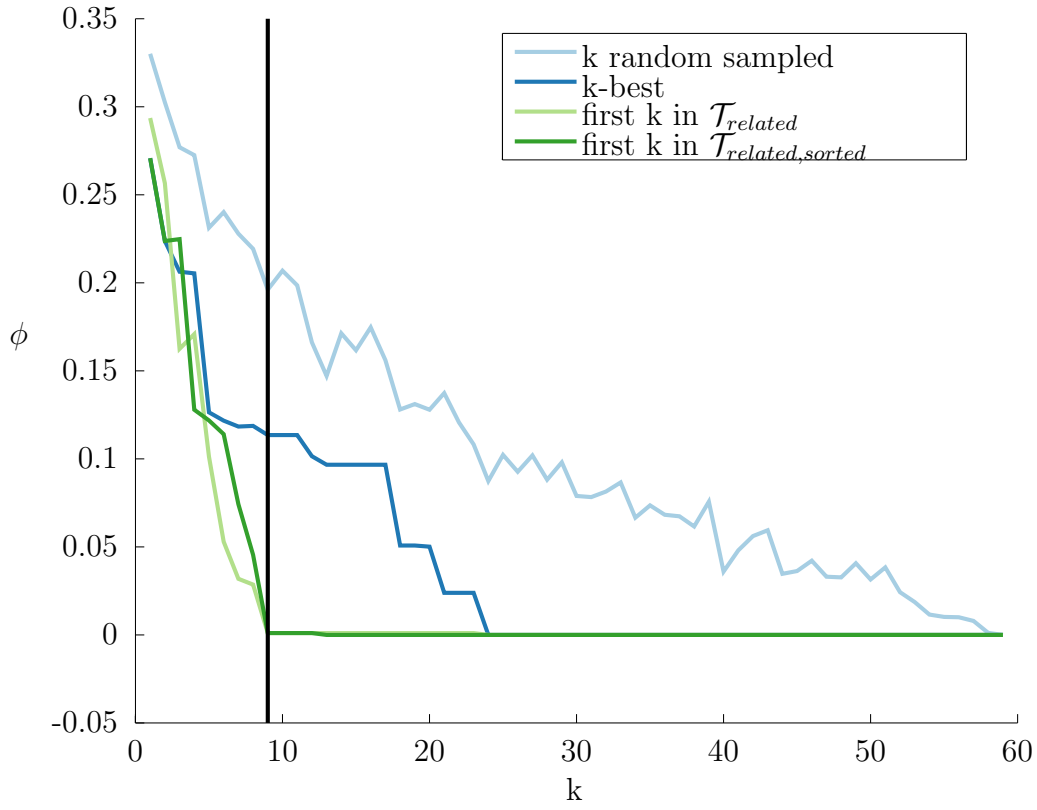

Figure 6.3: **Approximation quality:** This figure depicts depicts ϕ versus k for the 6-vertex eTSP shown in Fig. 4.1. $k = |\mathcal{T}'|$, i.e., the cardinality of the subset of tours $\mathcal{T}'$ used to construct an over approximation of the stability region and ϕ is the similarity measure defined in (6.41). Four different subset generation methods are compared.

Fig. 6.4 the black dot indicates the choice of vertex v_k. The blue edge indicates an edge that is contained in the optimal tour $T^\star$ but not in the minimum 1-tree $M1T_k$. Note that even though the set of edges contained in $M1T_3$ is equal to the set of edges contained in $M1T_4$ for example, the obtainable stability information may be different.

6.7.4 Over and under approximation of edge cost tolerances

Over and under approximations of edge cost tolerances can be computed from approximate stability regions as shown in Section 6.3.4 and Section 6.4.7 respectively. In this section, exact edge cost tolerances, over approximations of the edge cost tolerances

based on an over approximation of the stability region based on the 2-neighborhood, and under approximations of the edge cost tolerances based on the $M1T_k$ approach are obtained for the 6-vertex Euclidean TSP depicted in Section 4.7.1, for which the optimal tour is shown in Fig. 4.1. Let Δc^+ denote the upper edge cost tolerance, $\overline{\Delta} c^+$ denote the over approximation of an upper edge cost tolerance, and $\underline{\Delta} c^+$ denote the under approximation of an upper edge cost tolerance. Similarly, let c^- denote the lower edge cost tolerance, $\overline{c}^-$ denote the over approximation of a lower edge cost tolerance, and $\underline{c}^-$ denote the under approximation of an lower edge cost tolerance.

Fig. 6.5 provides a qualitative assessment of the under and over approximation of edge cost tolerances by these two specific methods. Edges contained in the optimal tour (red) are labeled as follows: $[\frac{\underline{\Delta} c^+}{\Delta c^+}, \frac{\overline{\Delta} c^+}{\Delta c^+}]$. Similarly, edges that are not contained in the optimal tour are labeled: $[\frac{\underline{c}^-}{\Delta c^-}, \frac{\overline{c}^-}{\Delta c^-}]$. For under approximations all six M1Ts are considered and the maximizer of the magnitude of the under approximation is chosen as described in Section 6.4.7. The figure shows that the upper bound on upper edge cost tolerances is close to the actual tolerance in all cases and equal to the actual tolerance in most cases for this instance. The under approximations of the edge cost tolerances are good, where some are close to the actual value, two are equal to the actual value, and all but one attain at least 30% of the actual value. The average under approximation is 55% of the actual value.

Table 6.1 and table 6.2 show the numerical values for the approximate and exact upper and lower edge cost tolerances respectively. Table 6.3 and table 6.4 give the numerical value of the under approximation of the upper and lower edge cost tolerances for each choice of v_k. As can be seen from the data, considering all choices of v_k and choosing the one that maximizes the magnitude of the under approximation for each edge individually is beneficial when obtaining under approximations of edge cost tolerances.

For completeness, considering stability regions rather than tolerances, the numer-

ical values of the similarity metric as defined in (6.41) are as follows. The similarity value of the over approximation of the stability region is $\phi_{over} = 0.001$. The over approximation is similar to the actual stability region. As expected, a good over approximation of the stability region leads to a good over approximation of edge cost tolerances as shown in Fig. 6.5. The average similarity value of all 6 under approximations of the stability region is $\phi_{under} = -0.42$. Finally, table 6.5 gives the value of ϕ_{under} for each choice of v_k.

The above examples suggest that approximating the stability region by means of an over approximation based on the 2-neighborhood of an optimal tour is promising. It is easy to construct once the optimal solution to the problem instance is known, does not require the solution of any additional optimization problems, and the achievable approximation quality is high for the examples shown. If an under approximation is required, considering the unions of stability regions of $M1T_k$ relaxations is a viable approach.

	e_{12}	e_{16}	e_{23}	e_{34}	e_{45}	e_{56}
$\overline{\Delta}c^+$	43.70	84.60	76.85	81.78	114.37	43.70
Δc^+	43.70	80.78	76.85	81.78	114.37	43.70
$\underline{\Delta}c^+$	43.70	33.63	23.23	28.63	56.76	19.50

Table 6.1: Numerical values for the approximate and exact upper edge cost tolerances.

	e_{13}	e_{14}	e_{15}	e_{24}	e_{25}	e_{26}	e_{35}	e_{36}	e_{46}
$\overline{\Delta}c^-$	-84.60	-176.61	-43.70	-114.37	-76.85	-43.70	-81.78	-76.85	-81.78
Δc^-	-84.60	-133.87	-43.70	-114.37	-76.85	-43.70	-81.78	-76.85	-81.78
$\underline{\Delta}c^-$	-75.12	-98.79	-43.70	-64.23	-42.79	0.00	-28.63	-47.16	-46.69

Table 6.2: Numerical values for the approximate and exact lower edge cost tolerances.

v_k	e_{12}	e_{16}	e_{23}	e_{34}	e_{45}	e_{56}
1	3.42	33.63	0.00	0.00	15.66	0.00
2	0.00	33.63	0.00	0.00	16.48	0.00
3	0.00	3.02	0.00	7.90	41.62	19.50
4	0.00	3.02	0.00	13.49	41.62	13.92
5	0.00	3.02	0.00	13.49	36.04	13.92
6	43.70	3.02	23.23	28.63	56.76	0.00

Table 6.3: Numerical values for the approximate upper edge cost tolerances obtained for choices of v_k.

v_k	e_{13}	e_{14}	e_{15}	e_{24}	e_{25}	e_{26}	e_{35}	e_{36}	e_{46}
1	-54.40	-58.51	-3.42	-44.67	-23.23	0.00	0.00	0.00	0.00
2	-69.10	-79.23	-24.14	-23.95	-2.51	0.00	0.00	0.00	0.00
3	-54.40	-98.79	-43.70	-64.23	-42.79	0.00	0.00	0.00	-19.50
4	-54.40	-92.78	-43.70	-58.22	-42.79	0.00	0.00	0.00	-13.49
5	-54.40	-58.51	-43.70	-23.95	-42.79	0.00	-13.92	0.00	0.00
6	-75.12	-79.23	-24.14	-44.67	-23.23	0.00	-28.63	-47.16	-46.69

Table 6.4: Numerical values for the approximate lower edge cost tolerances obtained for choices of v_k.

v_k	1	2	3	4	5	6
ϕ_{under}	-0.49	-0.48	-0.39	-0.40	-0.41	-0.34

Table 6.5: Similarity metric ϕ for under approximations of the stability region obtained through consideration of $M1T_k$ by choice of v_k.

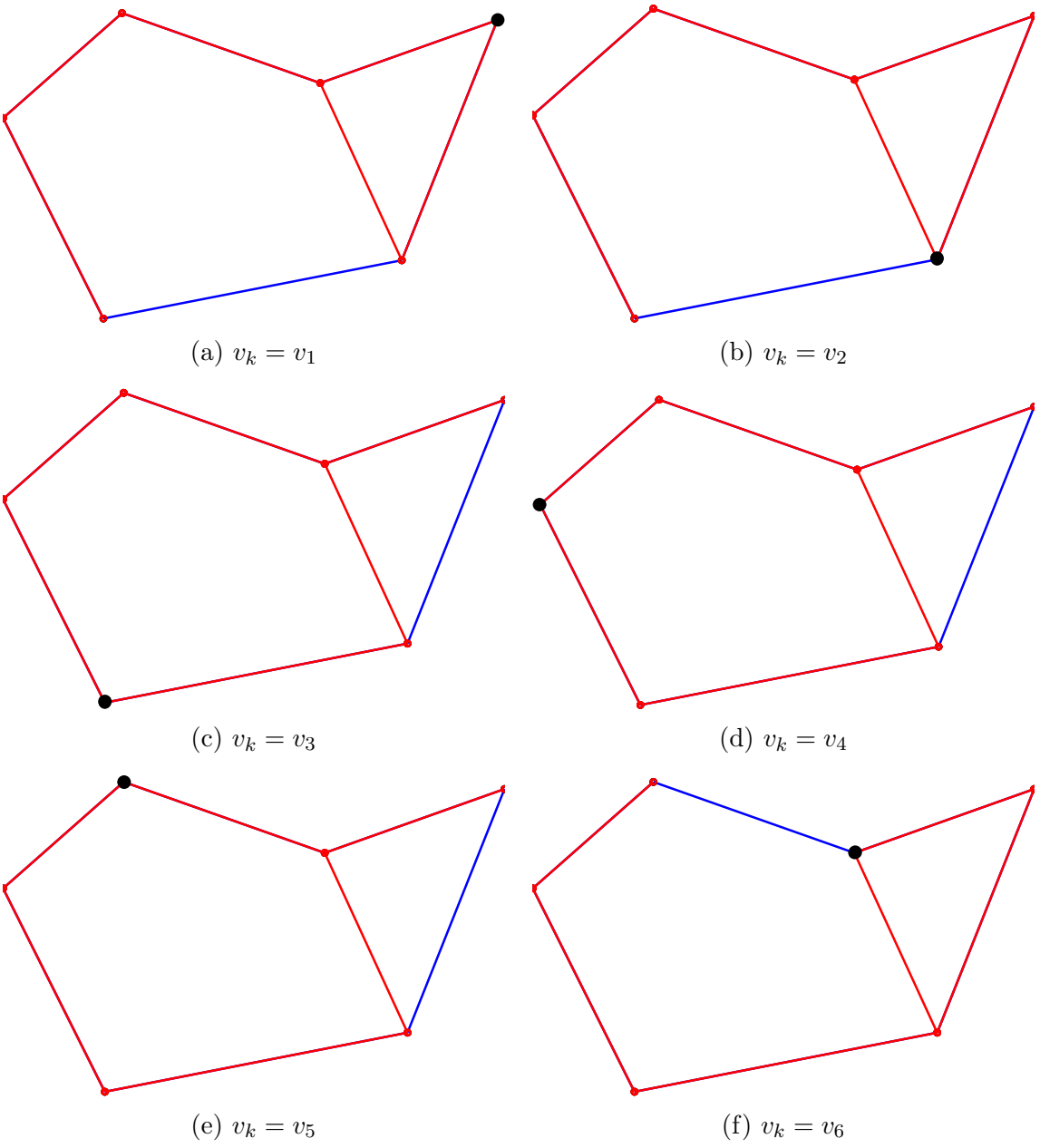

(a) $v_k = v_1$ (b) $v_k = v_2$

(c) $v_k = v_3$ (d) $v_k = v_4$

(e) $v_k = v_5$ (f) $v_k = v_6$

Figure 6.4: **Minimum 1-trees:** This figure depicts the M1Ts on the graph depicted in Section 4.7.1. The complete graph is shown in Fig. 4.1. In each of the subfigures the black dot indicates vertex v_k, i.e., the vertex that defines the subgraphs $G_1(V_{MST_k}, E_{MST_k})$ and the set of edges E_k. The blue edge indicates an edge that is contained in the optimal tour $T^\star$ but not in the minimum 1-tree $M1T_k$.

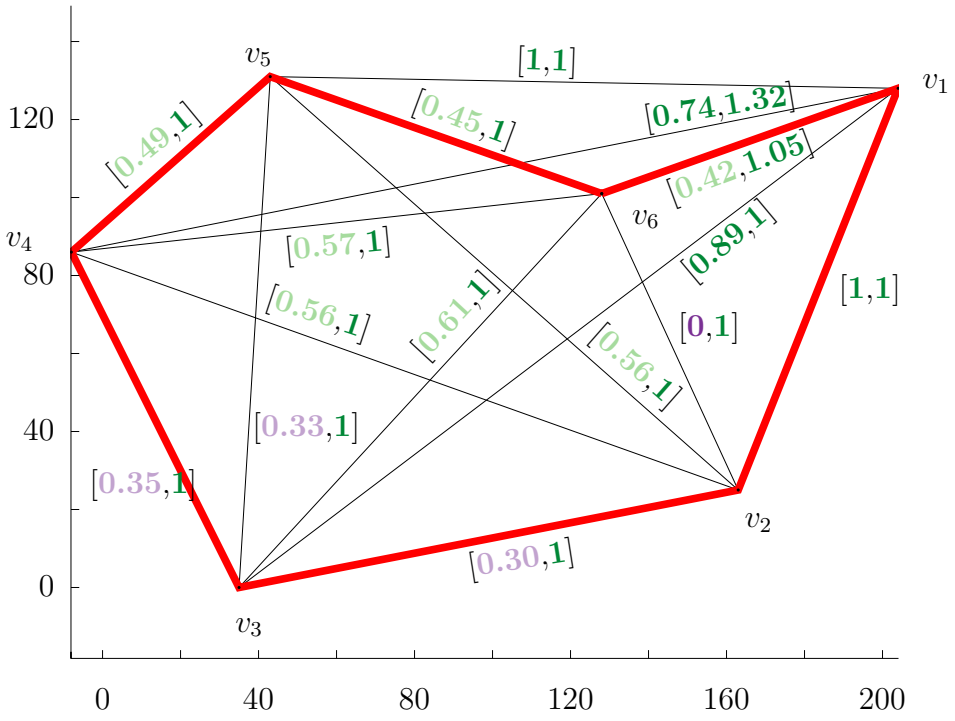

Figure 6.5: **Approximation quality for edge cost tolerances:** For the optimal tour to the eTSP depicted in Fig. 4.1 this figure provides an assessment of the under and over approximation quality for edge cost tolerances.

CHAPTER 7

Alternative applications

The previous chapters present methods for stability analysis of solutions to the TSP, the MST problem, and the M1T problem. These are combinatorial optimization problems. Many planning problems in real world applications can be formulated as combinatorial optimization problems. This chapter outlines two other applications of robustness analysis to solutions of combinatorial optimization problems. The author's publications presenting the results for each of the problems in detail are referenced at the end of the sections.

7.1 Stability analysis for ILP with Markovian problem data

This research thrust is motivated by optimal sensor placement problems and is joint work with Jonathan Las Fargeas. In particular, we consider a problem motivated by [95], where a phenomenon is present in an area modeled as a graph that is to be monitored using sensors (e.g., the spread of a disease in a network). A model of how the phenomenon traverses the graph is given as a first order Markov chain. Given this model, the goal is to place perfect sensors that detect the presence of the phenomenon on the vertices and edges of the graph such that a weighted likelihood of detecting the phenomenon is maximized. Related problems arise in various domains,

e.g., sensors to monitor chemical processes in plants, sensors to track pollutants in the ocean, sensors to track radiation levels, and sensors for surveillance tasks. Let u be a candidate sensor placement and let c be a vector containing the coefficients of the objective function for different sensor locations, then the problem can be formulated as:

$$\underset{u}{\operatorname{argmax}}(c^T \cdot u). \tag{7.1}$$

The cost vector c is a function of the probabilities that define the Markov chain. Therefore, these probabilities affect the optimal sensor placement. Hence, the following questions arise if the probabilities change after the sensors have been placed:

- Is the current sensor placement still optimal?
- How stable is the sensor placement to perturbations in the probabilities?
- How sensitive is the objective function to perturbations in the probabilities?
- How critical is each element in the problem data with respect to the other elements in the problem data?

Our work analyzes stability and criticality of solutions to integer linear programs with respect to perturbations in stochastic data given as Markov chains building upon and adapting the methods presented in Chapter 4 to explicitly address the stochasticity of the problem data. We give expressions for stability regions for perturbations in the initial distribution, the transition matrix, the stationary distribution, and the product of elements of the transition matrix and the stationary distribution. Furthermore, criticality measures that describe the sensitivity of the objective function with respect to an element of the problem data are derived. Stability regions that preserve the stochasticity of the problem data are given. Finally, stability regions for perturbations of elements of the transition matrix, given that the problem is not linear in the initial distribution or the transition matrix, are obtained using a small

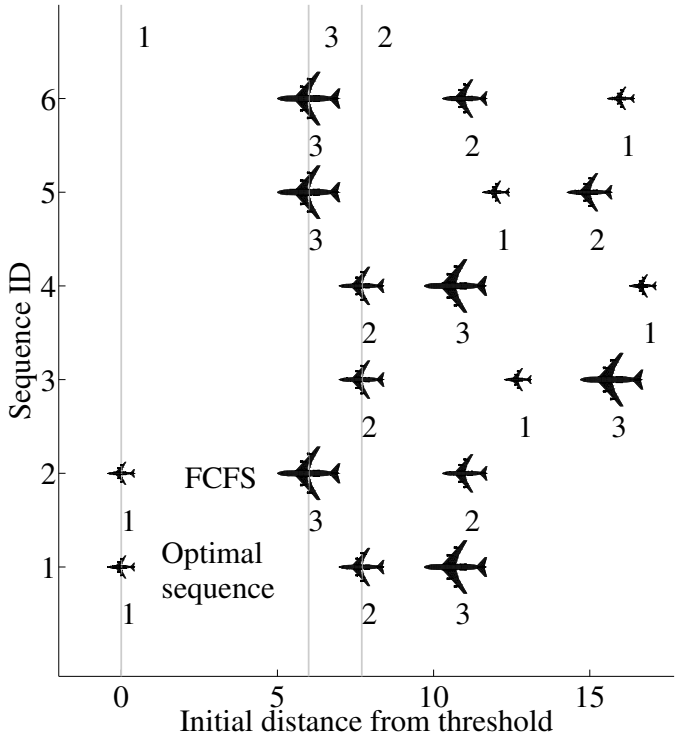

Figure 7.1: **Runway scheduling:** All possible schedules for a problem with three aircraft belonging to three different aircraft classes. Earliest availability is indicated by the vertical lines with the respective aircraft id. The first-come first-serve sequence and the optimal sequence are indicated.

perturbation analysis. The results stemming from this effort are presented in detail in Refs. [9, 16].

7.2 Stability analysis of runway schedules

This research thrust is motivated by runway scheduling problems. The runway scheduling problem is the problem of finding a sequence and corresponding arrival or departure times that optimize an objective of the schedule, for example its makespan, subject to several constraints such as position shift constraints and minimum spacing requirements based on different aircraft classes. Consider the following example de-

picted in Fig. 7.1: Three aircraft, each belonging to a different category numbered 1 to 3 with increasing weight, need to be scheduled. The minimum separation between two aircraft depends on the category of the preceding and the trailing aircraft. It increases with increasing weight of the preceding aircraft relative to the weight of the trailing aircraft and decreases with decreasing weight of the preceding aircraft relative to the trailing aircraft. The earliest availability for all three aircraft is indicated by the vertical lines in the figure. All feasible schedules are depicted and the first sequence, sequence 1, is optimal. Sequence 2 is in first-come first-serve order. In this example, first-come first-serve is not the optimal policy that minimizes the makespan of the sequence.

Minimizing the makespan of the sequence is a well studied objective amongst others in runway scheduling [96–98] as it addresses the problem of maximizing throughput. It therefore captures one of the essential objectives of optimizing runway usage.

Solving this type of scheduling problem is computationally hard due to its combinatorial nature and the availability constraints. Hence, once delays occur the following question is raised: How stable is the optimal schedule with respect to changes in the problem data, i.e., the arrival times of the aircraft. Building upon the methods presented in Chapter 4 a method to compute stability regions for a set of schedules is given. Sensitivity analysis of the linear programming relaxation and a nonlinear relationship between the delay of individual aircraft and the incurred cost change for all landing sequences yield the stability information. Furthermore, the properties of a first-come first-serve policy are studied by giving sufficient conditions and a heuristic condition for the optimality of first-come first-serve sequences. The above results are shown to be also applicable to landing sequences obtained through local neighborhood search, sequences that obey a position shift constraint, and subsequences of landing sequences as used in a rolling horizon approach. The results stemming from this effort are presented in detail in Refs. [15, 99].

CHAPTER 8

Conclusions

The use of UAVs has grown steadily in recent years. With the increase in their use and the advances in technology, these aircraft are tasked with increasingly large and complex missions. These missions are typically designed such that given the circumstances of the mission, e.g., the tasks to be completed, vehicle specifications, and a model of the environment, a flight path and sequence of actions to be performed by the aircraft are selected such that they optimize a mission objective. This thesis studies the robustness of a given mission plan, i.e., how changes in the circumstances of the mission affect the optimality of a given mission plan.

8.1 Summary

This thesis identifies variants of the traveling salesman problem as prototypical UAV mission planning problems as they inherently capture the combinatorial nature of the task planning problem and the continuous nature of the path planning problem as discussed in Chapter 1. The results developed in this thesis are agnostic to the specific implementation of the path planning layer and are therefore applicable to a variety of path planning methods, performance metrics, and world models. Furthermore, the minimum spanning tree problem is chosen to study the robustness of communication topologies in multi-UAV missions.

A literature survey relevant to mission planning problems for unmanned aircraft, stability analysis for combinatorial optimization problems, and exact and approximate stability analysis for solutions to traveling salesman problems is given in Chapter 2.

Chapter 3 formulates several relevant variants of the traveling salesman problem, minimum spanning tree problems, and defines the concepts used for stability analysis throughout this thesis.

Chapter 4 presents the analysis of the stability region of solutions to classes of the TSP with respect to perturbations in the edge costs through a linear programming relaxation of an auxiliary problem. A description and the representation of the stability regions are given. The derivation of edge cost tolerances from the stability regions is demonstrated and edge criticalities are defined. Finally, for the special case of Euclidean TSPs, the derivation of approximate stability regions with respect to perturbations in vertex locations is presented, safe radii and vertex criticalities are defined. Stability regions for optimal solutions to weighted-sum multi-objective TSPs in the space of weight changes with respect to a given set of tours are computed. From the stability region, most critical weight perturbations are derived. Furthermore, stability regions for optimal solutions to wsmoTSPs in the space of edge cost changes with respect to each cost function are presented. Finally, linearized stability regions for optimal solutions to wsmoTSPs for simultaneous perturbations in the individual cost functions and weights are derived.

Chapter 5 presents a polyhedral description of stability regions of MSTs based on results in the literature to study the robustness of optimal communication topologies for teams of unmanned aircraft. It follows the ideas outlined in the previous chapter in deriving stability measures from the stability regions such as tolerances, stability balls, and criticalities. Finally, following the approach in Chapter 4, this analysis is extended to eMST.

As computing exact stability regions for solutions to the TSP can become com-

putationally intractable for large instances, Chapter 6 discusses computationally tractable methods to obtain over and under approximations of the stability regions of optimal solutions to symmetric non sequence-dependent TSP. Upper and lower bounds on edge cost tolerances, approximate edge criticalities, approximate stability regions with respect to perturbations in vertex locations, safe radii, and vertex criticalities are shown to be obtainable.

The results presented in this thesis are applicable to other combinatorial optimization problems such as sensor placement problems and runway scheduling problems. Chapter 7 outlines these applications.

8.2 Concluding remarks

There exist numerous missions for unmanned aircraft. In almost all cases, these mission involve a combinatorial planning problem and a continuous planning problem. This commonality can be leveraged to formulate a wide class of mission planning problems in a similar fashion. The content of this thesis addresses the robustness of optimal mission plans with respect to changes in the problem data for missions that exhibit the above characteristics.

Regarding the interaction between scheduling and path planning, this includes the more general case of vehicle routing as for example found in delivery truck routing applications. Changing external conditions such as weather, dominant wind directions, or traffic may alter the problem instance, which can render an itinerary suboptimal. Specifically, this thesis addresses the problem of stability analysis for solutions to classes of the traveling salesman problem.

The robustness of a given solution with respect to changing parameters could be analyzed by exhaustively sampling the space of input parameters. However, solving the underlying optimization problem might be computationally expensive and the

quality of the analysis depends on the chosen sampling density. This thesis presents multiple alternative approaches to perform robustness analysis by obtaining the exact or approximate stability regions of an optimal solution. The stability region associated with an optimal solution is the set of all perturbations to the input parameters for which that solution remains optimal. From the stability regions, other stability measures such as tolerances and criticality for elements of the problem data can be derived.

This approach differs from an alternative way to address uncertain data, where the uncertainty is modeled and stochastic optimization techniques are employed to find a solution that minimizes the expected value of the objective function. Stability analysis as presented in this thesis does not require any a priori knowledge of the nature of the uncertainty. Additional insight, such as criticality of elements of the input data as well as the smallest perturbation that causes a solution to become suboptimal, can be derived.

This work has multiple potential benefits such as providing insight into theoretical properties of stability regions of traveling salesman tours, minimum spanning trees, and minimum 1-trees, but also insight into how robust a solution is with respect to modeling uncertainties and how limited intelligence resources should be allocated. For example, modeling and data acquisition efforts should be directed towards elements of the problem data that have a smaller robustness margin. While this thesis is not concerned with developing algorithms for solving instances of the TSP but rather with providing insight into properties of optimal solutions to classes of traveling salesman problems, the presented methods could be used in a supervisory control system for an agent executing a mission to assess the optimality of a plan if changes occur.

8.3 Future directions

Several future directions exist for the work presented in this thesis:

- **Alternative approximations:** Building upon the results on under approximation by relaxations and over approximation by subsets of tours, approximations using other relaxations and subset construction methods could be investigated. Furthermore, many specialized algorithms exist to solve instances of traveling salesman problems. It should be investigated if stability information is obtainable by exploiting the mechanisms implemented by these methods. Ref. [79] suggests using information obtained from branch and bound algorithms to obtain approximate stability information.

- **Approximation quality:** This thesis presents certain methods to obtain under and over approximations of stability regions and metrics derived from them in Chapter 6. Even though it is most likely intractable to obtain ϵ-approximate stability regions, the approximation quality should be assessed. Section 6.7 provides some insight into the approximation quality achieved by the methods discussed in this work. Furthermore, an easy to compute metric to compare stability regions is given. It would be interesting to evaluate other metrics and to use these metrics to guide the search for other approximation methods.

- **Mission replanning:** The results presented in this thesis can help to establish whether a tour remains optimal after changes to the problem data occur. One important extension to this work is to design efficient algorithms that exploit previous planning efforts and the nature of the change to re-optimize tours after a tour has become suboptimal. Furthermore, the problem of assessing optimality and re-optimizing tours if edge cost changes vary once an agent has already started executing a tour has not yet been studied systematically. The search space decreases as the agent starts executing a mission plan as the number

of candidate solutions at each step of execution is a subset of the previous set of solutions. Hence, some stability information for traveling agents is obtainable from the stability information obtained for the initial solution. Let $T^{\star}_{vis}(m)$ denote the sequence of vertices visited at the m-th step. Then the stability region of $T^{\star}$ at step zero, i.e., before traversal of the graph, is contained in the stability region of $T^{\star}$ at the m-th step with respect to the set of tours that share the same sequence $T^{\star}_{vis}(m)$, because the set of tours that share the same sequence $T^{\star}_{vis}(m)$ is a subset of the set of all tours.

- **Robust planning:** Efficient algorithms exist to solve the shortest tour TSP to optimality. Trading optimality for robustness, it would be interesting to investigate whether an optimization problem could be formulated that simultaneously minimizes tour length and maximizes a robustness measure such as the minimal tolerance or the largest inscribed ball in the stability region.

- **Alternative mission formulations:** This thesis identifies classes of the traveling salesman problem as prototypical problems to assess the robustness of UAV missions. While the author believes that the discussed classes capture a wide variety of real world mission planning problems for unmanned aircraft, one might argue that the constraint that each location can only be visited once is too restrictive in some real world applications. A variant of the TSP that allows returning to a priori visited locations is the Steiner TSP [100–102]. The application of the above robustness results to Steiner TSPs could be approached using a similar method as chosen for sequence-dependent problems through appropriate representation of the increased search space. However, for UAV applications, mission planning, as described in Chapter 1, already allows for flight paths to return to previously visited locations, as scheduling is performed on an auxiliary tactical graph and the path planner is not constrained in the

selection of flight paths.

Finally, an extension of the instance of asymmetric sequence-dependent TSP with intelligent adversaries as shown in Section 4.7.4.2 is a multi evader single pursuer pursuit evasion game [103]. In this game, multiple adversaries try to maximize the time at which the UAV is colocated with the last adversary to be visited by leaving their initial locations, while the UAV is tasked to select a sequence in which it pursues the adversaries that minimizes the time at which it is above the last adversary to be visited. It would be interesting to study the robustness of such an optimal sequence.

BIBLIOGRAPHY

[1] M. Niendorf, F. Schmitt, and F.-M. Adolf, "Multi-query path planning for an unmanned fixed-wing aircraft," in *AIAA Guidance, Navigation and Control Conference*, August 2013.

[2] H. Pollaris, K. Braekers, A. Caris, G. K. Janssens, and S. Limbourg, "Vehicle routing problems with loading constraints: state-of-the-art and future directions," *OR Spectrum*, vol. 37, no. 2, pp. 297–330, 2014.

[3] K. Barton and D. Kingston, "Systematic surveillance for uavs: A feedforward iterative learning control approach," in *American Control Conference (ACC), 2013*, 2013, pp. 5917–5922.

[4] E. Garcia and D. Casbeer, "Uav coordinated decision making and mission management," in *Proceedings of the ASME 2014 Dynamic Systems and Control Conference*, October 2014.

[5] M. Ehrgott and X. Gandibleux, "A survey and annotated bibliography of multiobjective combinatorial optimization," *OR-Spektrum*, vol. 22, no. 4, pp. 425–460, 2000.

[6] L. N. Kozeratskaya, T. T. Lebedeva, and I. V. Sergienko, "Stability, parametric, and postoptimality analysis of discrete optimization problems," *Cybernetics*, vol. 19, no. 4, pp. 522–535, 1983.

[7] F.-M. Adolf and A. Mueller, "Asymmetric 2-opt scheduling for roadmap-based task planning in urban terrain," in *AIAA Infotech@Aerospace*, 2013.

[8] S. V. Hoesel and A. Wagelmans, "On the complexity of postoptimality analysis of 01 programs," *Discrete Applied Mathematics*, vol. 91, no. 1, pp. 251 – 263, 1999.

[9] M. Niendorf, P. T. Kabamba, and A. R. Girard, "Polynomial time sensitivity analysis of task schedules," in *American Control Conference (ACC), 2014*, June 2014, pp. 4593–4598.

[10] ——, "Stability of solutions to classes of traveling salesman problems," *IEEE Transactions on Cybernetics*, vol. 46, no. 4, pp. 973–985, 2016.

[11] ——, "Stability analysis of multi-objective planning problems for unmanned aircraft," in *2015 IEEE 54rd Annual Conference on Decision and Control (CDC)*, December 2015, pp. 7238–7243.

[12] M. Niendorf and A. R. Girard, "Robustness of communication links for teams of unmanned aircraft by sensitivity analysis of minimum spanning trees," in *American Control Conference (ACC), 2016*, July 2016.

[13] M. Niendorf and A. Girard, "Exact and approximate stability of solutions to traveling salesman problems," *Submitted: IEEE Transactions on Automatic Control*, 2016.

[14] M. Niendorf, J. C. Las Fargeas, P. T. Kabamba, and A. R. Girard, "Stability analysis of stochastic integer optimization problems," in *2014 IEEE 53rd Annual Conference on Decision and Control (CDC)*, December 2014, pp. 402 – 407.

[15] M. Niendorf, P. T. Kabamba, and A. R. Girard, "Stability analysis of optimal runway schedules," in *American Control Conference (ACC), 2015*, July 2015.

[16] J. Las Fargeas, M. Niendorf, P. Kabamba, and A. Girard, "Stability and criticality analysis for integer linear programs with markovian problem data," *IEEE Transactions on Automatic Control*, 2015.

[17] C. S. Orloff, "A fundamental problem in vehicle routing," *Networks*, vol. 4, no. 1, pp. 35–64, 1974.

[18] S. Lin and B. W. Kernighan, "An effective heuristic algorithm for the traveling-salesman problem," *Operations research*, vol. 21, no. 2, pp. 498–516, 1973.

[19] J. W. Pepper, B. L. Golden, and E. A. Wasil, "Solving the traveling salesman problem with annealing-based heuristics: a computational study," *IEEE Transactions on Systems, Man and Cybernetics, Part A: Systems and Humans*, vol. 32, no. 1, pp. 72–77, 2002.

[20] H.-K. Tsai, J.-M. Yang, Y.-F. Tsai, and C.-Y. Kao, "An evolutionary algorithm for large traveling salesman problems," *IEEE Transactions on Systems, Man, and Cybernetics, Part B: Cybernetics*, vol. 34, no. 4, pp. 1718–1729, 2004.

[21] H. D. Nguyen, I. Yoshihara, K. Yamamori, and M. Yasunaga, "Implementation of an effective hybrid ga for large-scale traveling salesman problems," *IEEE Transactions on Systems, Man, and Cybernetics, Part B: Cybernetics*, vol. 37, no. 1, pp. 92–99, 2007.

[22] X.-F. Xie and J. Liu, "Multiagent optimization system for solving the traveling salesman problem (tsp)," *IEEE Transactions on Systems, Man, and Cybernetics, Part B: Cybernetics*, vol. 39, no. 2, pp. 489–502, 2009.

[23] V. A. Shim, K. Tan, and C. Cheong, "A hybrid estimation of distribution algorithm with decomposition for solving the multiobjective multiple traveling salesman problem," *IEEE Transactions on Systems, Man, and Cybernetics, Part C: Applications and Reviews*, vol. 42, no. 5, pp. 682–691, 2012.

[24] L. Ke, Q. Zhang, and R. Battiti, "Moea/d-aco: A multiobjective evolutionary algorithm using decomposition and antcolony," *IEEE Transactions on Cybernetics*, vol. 43, no. 6, pp. 1845–1859, 2013.

[25] D. L. Applegate and I. ebrary, *The traveling salesman problem a computational study*. Princeton: Princeton University Press, 2006.

[26] J. Jackson, M. Faied, and A. Girard, "Comparison of tabu/2-opt heuristic and optimal tree search method for assignment problems," *International Journal of Robust and Nonlinear Control*, vol. 21, no. 12, pp. 1358–1371, 2011.

[27] E. Kivelevitch, K. Cohen, and M. Kumar, "Market-based solution to the allocation of tasks to agents," *Procedia Computer Science*, vol. 6, no. 0, pp. 28 – 33, 2011.

[28] J. Las Fargeas, B. Hyun, P. Kabamba, and A. Girard, "Persistent visitation under revisit constraints," in *International Conference on Unmanned Aircraft Systems*, 2013.

[29] F. Pasqualetti, A. Franchi, and F. Bullo, "On cooperative patrolling: Optimal trajectories, complexity analysis, and approximation algorithms," *IEEE Transactions on Robotics*, vol. 28, no. 3, pp. 592–606, 2012.

[30] P. Oberlin, S. Rathinam, and S. Darbha, "Today's traveling salesman problem," *IEEE Robotics Automation Magazine*, vol. 17, no. 4, pp. 70–77, 2010.

[31] F. Bullo, E. Frazzoli, M. Pavone, K. Savla, and S. Smith, "Dynamic vehicle routing for robotic systems," *Proceedings of the IEEE*, vol. 99, no. 9, pp. 1482–1504, 2011.

[32] K. J. Obermeyer, P. Oberlin, and S. Darbha, "Sampling-based path planning for a visual reconnaissance unmanned air vehicle," *Journal of Guidance, Control, and Dynamics*, vol. 35, no. 2, pp. 619–631, 2012.

[33] J. T. Isaacs and J. P. Hespanha, "Dubins traveling salesman problem with neighborhoods: A graph-based approach," *Algorithms*, vol. 6, no. 1, pp. 84–99, 2013.

[34] S. Karaman and E. Frazzoli, "Sampling-based algorithms for optimal motion planning with deterministic μ-calculus specifications," in *American Control Conference (ACC), 2012*, 2012.

[35] L. Dubins, "On curves of minimal length with a constraint on average curvature, and with prescribed initial and terminal positions and tangents," *American Journal of Mathematics*, vol. 79, no. 3, pp. 497–516, 1957.

[36] M. Hwangbo, J. Kuffner, and T. Kanade, "Efficient two-phase 3d motion planning for small fixed-wing uavs," in *Proceedings of the 2007 IEEE International Conference on Robotics & Automation*, 2007.

[37] M. Niendorf, F.-M. Adolf, and T. Gerhard, "Behavior-based onboard mission management for an unmanned fixed-wing aircraft," in *AIAA Infotech@Aerospace*, 2012.

[38] K. Savla, E. Frazzoli, and F. Bullo, "Traveling salesperson problems for the dubins vehicle," *IEEE Transactions on Automatic Control*, vol. 53, no. 6, pp. 1378–1391, 2008.

[39] M. Cons, T. Shima, and C. Domshlak, *Integrating Task Assignment and Guidance via Motion Planning for Unmanned Aerial Vehicles.* American Institute of Aeronautics and Astronautics, 2011.

[40] J. Le Ny, E. Feron, and E. Frazzoli, "On the dubins traveling salesman problem," *IEEE Transactions on Automatic Control*, vol. 57, no. 1, pp. 265–270, 2012.

[41] M. Adbelhafiz, A. Mostafa, and A. Girard, "Vehicle routing problem instances: Application to multi-uav mission planning," in *AIAA Guidance, Navigation, and Control Conference.* American Institute of Aeronautics and Astronautics, 2010.

[42] M. Gendreau, M. Iori, G. Laporte, and S. Martello, "A tabu search algorithm for a routing and container loading problem," *Transportation Science*, vol. 40, no. 3, pp. 342–350, 2006.

[43] K. F. Doerner, G. Fuellerer, R. F. Hartl, M. Gronalt, and M. Iori, "Metaheuristics for the vehicle routing problem with loading constraints," *Networks*, vol. 49, no. 4, pp. 294–307, 2007.

[44] V. Lurkin and M. Schyns, "The airline container loading problem with pickup and delivery," *European Journal of Operational Research*, vol. 244, no. 3, pp. 955–965, 2015.

[45] R. Beard, T. McLain, M. Goodrich, and E. Anderson, "Coordinated target assignment and intercept for unmanned air vehicles," *IEEE Transactions on Robotics and Automation*, vol. 18, no. 6, pp. 911–922, Dec 2002.

[46] S. Scherer and S. Singh, "Multiple-Objective Motion Planning for Unmanned Aerial Vehicles," in *Proceedings of the 2011 IEEE/RSJ International Conference on Intelligent Robots and Systems (IROS 2011)*, Sep. 2011.

[47] D. Tezcaner and M. Köksalan, "An interactive algorithm for multi-objective route planning," *Journal of Optimization Theory and Applications*, vol. 150, no. 2, pp. 379–394, 2011.

[48] L. Benyoucef, J.-C. Hennet, M. K. Tiwari, N. Labadie, and C. Prodhon, *A Survey on Multi-criteria Analysis in Logistics: Focus on Vehicle Routing Problems*. Springer London, 2014, pp. 3–29.

[49] V. Pillac, M. Gendreau, C. Guéret, and A. L. Medaglia, "A review of dynamic vehicle routing problems," *European Journal of Operational Research*, vol. 225, no. 1, pp. 1–11, 2013.

[50] M. Pavone, E. Frazzoli, and F. Bullo, "Adaptive and distributed algorithms for vehicle routing in a stochastic and dynamic environment," *IEEE Transactions on Automatic Control*, vol. 56, no. 6, pp. 1259–1274, 2011.

[51] G. Laporte, F. Louveaux, and H. Mercure, "The vehicle routing problem with stochastic travel times," *Transportation Science*, vol. 26, no. 3, pp. 161–170, 1992.

[52] M. Gendreau, G. Laporte, and R. Séguin, "Stochastic vehicle routing," *European Journal of Operational Research*, vol. 88, no. 1, pp. 3–12, 1 1996.

[53] A. S. Kenyon and D. P. Morton, "Stochastic vehicle routing with random travel times," *Transportation Science*, vol. 37, no. 1, pp. 69–82, 2003.

[54] Z. Wang, J. Guo, M. Zheng, and Y. Wang, "Uncertain multiobjective traveling salesman problem," *European Journal of Operational Research*, vol. 241, no. 2, pp. 478–489, 3 2015.

[55] T. Cheong and I. White, C.C., "Dynamic traveling salesman problem: Value of real-time traffic information," *IEEE Transactions on Intelligent Transportation Systems*, vol. 13, no. 2, pp. 619–630, 2012.

[56] A. Toriello, W. B. Haskell, and M. Poremba, "A dynamic traveling salesman problem with stochastic arc costs," *Operations Research*, vol. 62, no. 5, pp. 1107–1125, 2014.

[57] U. Ritzinger, J. Puchinger, and R. F. Hartl, "A survey on dynamic and stochastic vehicle routing problems," *International Journal of Production Research*, vol. 54, no. 1, pp. 1–17, 2015.

[58] D. Kingston, R. Holt, R. Beard, T. McLain, and D. Casbeer, "Decentralized perimeter surveillance using a team of uavs," in *AIAA Guidance, Navigation, and Control Conference and Exhibit*. American Institute of Aeronautics and Astronautics, 2005.

[59] D. W. Casbeer, D. B. Kingston, R. W. Beard, and T. W. McLain, "Cooperative forest fire surveillance using a team of small unmanned air vehicles," *International Journal of Systems Science*, vol. 37, no. 6, pp. 351–360, 2006.

[60] J. Las Fargeas, P. Kabamba, and A. Girard, "Cooperative surveillance and pursuit using unmanned aerial vehicles and unattended ground sensors," *Sensors*, vol. 15, no. 1, pp. 1365–1388, 2015.

[61] T. Shima and S. J. Rasmussen, *UAV cooperative decision and control challenges and practical approaches*. Philadelphia: Society for Industrial and Applied Mathematics, 2009.

[62] K. P. Valavanis, G. J. Vachtsevanos, A. Kopeikin, S. Ponda, and G. Inalhan, *Control of Communication Networks for Teams of UAVs*. Springer Netherlands, 2014, pp. 1619–1654.

[63] D. Pike, S. Givigi, J. Marshall, A. Taylor, and A. Beaulieu, "Robust vehicle routing policies using local communications amp; sensing," in *American Control Conference (ACC), 2013*, June 2013, pp. 6351–6357.

[64] S. Kim, H. Oh, J. Suk, and A. Tsourdos, "Coordinated trajectory planning for efficient communication relay using multiple uavs," *Control Engineering Practice*, vol. 29, no. 0, pp. 42–49, 2014.

[65] B. Newton, J. Aikat, and K. Jeffay, "Analysis of topology algorithms for commercial airborne networks," in *2014 IEEE 22nd International Conference on Network Protocols (ICNP)*, Oct 2014, pp. 368–373.

[66] L. N. Kozeratskaya, T. T. Lebedeva, and I. V. Sergienko, "Stability of discrete optimization problems," *Cybernetics and Systems Analysis*, vol. 29, no. 3, pp. 367–378, 1993.

[67] T. Gal, *Postoptimal Analyses, Parametric Programming, and Related Topics: Degeneracy, Multicriteria Decision Making, Redundancy*. Walter De Gruyter Incorporated, 1995.

[68] H. J. Greenberg, *An Annotated Bibliography for Post-Solution Analysis in Mixed Integer Programming and Combinatorial Optimization*. Boston, MA: Springer US, 1998, pp. 97–147.

[69] D. Fernández-Baca and B. Venkatachalam, "Sensitivity analysis in combinatorial optimization," *Handbook of Approximation Algorithms and Metaheuristics*, pp. 30–1—30–17, 2007.

[70] N. Hall and M. Posner, "Sensitivity analysis for scheduling problems," *Journal of Scheduling*, vol. 7, no. 1, pp. 49–83, 2004.

[71] B. Goldengorin, G. Jäger, and P. Molitor, "Tolerances applied in combinatorial optimization," *Journal of Computer Science*, vol. 2, pp. 716–734, 2006.

[72] ——, "Some basics on tolerances," in *Algorithmic Aspects in Information and Management*. Springer, 2006, pp. 194–206.

[73] Y. Sotskov, V. Leontev, and E. Gordeev, "Some concepts of stability analysis in combinatorial optimization," *Discrete Applied Mathematics*, vol. 58, no. 2, pp. 169 – 190, 1995.

[74] M. Libura, "A note on robustness tolerances for combinatorial optimization problems," *Information Processing Letters*, vol. 110, no. 16, pp. 725 – 729, 2010.

[75] G. Jäger, B. Goldengorin, and P. Pardalos, "The theory of set tolerances," in *Learning and Intelligent Optimization*, ser. Lecture Notes in Computer Science, P. M. Pardalos, M. G. Resende, C. Vogiatzis, and J. L. Walteros, Eds. Springer International Publishing, 2014, pp. 362–377.

[76] D. R. Shier and C. Witzgall, "Arc tolerances in shortest path and network flow problems," *Networks*, vol. 10, no. 4, pp. 277–291, 1980.

[77] R. E. Tarjan, "Sensitivity analysis of minimum spanning trees and shortest path trees," *Information Processing Letters*, vol. 14, no. 1, pp. 30–33, 1982.

[78] D. Gusfield, "A note on arc tolerances in sparse shortest-path and network flow problems," *Networks*, vol. 13, no. 2, pp. 191–196, 1983.

[79] E. van der Poort, "Aspects of sensitivity analysis for the traveling salesman problem," Ph.D. dissertation, University of Groningen, 1997.

[80] G. Jaeger, "The theory of tolerances with application to the travelling salesman problem," Habilitationsschrift, Martin-Luther University of Halle-Wittenberg, 2010.

[81] P. Hansen, M. Labbé, and R. E. Wendell, "Sensitivity analysis in multiple objective linear programming: The tolerance approach," *European Journal of Operational Research*, vol. 38, no. 1, pp. 63–69, 1 1989.

[82] E. Triantaphyllou and A. Sánchez, "A sensitivity analysis approach for some deterministic multi-criteria decision-making methods*," *Decision Sciences*, vol. 28, no. 1, pp. 151–194, 1997.

[83] M. Libura, E. van der Poort, G. Sierksma, and J. van der Veen, "Stability aspects of the traveling salesman problem based on k-best solutions," *Discrete Applied Mathematics*, vol. 87, no. 1, pp. 159–185, 1998.

[84] M. Libura, "Sensitivity analysis for minimum hamiltonian path and traveling salesman problems," *Discrete Applied Mathematics*, vol. 30, no. 2, pp. 197–211, 1991.

[85] K. Helsgaun, "An effective implementation of the lin–kernighan traveling salesman heuristic," *European Journal of Operational Research*, vol. 126, no. 1, pp. 106–130, 2000.

[86] D. Richter, "Toleranzen in helsgauns lin-kernighan heuristik fuer das tsp," Universitaet Halle-Wittenberg, Diploma Thesis, 2006.

[87] A. Schrijver, *Theory of linear and integer programming.* John Wiley & Sons, 1999.

[88] D. G. Luenberger and Y. Ye, *Linear and Nonlinear Programming.* Boston, MA: Springer Science+Business Media, LLC, 2008.

[89] R. K. Ahuja, T. L. Magnanti, and J. B. Orlin, *Network flows : theory, algorithms, and applications.* Upper Saddle River (N.J.): Prentice Hall, 1993.

[90] M. R. Garey and D. S. Johnson, *Computers and intractability: a guide to the theory of NP-completeness.* New York: W. H. Freeman & Co, 1979.

[91] G. Croes, "A method for solving traveling-salesman problems," *Operations Research*, vol. 6, no. 6, pp. 791–812, 1958.

[92] M. Held and R. M. Karp, "The traveling-salesman problem and minimum spanning trees," *Operations Research*, vol. 18, no. 6, pp. 1138–1162, 1970.

[93] S. Boyd and L. Vandenberghe, *Convex Optimization.* Cambridge University Press, 2004.

[94] G. C. Calafiore and L. El Ghaoui, *Optimization Models.* Cambridge University Press, 2007.

[95] J. Las Fargeas, P. Kabamba, and A. Girard, "Optimal configuration of alarm sensors for monitoring mobile ergodic markov phenomena on arbitrary graphs," *IEEE Sensors*, vol. 15, no. 6, pp. 3622–3634, June 2015.

[96] J. Bennell, M. Mesgarpour, and C. Potts, "Airport runway scheduling," *Annals of Operations Research*, vol. 204, no. 1, pp. 249–270, 2013.

[97] B. Chandran and H. Balakrishnan, "A dynamic programming algorithm for robust runway scheduling," in *American Control Conference (ACC) 2007*, July 2007, pp. 1161–1166.

[98] H. Balakrishnan and B. G. Chandran, "Algorithms for scheduling runway operations under constrained position shifting," *Operations Research*, vol. 58, no. 6, pp. 1650–1665, 2010.

[99] M. Niendorf, P. Kabamba, and A. Girard, "Stability analysis of runway schedules," *accepted: IEEE Transactions on Intelligent Transportation Systems*, 2016.

[100] D. H. Ratliff and A. S. Rosenthal, "Order-picking in a rectangular warehouse: A solvable case of the traveling salesman problem," *Operations Research*, vol. 31, no. 3, pp. 507–521, 1983.

[101] B. Fleischmann, "A cutting plane procedure for the travelling salesman problem on road networks," *European Journal of Operational Research*, vol. 21, no. 3, pp. 307–317, 1985.

[102] G. Cornuéjols, J. Fonlupt, and D. Naddef, "The traveling salesman problem on a graph and some related integer polyhedra," *Mathematical Programming*, vol. 33, no. 1, pp. 1–27, 1985.

[103] D. W. Oyler, "Contributions to pursuit-evasion game theory," Ph.D. dissertation, University of Michigan, 2016.